

**The maximum wind effect
on wave overtopping at dikes
with crest elements**

R.J. van der Bijl

The maximum wind effect on wave overtopping at dikes with crest elements

MSc. Thesis

Ruben Johan van der Bijl

in partial fulfilment of the requirements for the degree of

Master of Science
in Civil Engineering

at Delft University of Technology,
Faculty of Civil Engineering and Geosciences,
Department of Hydraulic Engineering,
Section of Coastal Engineering,

to be defended publicly on Tuesday September 20, 2022 at 9:00 AM.

Thesis committee

Prof. dr. ir. M. R. A. van Gent	Delft University of Technology & Deltares
Dr. ir. D. Wüthrich	Delft University of Technology
Dr. ir. G. Wolters	Deltares

This thesis is confidential and cannot be made public until September 20, 2023.
An electronic version of this thesis is available at <http://repository.tudelft.nl/>.

Preface

This thesis finalises the master Hydraulic Engineering at Delft University of Technology. Physical model tests were performed in the Pacific Basin at Deltares, which was an interesting and enjoyable learning experience. To me, working in the laboratory was a unique adventure and I am glad that I had the opportunity.

After conducting the experiments, I moved to the office for the data analysis and report writing. During this theoretical part of the research, the thesis committee guided me when needed. I would like to thank the thesis committee, starting with Marcel van Gent, the chairman of the committee and main sparring partner. Whenever I had some remarkable results or I was in doubt how to approach the data, you were willing to give some tips or guidance based on your broad experience. Moreover, thanks to you I had the opportunity to graduate at Deltares and perform physical model tests. Next, I would like to thank Davide Wüthrich, for being curious to know more about this research topic and therefore encouraging me to keep investigating. Your open-minded view resulted in valuable feedback on the report and during the meetings. Last but not least, I would like to thank Guido Wolters for this critical view on the content I presented. Based on your comments, you made me think about possible explanations and the way the data fit these interpretations.

The experiments could not have been conducted without help of the model technicians. Wesley Stet, Danny van Doeveren and Peter Alberts, I would like to thank you for your help when it comes to changing the dike configuration or solving problems when pieces of the dike were floating in the basin and the dike had to be repaired. Whenever I asked for assistance, you were there. You are essential to all students and Deltares employees that want to perform experiments and you create a pleasant atmosphere in the Hydrohall.

As always, being supported by the experts in the hydraulic engineering field is as important to me as being supported by friends and family. I would like to express special thanks to my parents and brother. Since you are the ones closest to me, you are the first to see joy, frustration, eureka moments and more. Whatever happened, you stood behind me, supported me and encouraged me to go on. Although you are not familiar with in depth Coastal Engineering concepts, your views are valuable. Simplicity sometimes is the best way, especially when it comes to explaining certain theories. My friends are just as important. On the one hand, you gave me the opportunity to relax. On the other hand, the more hydraulic educated friends were able to give useful substantive feedback and keep me open minded. Thank you for your support.

Enjoy reading my thesis!

*Ruben van der Bijl
Delft, September 2022*

Abstract

Climate change affects sea level rise and the safety of the people living behind seadikes. In order to prepare for this, several adaptation measures are available. One option to reduce the wave attack on dikes is constructing a foreshore breakwater or nourishments, which affect the foreshore instead of the dike. It is also possible to adapt the dike itself by means of raising the dike. However, this measure comes with widening of dikes and higher loading on the subsoil. Wave overtopping can be reduced by including roughness elements or adding a berm as well. Another possibility is to employ crest elements such as a vertical crest wall, promenade or parapet on the crest wall to reduce wave overtopping discharges.

The overtopping discharge is key when defining the dike dimensions. Despite the fact that several overtopping reduction measures are researched, the combination of those influence factors is still not fully understood (Van Gent, 2019). Moreover, the effect of wind on the overtopping discharge is not included in existing guidelines, whereas wind is complex due to its dynamic behaviour. Also, the knowledge niche regarding the position and height of the vertical crest wall is the reason for performing more research. Physical model tests are conducted to gain more knowledge about the maximum wind effect to obtain a better understanding of how it affects the overtopping discharge and the loading on seadikes.

The following research question is covered in this master thesis: *What is the maximum wind effect on wave overtopping at dikes with crest elements?* The aim of the present research is to examine this wind effect based on physical model tests, which are performed at Deltares in Delft, the Netherlands. Experiments on a small-scale model of a seadike with a smooth outer slope at an angle of $\tan(\alpha) = 1:3$ are conducted using a significant wave height between 0.1 and 0.2 m with a wave steepness between 0.02 and 0.04. In total, four dike configurations were tested, consisting of a crest wall (0.05 and 0.08 m), which is placed at the seaside of the dike crest in one case and on the land side in another. In the latter case, the promenade between the crest wall and the seaward edge of the crest is 0.15 m. Additionally, some experiments were conducted with varying water levels in order to quantify the importance of water level differences on the maximum wind effect. A paddle wheel is used to simulate the maximum effect of wind, based on the idea that all vertical spray exceeding the dike crest is transported over the crest by onshore wind. The maximum wind effect is determined by comparing the tests with and without the use of the paddle wheel.

The results of this investigation show that existing guidelines, such as TAW (2002), should be optimised to fit the measured overtopping discharges for the situation without wind. For non-breaking waves, the wave steepness is not included in the TAW (2002) overtopping formula, but the data show a clear dependency on this parameter. Regarding breaking waves, one of the numerical coefficients used in the overtopping equation is optimised. When a crest wall or crest wall with promenade is added to the dike, it depends on the type of waves (breaking or non-breaking) and dike configuration whether the coefficients in the expressions should be adapted to account for the crest elements. However, it has to be mentioned that the proposed formulas should be validated against larger databases before they are being adopted.

One of the most significant findings from this study is a quantification of the maximum wind effect (Equation 28). It provides an amplification factor (γ_{wind}) on the overtopping discharge. This maximum wind effect is defined as the ratio q_{wind}/q , which indicates the overtopping discharge with maximum wind effect due to onshore blowing winds (q_{wind}) over the overtopping discharges without wind effects (q). For the data obtained during this research, the maximum wind effect ranged from 1.0 to 4.0, where a γ_{wind} of 1.0 indicates no increase in overtopping discharge due to wind. Although the different dike configurations can each be assigned to a calibrated version of Equation 28, this equation is a reasonably good estimation and could also be applied as a first estimate to configurations that are not tested in this research.

$$\gamma_{wind} = 0.011 q^{*-0.43} + 1$$

Equation 28

Table of contents

Preface	iii
Abstract	v
List of symbols	ix
List of figures	xi
List of tables	xv
I State of the art	1
1 Problem analysis	3
1.1 Introduction.....	3
1.2 Problem statement	4
1.3 Objective	5
1.4 Methodology.....	5
1.5 Outline of the thesis.....	6
2 Literature study	9
2.1 Wave overtopping as failure mechanism.....	9
2.2 Overtopping discharge	10
2.3 Influence factors determining wave overtopping	12
2.3.1 Berm	12
2.3.2 Roughness.....	13
2.3.3 Oblique waves	14
2.3.4 Promenade and vertical wall.....	15
2.4 The influence of wind.....	16
2.5 Summary	18
II Analysing physical model tests	19
3 Physical model tests	21
3.1 Model set-up.....	21
3.2 Measurement programme	23
3.3 Froude scaling	24
4 Data analysis	25
4.1 Comparing reference tests with existing guidelines.....	25
4.2 Wave characteristics and dike configuration influencing the overtopping discharge	28

4.3	Comparing crest element tests with existing guidelines	31
4.3.1	Influence factors of crest elements for non-breaking waves	33
4.3.2	Influence factors of crest elements for breaking waves	37
4.4	Maximum wind effect.....	40
4.4.1	The impact of wave characteristics and dike configurations	40
4.4.2	The impact of water level variations.....	45
4.4.3	Creating a wind influence factor.....	47
III	Wrap-up	51
5	Discussion	53
5.1	Physical model tests.....	53
5.2	Applicability and limitations of the research.....	54
6	Conclusions and recommendations.....	57
6.1	Conclusions.....	57
6.1.1	How do wave characteristics, such as the significant wave height and wave steepness, influence wave overtopping at dikes with and without crest elements?	58
6.1.2	What is the influence of the height of crest elements on the overtopping discharge?.....	59
6.1.3	What is the influence of the position of crest elements on the overtopping discharge?.....	59
6.1.4	How do wave characteristics, such as the significant wave height and wave steepness, influence the maximum wind effect on wave overtopping at dikes with crest elements?	60
6.1.5	What is the influence of the height of crest elements on the maximum wind effect on wave overtopping at dikes with crest elements?	60
6.1.6	What is the influence of the position of crest elements on the maximum wind effect on wave overtopping at dikes with crest elements?	60
6.2	Recommendations.....	60
	References	63
IV	Appendices.....	65
A	Technical drawing model set-up.....	67
B	Pictures from the test facility	71
C	Measurement programme.....	77
D	Overtopping discharges with wind.....	79

List of symbols

Symbol	Unit	Description
α	$^{\circ}$	Averaged angle of the waterside slope
β	$^{\circ}$	Angle of wave attack
γ_{β}	-	Influence factor for oblique wave attack
γ_b	-	Berm influence factor
γ_f	-	Roughness influence factor
γ_{prom}	-	Influence factor for a promenade
$\gamma_{prom,v}$	-	Influence factor for a promenade combined with a vertical crest wall
γ_v	-	Influence factor for a vertical wall
γ_{wind}	-	Wind influence/amplification factor
γ^*	-	Influence factor for crest elements
ξ_0	-	Breaker/Iribarren parameter based on H_{m0} and $T_{m-1,0}$
a	-	Empirical coefficient
b	-	Empirical coefficient
B	m	Promenade width
b_0	-	Empirical coefficient
B_{berm}	m	Berm width
c_0	-	Empirical coefficient for the roughness influence factor
$c_{h2\%}$	-	Empirical coefficient
$c_{v2\%}$	-	Empirical coefficient
d	m	Water depth at the toe of the seadike
d_h	m	Water depth at the centre of the berm
g	m/s^2	Gravitational acceleration
$h_{2\%}$	m	Layer thickness at the seaward edge of the dike crest
H_{m0}	m	Significant wave height based on the wave energy spectrum
h_{wall}	m	Height of the crest wall
L_{berm}	m	Berm length
$L_{m-1,0}$	m	Wave length based on $T_{m-1,0}$
q	$m^3/s/m$	Averaged overtopping discharge per metre crest width
q_{wind}	$m^3/s/m$	Averaged overtopping discharge per metre crest width for tests with wind
q^*	-	Dimensionless overtopping discharge based on H_{m0}
q^*_{wind}	-	Dimensionless overtopping discharge based on H_{m0} with wind
R_c	m	Crest freeboard; distance between the crest height and the still water level
$R_{u2\%}$	m	Wave run-up height, exceeded by 2% of the incident waves
s_0	-	Wave steepness based on H_{m0} and $T_{m-1,0}$
$T_{m-1,0}$	s	Spectral wave period based on the ratio of the spectral moments m_{-1} and m_0 of the incident wave spectrum
$u_{2\%}$	m/s	Extreme flow velocity

List of figures

Figure 1.1: (a) Waves overtopping a jetty (De Lange, 2022); (b) A map of the Netherlands, which indicates the highest measured wind speeds in km/h during storm Corrie (Klaassen, 2022).....	4
Figure 1.2: Overview of the model set-up with paddle wheel above the seadike with crest wall and promenade.....	6
Figure 2.1: Failure mechanisms of dikes (Bakkenist et al., 2012).....	9
Figure 2.2: Wave overtopping at a dike (TAW, 2002).....	10
Figure 2.3: Definition of parameters in the berm influence factor γb (TAW, 2002). ..	13
Figure 2.4: Obliquely incident waves under angle β (EurOtop, 2018). ..	14
Figure 3.1: Schematic overview of the model set-up with paddle wheel above the seadike with crest wall and promenade.	22
Figure 3.2: Vertical splashing of water when waves hit the crest wall on the dike with crest wall only.	22
Figure 3.3: Vertical splashing of water when waves hit the crest wall on the dike with crest wall and promenade.....	23
Figure 3.4: Schematic close-up with tested crest wall heights and positions; (a) Crest wall at seaside; (b) Crest wall at land side, thus introducing a promenade.	23
Figure 4.1: Measured overtopping discharges for reference tests, with a distinction between breaking and non-breaking waves, but also between different wave steepnesses.	26
Figure 4.2: Measured overtopping discharges for reference tests compared with TAW (2002) and EurOtop (2018); (a) Non-breaking waves; (b) Breaking waves.	27
Figure 4.3: Measured overtopping discharges for the reference tests for non-breaking waves compared with the proposed expression in Equation 23.	27
Figure 4.4: Measured overtopping discharges; (a) Measurements in absence of wind; (b) Measurements in presence of wind.....	29
Figure 4.5: Measured overtopping discharges sorted on wave steepness; (a) Measurements with wave steepness of 0.02; (b) Measurements with wave steepness of 0.03; (c) Measurements with wave steepness of 0.04.....	30
Figure 4.6: Measured overtopping discharges sorted on dike configuration; (a) Measurements with crest wall of 5 cm; (b) Measurements with crest wall of 8 cm; (c) Measurements with crest wall of 5 cm and promenade; (d) Measurements with crest wall of 8 cm and promenade.....	30
Figure 4.7: Measured overtopping discharge versus breaker parameter; (a) Measurements for non-breaking waves; (b) Measurements for breaking waves.....	31

Figure 4.8: Measured overtopping discharges without wind compared with the TAW (2002) and Van Doorslaer et al. (2015) formulas.....	32
Figure 4.9: Comparison of measured overtopping discharges with calculated overtopping discharges for breaking and non-breaking waves (TAW, 2002); (Van Doorslaer et al., 2015).	33
Figure 4.10: Comparison of the hypothetical influence factors for a crest wall, which are needed to connect the measurements with the TAW (2002) formula, with the proposed formula by Van Doorslaer et al. (2015) for non-breaking waves.....	33
Figure 4.11: Measured overtopping discharges and the effect of adding the influence factor for a crest wall for non-breaking waves; (a) Without taking the reduction factor into account; (b) Taking the reduction factor into account.	34
Figure 4.12: Measured overtopping discharges and the effect of adding the influence factor for a crest wall for non-breaking waves compared with the proposed expression in Equation 23, but with $s_0 = 1.95$ and γ	34
Figure 4.13: Comparison of the influence factors for a crest wall with promenade related to the measurements with the proposed formula by Van Doorslaer et al. (2015) for non-breaking waves.	35
Figure 4.14: Measured overtopping discharges and the effect of adding the influence factor for a crest wall with promenade for non-breaking waves; (a) Without taking the reduction factor into account; (b) Taking the reduction factor into account.....	36
Figure 4.15: Measured overtopping discharges and the effect of adding the influence factor for a crest wall with promenade for non-breaking waves compared with the proposed expression in Equation 23, but with $s_0 = 2.07$ and γ	36
Figure 4.16: Comparison of the influence factor for a crest wall related to the measurements with the proposed formula by Van Doorslaer et al. (2015) for breaking waves.	37
Figure 4.17: Measured overtopping discharges and the effect of adding the influence factor for a crest wall for breaking waves; (a) Without taking the reduction factor into account; (b) Taking the reduction factor into account.	38
Figure 4.18: Comparison of the influence factor for a crest wall with promenade related to the measurements with the proposed formula by Van Doorslaer et al. (2015) for breaking waves.	38
Figure 4.19: Measured overtopping discharges and the effect of adding the influence factor for a crest wall with promenade for breaking waves; (a) Without taking the reduction factor into account; (b) Taking the reduction factor into account.....	39
Figure 4.20: Measured overtopping discharges and the effect of adding the influence factor for crest elements for breaking waves compared with the proposed expressions in Equation 22 and Equation 26.....	39
Figure 4.21: The influence of the relative crest freeboard on the maximum wind effect.....	41

Figure 4.22: Maximum wind effect sorted on wave steepness; (a) Measurements with wave steepness of 0.02; (b) Measurements with wave steepness of 0.03; (c) Measurements with wave steepness of 0.04.	42
Figure 4.23: Schematic close-up of the dike. When the striped blue triangle above the promenade is filled with water, the wave will overtop the crest element more easily.	42
Figure 4.24: The influence of the crest wall height on the maximum wind effect; (a) Measurements with a crest wall only; (b) Measurements with a crest wall and promenade.	43
Figure 4.25: Maximum wind effect sorted on dike configuration; (a) Measurements with crest wall of 5 cm; (b) Measurements with crest wall of 8 cm; (c) Measurements with crest wall of 5 cm and promenade; (d) Measurements with crest wall of 8 cm and promenade.	44
Figure 4.26: The influence of the breaker parameter on the maximum wind effect. .	45
Figure 4.27: Measured overtopping discharges for different tests with variations in water level; (a) Measurements in absence of wind; (b) Measurements in presence of wind.	45
Figure 4.28: Measured overtopping discharges without wind for varied water levels compared with Equation 23.	46
Figure 4.29: Maximum wind effect for different tests with variations in water level. ...	47
Figure 4.30: The influence of the overtopping discharge on the maximum wind effect; (a) Maximum wind effect on linear scale; (b) Maximum wind effect on logarithmic scale.	48
Figure 4.31: The influence of the overtopping discharge on the maximum wind effect and fitted curves (Equation 27); (a) Maximum wind effect on linear scale; (b) Maximum wind effect on logarithmic scale.	48
Figure 4.32: The influence of the overtopping discharge on the maximum wind effect and fitted curve (Equation 28) with the 90% confidence interval based on the relative error; (a) Maximum wind effect on linear scale; (b) Maximum wind effect on logarithmic scale.	49
Figure 4.33: Measured overtopping discharges of all tests compared with the proposed equations in Table 4.9.	50
Figure A.1: Front view of the model set-up, which contains the dimensions of the paddle wheel (blue) and the seadike (green) with and without the two crest walls (W. Stet, personal communication, March, 2022).	67
Figure A.2: Side view of the model set-up, which contains dimensions of the promenade, the concrete walls on both sides of the dike and the dike length (W. Stet, personal communication, March, 2022).	68
Figure A.3: Top view of the model set-up, which contains the dimensions of the dike width, the width of the paddle wheel and the two different overtopping chutes (W. Stet, personal communication, March, 2022).	69
Figure B.1: Side view; dike configuration with a crest wall and promenade with paddle wheel.	71

Figure B.2: Front view; dike configuration with a crest wall and promenade with paddle wheel.	72
Figure B.3: Side view; dike configuration with a crest wall with paddle wheel.	72
Figure B.4: Side view; dike configuration with a crest wall with paddle wheel.	73
Figure B.5: General overview of the basin with the machines of the wave generator in green; dike configuration with a crest wall.	73
Figure B.6: Front view with the three wave gauges measuring the wave height and period in front of the dike; dike configuration with a crest wall.	74
Figure B.7: Side view; dike configuration with a crest wall.....	74
Figure B.8: General overview of the basin from behind the dike; at the top, the wave generator is visible; at the bottom, the overtopping box behind the dike is visible.	75
Figure D.1: Measured overtopping discharges with wind sorted on wave steepness; (a) Measurements with wave steepness of 0.02; (b) Measurements with wave steepness of 0.03; (c) Measurements with wave steepness of 0.04.....	79
Figure D.2: Measured overtopping discharges with wind sorted on dike configuration; (a) Measurements with crest wall of 5 cm; (b) Measurements with crest wall of 8 cm; (c) Measurements with crest wall of 5 cm and promenade; (d) Measurements with crest wall of 8 cm and promenade.	80
Figure D.3: Measured overtopping discharge with wind versus breaker parameter; (a) Measurements for non-breaking waves; (b) Measurements for breaking waves.	80

List of tables

Table 3.1: Parameter ranges of the test programme.	24
Table 4.1: RMSLE for overtopping discharges of reference tests described by TAW (2002) and the newly proposed Equation 23 (non-breaking waves) or Equation 22 (breaking waves).	28
Table 4.2: RMSLE for overtopping discharges of crest element tests described by TAW (2002) and Van Doorslaer et al. (2015).	32
Table 4.3: RMSLE for overtopping discharges of non-breaking crest wall tests described by TAW (2002) and the newly proposed Equation 23.	35
Table 4.4: RMSLE for overtopping discharges of crest wall with promenade tests for non-breaking described by TAW (2002) and the newly proposed Equation 23.	37
Table 4.5: RMSLE for overtopping discharges of crest element tests for breaking waves described by TAW (2002) and the expressions with the fitted exponents (Equation 22 and Equation 26).	39
Table 4.6: Ranges of the maximum wind effect for different wave characteristics per dike configuration.	41
Table 4.7: RMSLE for overtopping discharges of tests with water level variations described by TAW (2002) and the newly proposed Equation 23 (non-breaking waves).	46
Table 4.8: RMSE for the amplification factor γ_{wind} described by the newly proposed Equation 27 and Equation 28.	50
Table 4.9: RMSLE for overtopping discharges of all tests described by the newly proposed formulas in this thesis.	50
Table 5.1: One test series repeated to measure the deviations in overtopping discharge.	54
Table 6.1: Parameter ranges of the test programme used in the analysis and the results.	58
Table C.1: Wave characteristics for each test series as defined in chapter 2.	77
Table C.2: Expected dimensionless overtopping discharges for tests without wind based on equations from TAW (2002) and Van Doorslaer et al. (2015).	78
Table C.3: Wave characteristics and expected dimensionless overtopping discharges for tests with different water levels.	78

I

State of the art

1

Problem analysis

Chapter 1 contains the problem analysis. A short introduction to wave overtopping, the problem statement and research questions are part of this chapter. Subsequently, the methodology and outline of the thesis finish this chapter.

1.1 Introduction

Wave overtopping is one of the failure mechanisms of dikes, resulting in overtopping discharges damaging the dike revetment at the land side. The result can be disastrous, leading to instability or breaching of the dike. Flooding due to breaching has to be prevented, which has to be taken into account in the design and safety assessment of dikes.

Due to climate change, the risk on flooding events increases, leading to a possible breach of safety standards. As a consequence, new seadikes need to be higher and existing dikes may need to be reinforced (Chen et al., 2021). It is assumed that for each metre of sea level rise, the dikes need to be raised 2.5 m. Not only does it take more space, because the seadike will be wider landward, but it also results in higher loading on the subsoil. In order to overcome this problem of raising dikes, several options are available (Van Gent, 2019). The first option is not to adapt the dike itself, but the foreshore. This consists in constructing an offshore breakwater or decreasing the water depth through, for instance, nourishments. These two foreshore measures do not affect the dike, but reduce the wave loading. Adaptation of the dike can be achieved by various options. At the seaside of the dike it is possible to include a berm or increase the roughness by changing the type of armour layer. At the crest of the dike, crest elements such as a wall can diminish the amount of wave overtopping. At the inner side of the dike, the slope can be strengthened in order to allow larger overtopping discharges without the possibility of dike breaching.

Each adaptation measure can be optimised based on the amount of sea level rise. However, making a choice between the measures is difficult due to the large amount of uncertainty on both the impact of measures and the actual sea level rise. Moreover, in order to determine the height of a dike, the overtopping discharge has to be analysed, which consists of several parameters. One of the parameters affecting the overtopping discharge is the effect of wind.

The influence of wind on wave overtopping is most pronounced during storms. Onshore blowing winds induce increasing water levels and, as a result, higher waves that approach the coast. Figure 1.1 (a) displays the effect of waves hitting a jetty during a storm. The vertical water spray could all be blown onshore, which increases the overtopping discharge. A storm in January 2007 was closely monitored near Petten

(the Netherlands) by Rijkswaterstaat. Multiple wave and wind characteristics as well as wave overtopping discharges were measured. These field measurements revealed that wave overtopping occurred when high astronomical tide was combined with strong onshore blowing winds (Marsman et al., 2007). A more recent example of such a storm in the Netherlands is storm Corrie in January 2022, which resulted in wind speeds up to 110 km/h (Figure 1.1 (b)) and wave heights of 5 to 6 m at the Afsluitdijk (Visser, 2022).



Figure 1.1: (a) Waves overtopping a jetty (De Lange, 2022); (b) A map of the Netherlands, which indicates the highest measured wind speeds in km/h during storm Corrie (Klaassen, 2022).

1.2 Problem statement

The overtopping discharge is one of the main issues when determining the height of dikes and wave overtopping. Influencing parameters such as berm, roughness, obliquely incident waves and a vertical wall have already been widely investigated. As a result, these influencing parameters are included in current calculation methods, although Van Gent (2019) stated that the combination of some influence factors is still not fully understood. At the moment, such an influence factor for wind does not exist. Although some experiments were conducted, little is known about the effect of wind on wave overtopping at dikes with crest elements. Wind in itself is a complex phenomenon due to its dynamic behaviour, which adds up to all the different parameters that influence the overtopping discharge. This makes it difficult to construct a general formula including the effect of wind on wave overtopping. Additionally, scaling effects of water-air interaction are important.

Adding to that, several configurations of a vertical wall on a dike are possible. For vertical walls with a toe above the still water level, limited data and knowledge are available (EurOtop, 2018). Therefore, it is necessary to do more research and perform laboratory tests in order to reduce these knowledge gaps.

1.3 Objective

The objective of the research is to gather more information about a possible relationship between the maximum wind effect and wave overtopping at dikes. Furthermore, the crest elements may influence the wave overtopping and wind effect. To achieve this objective, the following research question is covered in this master thesis.

What is the maximum wind effect on wave overtopping at dikes with crest elements?

The basis for answering the research question is created by two groups of sub-questions. The first group of sub-questions is focussed on the relation between the data from the present research and comparison with previous research.

- 1. How do wave characteristics, such as the significant wave height and wave steepness, influence wave overtopping at dikes with and without crest elements?*
- 2. What is the influence of the height of crest elements on the overtopping discharge?*
- 3. What is the influence of the position of crest elements on the overtopping discharge?*

The second group of sub-questions is concentrated on the maximum wind effect.

- 4. How do wave characteristics, such as the significant wave height and wave steepness, influence the maximum wind effect on wave overtopping at dikes with crest elements?*
- 5. What is the influence of the height of crest elements on the maximum wind effect on wave overtopping at dikes with crest elements?*
- 6. What is the influence of the position of crest elements on the maximum wind effect on wave overtopping at dikes with crest elements?*

1.4 Methodology

In order to answer the research question, experiments form the basis of a possible solution. The Pacific Basin at Deltares in Delft, the Netherlands, was used to investigate the maximum wind effect for different wave characteristics based on physical model tests. This maximum wind effect was schematised by using a paddle wheel that mechanically collected the splashing water when waves attacked the dike.

Furthermore, the crest element was modified so the influence of reducing wave overtopping measures could be quantified. For instance, a vertical wall of which the height could be changed, was installed. In addition, the location of this wall could also be altered by adding a promenade seaward of the crest wall. The literature study preceding the analysis of the results gives an overview of the current state of knowledge and knowledge gaps. The gathered data are compared with the literature to answer the research question.

To get an impression of the model set-up related to this topic, Figure 1.2 is added. The paddle wheel simulating the maximum wind effect (rotating anti-clockwise in Figure 1.2), was positioned just above the crest wall on the dike and transported the overtopping discharge via the chute to an overtopping box, where the overtopping water volume was measured. For more detailed information about the model set-up and measurement programme, the reader is referred to section 3.1.

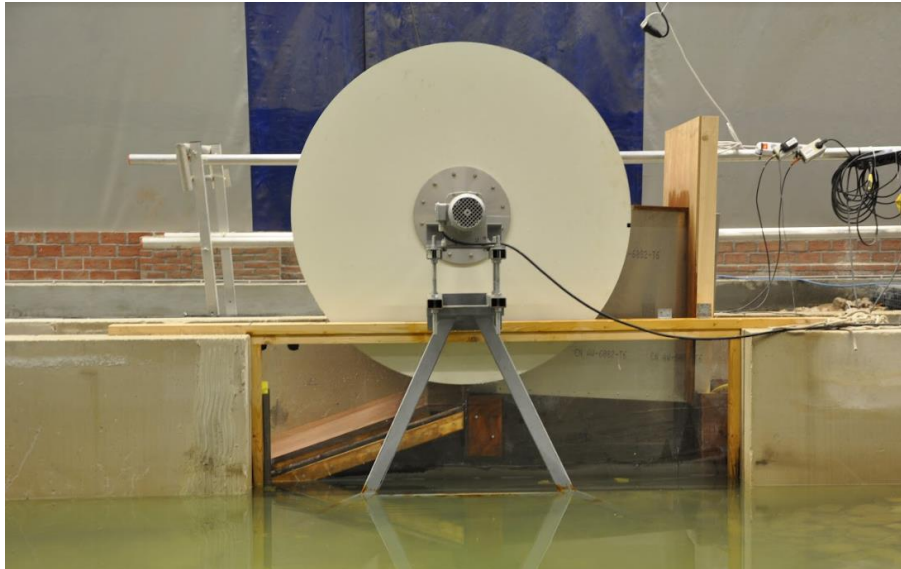


Figure 1.2: Overview of the model set-up with paddle wheel above the seadike with crest wall and promenade.

1.5 Outline of the thesis

This thesis is divided into three main parts, which describe the different elements of the research, and the appendices.

State of the art

The composition of the thesis starts with the introduction in chapter one. The research question, problem statement and methodology give the reader an impression of the focus of this research. Chapter two contains a literature study, where the concept ‘wave overtopping’ is clarified. Additionally, several parameters influencing wave overtopping and the current knowledge and knowledge gaps about the wind effect are presented.

Analysing physical model tests

The second part focusses on the physical model tests. Chapter three illustrates the methodology regarding the experiments. The set-up, the boundary conditions and possible variations are explained. Next, the data analysis follows in chapter four. This data analysis consists of verifying the connection between different parameters by means of interpreting and analysing the data.

Wrap-up

The third and last part before the appendices concludes the thesis. The discussion is the topic of chapter five. Chapter six contains the conclusions of the research with

respect to the research question and is completed with recommendations for further research.

Appendices

The appendices contain more detailed information about the model set-up of the physical model tests, the measurement programme and the experiments conducted with wind.

2

Literature study

In this chapter a literature study is presented to obtain knowledge and acquire an understanding of wave overtopping and parameters influencing wave overtopping. Several coastal structure configurations are analysed, including the outer slope of a dike, a berm and a vertical wall as crest modification. In addition, existing knowledge about the wind effect on wave overtopping is discussed.

2.1 Wave overtopping as failure mechanism

Climate change has an impact on a very wide range of engineering subjects. Sea level rise initiated by global warming will become more critical in the Netherlands over the coming decades. Some other countries also face the effect of land subsidence. Both effects require an evaluation on the risk of flooding events and associated safety standards of coastal structures. One group of coastal structures affected by sea level rise is seadikes. When focussing on the safety standards of dikes, several failure mechanisms have to be considered as displayed in Figure 2.1. In this thesis, the focus is on wave overtopping, and the other failure mechanisms are not evaluated.

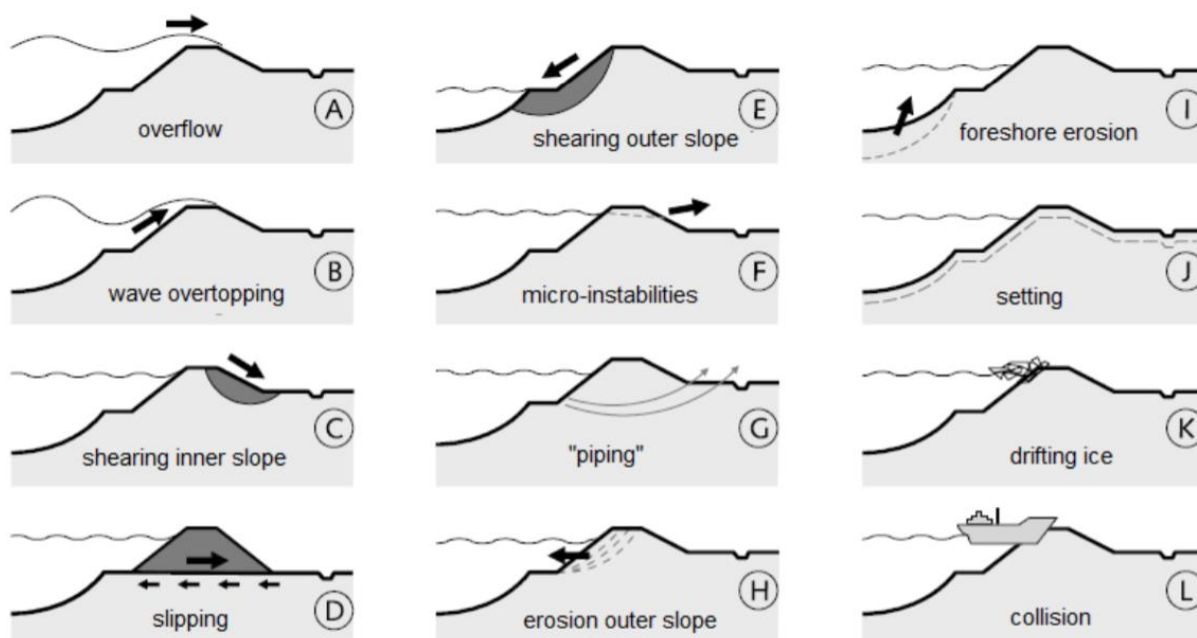


Figure 2.1: Failure mechanisms of dikes (Bakkenist et al., 2012).

Not only wave overtopping in itself can be dangerous in the sense that it may lead to damage of structures and salt intrusion. The resulting forces on the land side of the dike must not be underestimated.

The overtopping discharge may damage and erode the land side slope, which, in the end, has the ability to result in breaching of the dike. In order to prevent this complete dike failure, research was performed, and guidelines prescribed. Some influential parameters are described in the following sections.

Wave overtopping at dikes occurs when the wave run-up level is higher than the crest level of a dike. The principle is illustrated in Figure 2.2. R_c is the free crest height, which is defined as the outer crest level relative to the still water level (SWL).

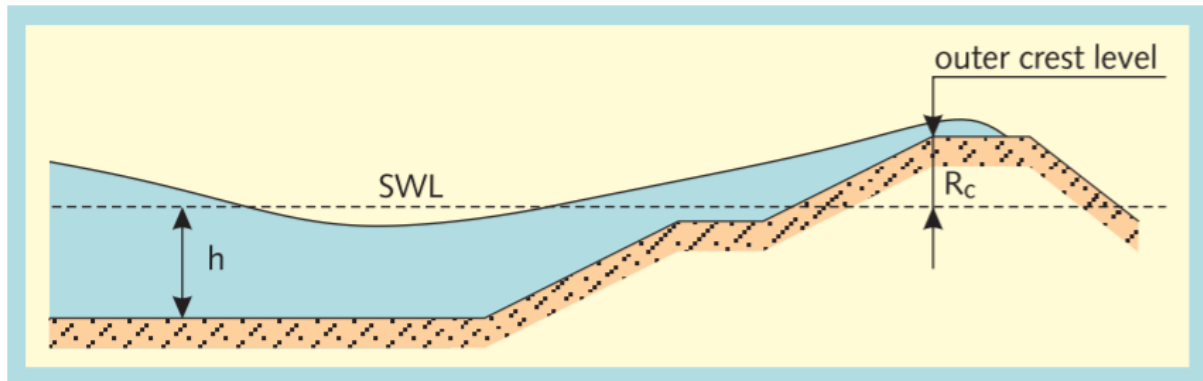


Figure 2.2: Wave overtopping at a dike (TAW, 2002).

2.2 Overtopping discharge

In order to quantify wave overtopping, the overtopping discharge is normally used. The average overtopping discharge, q , is expressed in $\text{m}^3/\text{s}/\text{m}$ or $\text{l}/\text{s}/\text{m}$. To prevent massive erosion at the inner slope of a dike, the following upper limits of overtopping discharges are prescribed (TAW, 2002):

- 0.1 $\text{l}/\text{s}/\text{m}$ for sandy soil with a poor grass cover;
- 1.0 $\text{l}/\text{s}/\text{m}$ for clayey soil with a reasonably good grass cover;
- 10 $\text{l}/\text{s}/\text{m}$ for a clay covering and a grass cover according to the requirements for the outer slope or for an armoured inner slope.

Many overtopping formulas are empirical formulas, which are validated using physical experiments or numerical modelling (Chen et al., 2021). Two important equations are given in the EurOtop manual (EurOtop, 2018) and the TAW report (TAW, 2002).

The overtopping discharge from Equation 1 and Equation 2 originate from the EurOtop manual (EurOtop, 2018) and can be used for predictions about and comparisons with measurements.

$$\frac{q}{\sqrt{g H_{m0}^3}} = \frac{0.023}{\sqrt{\tan(\alpha)}} \gamma_b \cdot \xi_{m-1,0} \cdot \exp\left(-\left(2.7 \frac{R_c}{H_{m0}} \frac{1}{\xi_{m-1,0} \cdot \gamma_b \cdot \gamma_f \cdot \gamma_\beta \cdot \gamma_v}\right)^{1.3}\right) \quad \text{Equation 1}$$

with a maximum of:

$$\frac{q}{\sqrt{g H_{m0}^3}} = 0.09 \cdot \exp\left(-\left(1.5 \frac{R_c}{H_{m0}} \frac{1}{\gamma_f \cdot \gamma_\beta \cdot \gamma_v}\right)^{1.3}\right) \quad \text{Equation 2}$$

The overtopping discharge from Equation 3 and Equation 4 originate from the TAW report (TAW, 2002).

$$\frac{q}{\sqrt{g} H_{m0}^3} = \frac{0.067}{\sqrt{\tan(\alpha)}} \gamma_b \cdot \xi_0 \cdot \exp\left(-4.3 \frac{R_c}{H_{m0}} \frac{1}{\xi_0 \cdot \gamma_b \cdot \gamma_f \cdot \gamma_\beta \cdot \gamma_v}\right) \quad \text{Equation 3}$$

with a maximum of:

$$\frac{q}{\sqrt{g} H_{m0}^3} = 0.2 \cdot \exp\left(-2.3 \frac{R_c}{H_{m0}} \frac{1}{\gamma_f \cdot \gamma_\beta}\right) \quad \text{Equation 4}$$

where q [m³/s/m] is the average wave overtopping discharge, g [m²/s] is the gravitational acceleration, H_{m0} [m] is the significant wave height at the toe of the dike, ξ_0 [-] is the breaker parameter (or Iribarren parameter), $\tan(\alpha)$ [-] is the average slope, R_c [m] is the free crest height above the still water level, and γ [-] is an influence factor for a berm, roughness elements, obliquely incident waves and a vertical wall. There is a maximum on the amount of overtopping discharge because non-breaking waves are assumed to be independent of the breaker parameter.

In Equation 1 and Equation 3, the breaker parameters are the same and defined as:

$$\xi_{m-1,0} = \xi_0 = \frac{\tan(\alpha)}{\sqrt{s_0}} \quad \text{Equation 5}$$

with:

$$s_0 = \frac{2 \cdot \pi \cdot H_{m0}}{g \cdot T_{m-1,0}^2} \quad \text{Equation 6}$$

s_0 [-] is the wave steepness and $T_{m-1,0}$ [s] is the spectral wave period at the toe of the dike.

Since in recent research (Den Bieman et al., 2020) the equations from TAW (2002) have shown to be more accurate than EurOtop (2018) for several datasets, the TAW (2002) equations are used for further analysis and as reference. Besides, there is some debate about the power coefficient of 1.3 that is used in the EurOtop formulas for the overtopping discharge (Equation 1 and Equation 2) (Chen et al., 2019). From the overtopping discharge formulas, it can be concluded that the overtopping discharge is dependent on influence factors (γ) and wave characteristics. The influence factors are discussed in section 2.3.

Two wave characteristic parameters that affect the overtopping discharge are the spectral wave period and significant wave height. The wave period is included in the overtopping discharge for breaking waves. For larger wave periods, the overtopping discharge shows an increase. The maximum discharge given is independent of the wave period according to current guidelines. Regarding the significant wave height, a similar relation exists as for the wave period. Increasing the wave height will increase the overtopping discharge as well.

The seaward slope of a dike is not accounted for in an influence factor, but is of importance for the overtopping discharge in Equation 1 and Equation 3, both directly and via the breaker parameter. However, the influence of the seaward slope on wave overtopping is not included in the maximum overtopping discharge in Equation 2 and Equation 4. Although a steeper slope results in more wave reflection, which means that more energy is reflected, and that the layer thickness of the overtopping bore is smaller, the effect is not significantly observed in experiments by Van Doorslaer et al. (2015).

According to Chen et al. (2021), failure of dikes is mainly caused by overtopping events. Extreme wave overtopping events can lead to much higher overtopping discharges, higher velocities and a thicker overtopping water layer. Because of this, these extreme conditions may be more governing regarding dike failure than the mean quantities (Van Gent, 2002). Average overtopping discharges are therefore less relevant as they do not account for extreme events. However, the average discharge is still one of the main parameters for determining the crest height of the dike. For overtopping events, parameters like overtopping flow velocity and layer thickness are certainly important. Breaching of a dike due to overtopping events is largely determined by the velocity of the overtopping waves at the crest. If the velocity is larger than the critical value, it will lead to erosion at the land side, which may result in breaching of the dike (Van Gent, 2020).

The equations for the extreme flow velocity and the extreme layer thickness at the seaward edge of the dike crest are empirical and can be formulated as follows (Chen et al., 2021).

$$u_{2\%} = c_{v2\%} \left(\sqrt{\frac{g(R_{u2\%} - R_c)}{\gamma_f^a}} \right)^b \quad \text{Equation 7}$$

$$h_{2\%} = c_{h2\%} \left(\frac{R_{u2\%} - R_c}{\gamma_f^a} \right)^b \quad \text{Equation 8}$$

Although these overtopping events may be more governing for dike breaching, further study focusses on the average wave overtopping discharge with corresponding parameters.

2.3 Influence factors determining wave overtopping

The exponential part of the overtopping discharge formula contains the influence factors (γ). Therefore, relatively small changes in these γ values may lead to large deviations in the calculated overtopping discharges. Several dike configurations have the ability to reduce wave overtopping. These configurations expressed as influence factors are explained here. If a certain influence is not present, its value is equal to 1.0.

2.3.1 Berm

Adding a berm at the seaward side of the dike certainly has an influence on the amount of wave overtopping. Introducing a berm reduces wave overtopping (Van Gent, 2020). The reason for this is that a berm decreases the average slope angle and therefore

decreases the amount of wave overtopping. Chen et al. (2021) compared numerical experiments with the formulas given in the EurOtop manual (EurOtop, 2018). The EurOtop manual explicitly included an influence factor γ_b in calculating the wave run-up. In contrast, EurOtop (2018) overestimates the run-up heights, but underestimates the berm influence factor with respect to experiments by Chen et al. (2021). Overall, the use of EurOtop (2018) results in too much reduction of a berm on wave overtopping with respect to the performed experiments by Chen et al. (2021).

The effect of a berm is affected by wave characteristics that are not included in the influence factor described by EurOtop (2018) and TAW (2002). The berm influence decreases as the wave steepness increases. Moreover, a higher permeability of a berm results in less reduction of wave overtopping. However, more research is needed to confirm these statements (Chen et al., 2019).

The existing formula for the berm influence factor updated by Chen et al. (2019) is

$$\gamma_b = 1 - \frac{b_0}{\sqrt{s_0}} \frac{B_{berm}}{L_{berm}} \left(0.5 + 0.5 \cdot \cos \left(\frac{\pi \cdot d_h}{x} \right) \right) \quad \text{with } 0.6 \leq \gamma_b \leq 1 \quad \text{Equation 9}$$

where:

$$\begin{aligned} x &= R_{u2\%} && \text{(berm above still water level)} \\ x &= 2 \cdot H_{m0} && \text{(berm below still water level)} \end{aligned} \quad \text{Equation 10}$$

If the berm is located more than $2 \cdot H_{m0}$ below or more than the run-up height above the still water level, γ_b is equal to 1.0 as the berm is located outside the influence area. The coefficient $b_0 = 0.21$ applies to impermeable slopes.

The definition of the berm parameters in Equation 9 is best explained in Figure 2.3. It is remarkable that the berm width has a significant reductive impact on wave overtopping while the berm level has not (Chen et al., 2021).

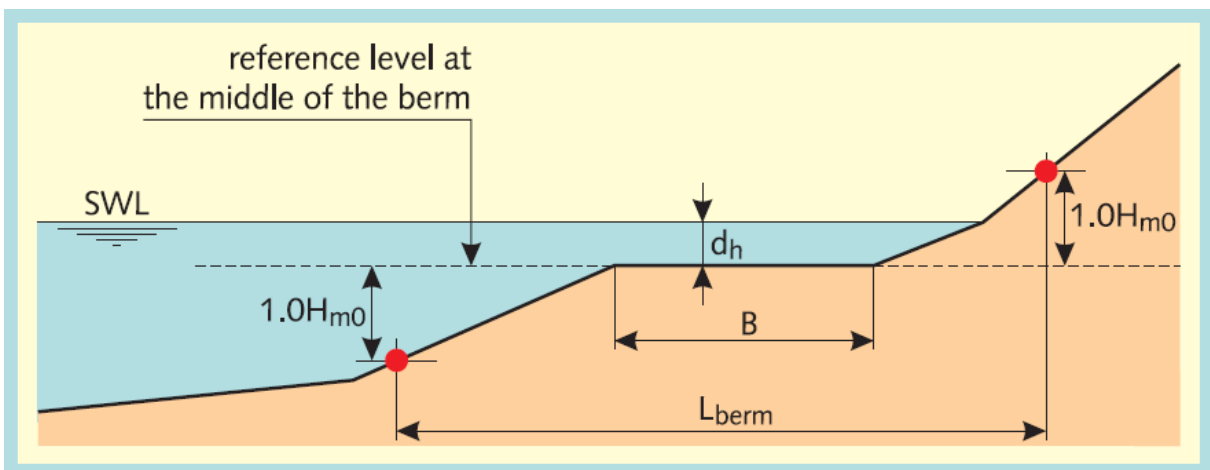


Figure 2.3: Definition of parameters in the berm influence factor γ_b (TAW, 2002).

2.3.2 Roughness

Another parameter influencing the amount of wave overtopping is the roughness of the seaward slope of a dike. The more rough the seaward slope, the less wave overtopping

will occur (Van Gent, 2020). Most dikes in the Netherlands have smooth slopes that are made of grass, conventional placed block revetments or asphalt. In these cases, the influence factor γ_f is equal to 1.0. The reductive effect that roughness has on wave overtopping depends on the configuration, among other factors. In order to increase roughness, it is possible to create a less flat pattern, where blocks have different heights. In these cases of protruding blocks, the block height as well as the spacing between the blocks of equal height are important parameters. Multiple configurations are possible.

Another way to introduce roughness is to increase the porosity of the dike revetment. When a wave runs up the dike, some of the water is absorbed and wave energy is dissipated. Subsequently, the wave run-up decreases hence there is a lower overtopping discharge (EurOtop, 2018).

The influence factor for roughness does not only depend on the type of material, but the crest freeboard, significant wave height and Iribarren parameter play a role as well (Chen et al., 2019). These parameters define the influence factor γ_f , shown in Equation 11, defined by Chen et al. (2019). Calibration coefficient c_0 is defined for several types of block revetments on permeable or impermeable slopes.

$$\gamma_f = 1 - \frac{c_0 R_c}{H_{m0} \xi_0} \quad \text{Equation 11}$$

2.3.3 Oblique waves

Obliquely incident waves have a reducing effect on wave overtopping with respect to normally incident waves. Moreover, the more oblique the waves are, the more wave overtopping is reduced (Van Gent, 2020). Van Gent (2020) expressed this in Equation 12, where β is the angle of wave incidence as displayed in Figure 2.4. In Equation 12, the berm width B_{berm} is included because the influence factor is larger for wider berms.

$$\gamma_\beta = \cos^2(\beta) + 0.35(1 - \cos^2(\beta)) \left(1 + \frac{B_{berm}}{H_{m0}}\right)^{-1} \quad \text{Equation 12}$$

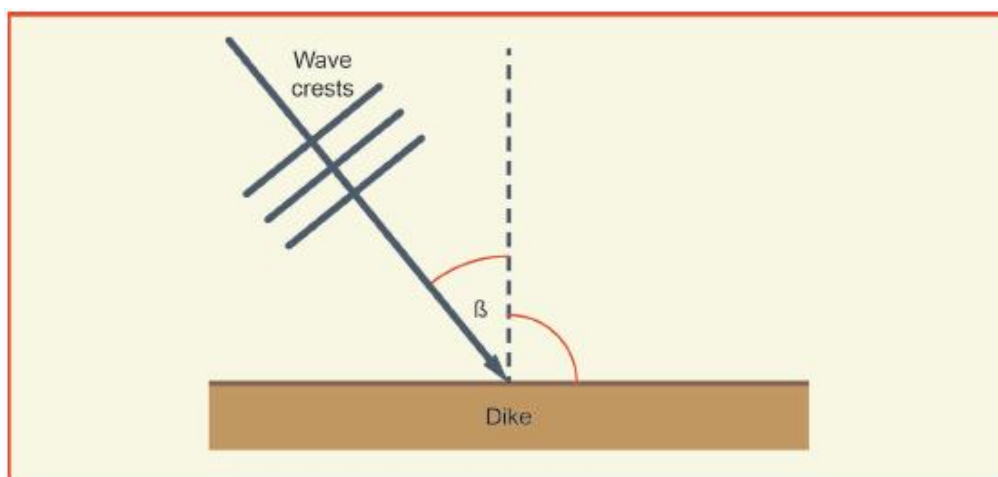


Figure 2.4: Obliquely incident waves under angle β (EurOtop, 2018).

Including both obliquely incident waves and a berm shows a dependency on each other. When the berm width increases, the influence factor of obliquely incident waves decreases. Hence the widening of a berm leads to less wave overtopping due to obliquely incident waves (Chen et al., 2021).

The methods by TAW (2002) and EurOtop (2018) for calculating the overtopping discharge are not fully correct for obliquely incident waves in combination with a berm. For very oblique waves, the existing methods overestimate the overtopping discharge by several orders of magnitude. When waves are normally incident, these methods agree with research performed by Van Gent (2020). It has to be mentioned that this statement holds for research focussed on breaking waves (Van Gent, 2020).

2.3.4 Promenade and vertical wall

Possible measures at the crest of the dike to reduce wave overtopping are a promenade, stilling wave basin and crest wall. The promenade acts as a berm at crest level. Adding a berm around the water level will reduce wave overtopping since the width increases. It has to be mentioned that a vertical wall is much more effective than a promenade solely (Van Doorslaer et al., 2015). The effect of a vertical wall is most pronounced when waves break on the dike slope, causing a jet which may overflow the dike. This jet is retained by a vertical wall.

The stilling wave basin is approximately the same as the promenade, but the difference is that the basin acts as an overspill. Drainage is one of the most important factors in the efficiency of the basin. Rapid drainage improves the quality of the basin. Because waves hit the seaward wall first and water is dropped in the stilling wave basin, most energy is dissipated. As a result, there is less overtopping at the vertical wall at the land side of the basin (Van Doorslaer et al., 2015).

Van Doorslaer et al. (2015) also investigated the combined effect of a promenade and vertical wall. The result is that the combination of both measures is even more effective than a multiplication of the two separate reduction factors. The outcome of the research consists of several influence factors for a vertical wall, a promenade and a combination. The influence of a parapet was also investigated. A parapet is a bull nose on top of the vertical wall used to guide incoming waves away from the dike. Although a parapet appears to be an efficient way to reduce wave overtopping in specific situations, it is not described in detail here.

Equation 3 takes the reduction in overtopping discharge due to a vertical wall into account, but this wall needs to be between $1.2 \cdot H_{m0}$ under and above the still water level. However, for non-breaking waves where $\xi_0 > 2$, approximately, this influence factor is absent (Equation 4). Van Doorslaer et al. (2015) argued that this is not correct, and an influence factor is needed in case a vertical wall is present or promenade is added. These influence factors are included in Equation 4 as follows, where γ^* is γ_v or $\gamma_{prom,v}$:

$$\frac{q}{\sqrt{g} H_{m0}^3} = 0.2 \cdot \exp\left(-2.3 \frac{R_c}{H_{m0}} \frac{1}{\gamma_f \cdot \gamma_\beta \cdot \gamma^*}\right) \quad \text{Equation 13}$$

For the dike configuration with a vertical crest wall, the influence factor is described in Equation 14.

$$\gamma_v = \begin{cases} \exp\left(-0.56 \frac{h_{wall}}{R_c}\right) & \text{if } \frac{h_{wall}}{R_c} < 1.24 \\ 0.5 & \text{if } \frac{h_{wall}}{R_c} \geq 1.24 \end{cases} \quad \text{Equation 14}$$

h_{wall} [m] is the height of the crest wall and R_c [m] is the distance from the still water level to the top of the wall.

To the configuration in which a promenade is present without a vertical wall, the following influence factor should be added:

$$\gamma_{prom} = 1 - 0.47 \cdot \frac{B}{L_{m-1,0}} \quad \text{Equation 15}$$

B [m] is the length of the promenade. $L_{m-1,0}$ [m] is the wave length corresponding to the mean spectral wave period $T_{m-1,0}$ [s] and can be calculated using the dispersion relation (Equation 16) with d [m] being the water depth (Holthuijsen, 2007).

$$L_{m-1,0} = \frac{gT_{m-1,0}^2}{2\pi} \tanh\left(\frac{2\pi d}{L_{m-1,0}}\right) \quad \text{Equation 16}$$

In case the vertical wall is combined with a promenade, the influence factor becomes:

$$\gamma_{prom,v} = 0.87 \cdot \gamma_{prom} \cdot \gamma_v \quad \text{Equation 17}$$

When a crest wall is introduced to reduce wave overtopping, several wave/structure interaction processes may take place. This depends among other factors on wave characteristics, such as the wave steepness, and the location of the vertical wall. If the vertical wall is positioned at the outer side of the dike crest, waves most likely have broken or will break. Waves breaking against the vertical wall may induce high forces and quite some splashing water. Another possibility is that the waves are already broken and have a high level of aeration. These waves also result in splashing water when arriving at the vertical wall (EurOtop, 2018). In the context of the influence of wind, this spraying is interesting as it may exceed the height of the wall hence it may contribute to the overtopping discharge. Section 2.4 elaborates on the influence of wind.

2.4 The influence of wind

Multiple influence factors account for geometrical variations of a dike and for obliquely incident waves. Nevertheless, one important external factor is not accounted for: wind.

As some people say: ‘nothing as changeable as the weather’. Hence the wind continuously changes in speed and direction. This dynamic behaviour of wind may result in different processes for waves attacking a dike. In general, winds blowing offshore reduce wave overtopping. For winds blowing onshore it is plausible that the result is an increase in the amount of wave overtopping. However, there are different

mechanisms that describe the behaviour of waves. On the one hand, onshore blowing winds may push a wave up the dike slope hence increase the wave run-up and overtopping. On the other hand, stirring up the waves on the dike slope may imply an earlier breaking point of waves on the dike slope. This process decreases the amount of wave overtopping (Lorke et al., 2012).

When focussing on onshore blowing winds, the effect of wind can be expressed in several ways. Wind can increase the overtopping discharge by blowing water (spray) that exceeds the crest height over the dike. Second, onshore winds can cause higher wave run-up and change of the breaker parameter. Third, wind can lead to spraying of water at open sea in general. In this study, the main focus is on the first option, where the maximum wind effect on wave overtopping is analysed. The focus is on the water volume that would not overtop the dike in case of no wind (De Waal et al., 1996).

De Waal et al. (1996) stated that, based on their experiments, a higher crest level with respect to the still water level results in a larger difference between the situation with and without wind. A possible explanation is that for higher crest levels, the horizontal velocity of the water rising above the crest is smaller. When a vertical wall as crest element is included, the influence of wind is increasing. The reason is that water is projected vertically upwards, so the horizontal velocity is zero. Winds may blow this volume over the dike (Wolters & Van Gent, 2007).

Another correlation is made between the water depth and the maximum wind effect. If the water level is decreased, more waves will be broken when they approach the dike. Because the spray effect originates from breaking or broken waves hitting the crest element, a shallower water depth is associated with more spraying and hence a larger maximum wind effect on the overtopping discharge (De Waal et al., 1996).

De Waal et al. (1996) concluded that the upper limit of the overtopping discharge with maximum wind effect with respect to the overtopping discharge without wind is approximately three. However, more recent research shows that this value may be exceeded (Wolters & Van Gent, 2007). Wolters and Van Gent (2007) carried out experiments in order to investigate the maximum wind effect on wave overtopping at breakwaters with crest elements. In order to do this, a rotating paddle wheel was used, with which all water exceeding the crest of the dike was determined as extra overtopping discharge due to the maximum wind effect. The research focussed on the low overtopping regime, where $q^* < 2 \cdot 10^{-4}$. The definition of the dimensionless overtopping discharge q^* [-] is given in Equation 18.

$$q^* = \frac{q}{\sqrt{gH_{m0}^3}} \quad \text{Equation 18}$$

Breaking waves on both rough and smooth slopes were investigated (Wolters & Van Gent, 2007). It appeared that for rough slopes there was some splashing water, which was not significant with respect to the wave overtopping volumes. For smooth slopes, breaking waves contain a jet under the wave crest which has a significant impact on the wave overtopping volume. Due to this jet that may reach the crest elements, the influence of wind is larger for smooth slopes than for rough slopes.

In addition, changing the crest freeboard and wave steepness changes the overtopping discharge. The relation between lowering the freeboard and the resulting increasing discharge is exponential and it is this parameter which influence is most notable. Increasing the wave steepness (the wave height with respect to the wave length) results, for smooth slopes only, to a linear increase of the overtopping discharge.

As a result, Wolters and Van Gent (2007) concluded that the maximum influence of wind expressed as the ratio q_{wind}/q could be up to 6.3. This indicates that the overtopping discharge with maximum wind effect (q_{wind}) is more than six times as much as the overtopping discharge without wind effects (q). Additionally, the research concluded that the ratio q_{wind}/q is largest for relatively small overtopping discharges.

It is interesting to see that the method used to measure the wind effect may lead to different conclusions. Wolters and Van Gent (2007) used a rotating paddle wheel, whereas Chowdhury et al. (2020) implemented fans to generate wind. For these two methods, different results were found for the relation between the wave height and the overtopping due to wind. The result was that for higher incoming waves, the jet overshooting the crest of the dike is thick and the effect of wind is small. In contrast, for smaller waves there is more wave overtopping due to wind as the mixing of air becomes easier for less thick jets (Chowdhury et al., 2020). Although the maximum wind effect was determined, the difference shows that still more research is needed in order to fill this knowledge gap.

2.5 Summary

The wave loading at dikes can be quantified using the average overtopping discharge q . The literature study has shown that this overtopping discharge is dependent on multiple parameters. Dike configurations such as including a berm, roughness elements or a vertical wall that may be combined with a promenade are represented as influence factors (γ) and reduce the overtopping discharge.

Nevertheless, wind is not included in the equations for overtopping discharge. Research has shown that the maximum wind effect may be significant, but more research is needed in order to confirm and quantify this statement. Moreover, when crest elements are implemented, the maximum wind effect may even become a more dominant parameter.

In order to extend the understanding of the principles behind wave overtopping at dikes, physical model tests were performed, and the results are analysed in the following chapters. It was assumed that the overtopping discharge would be up to three to six times as large as the situation without wind. Also, the crest element and promenade would most likely decrease the overtopping discharge but increase the difference between the situation with and without wind. In conclusion, the physical model tests and data analysis focus on the maximum wind effect in combination with the impact of crest elements in order to answer the research question.

II

Analysing physical model tests

3

Physical model tests

The main part of the research involved performing and analysing physical model tests. Chapter 3 describes the set-up of these physical model tests, which were conducted using facilities at Deltares, and the measurement programme.

3.1 Model set-up

Physical model tests were performed in the Pacific Basin at Deltares in Delft, the Netherlands, with dimensions of 28 by 14 square metres with a depth of 1.25 m (Deltares, n.d.). A one-metre wide cross-section of an impermeable dike was physically modelled in the basin with a smooth outer slope at an angle of $\tan(\alpha) = 1:3$. In order to measure the overtopping discharge, a chute was used to transport the discharge to a box. Within this box, a wave gauge was installed to measure the hydrostatic pressure and to convert this to overtopping discharge. This is the discharge q in $\text{m}^3/\text{s}/\text{m}$ as defined in section 2.2 and 2.3.4. For an impression on how the overtopping box fitted in the structure, see Figure 3.1, or for a picture of the overtopping box, see Figure B.8.

Experiments were conducted for several combinations of significant wave height H_{m0} and wave period $T_{m-1,0}$, which together define the wave steepness s_0 , as introduced in Equation 6. During the tests, a JONSWAP spectrum with peak enhancement factor of 3.3 was generated. In order to reproduce realistic wave characteristics, the wave steepness was defined to be between 0.015 and 0.04, which is a combination of swell and wind waves. The two wave characteristics (H_{m0} and $T_{m-1,0}$) were measured using three wave gauges in front of the dike in order to verify the settings of the wave generator.

Figure 3.1 displays a schematic view of the set-up, where the water depth d was 0.7 m. Changes were made to both the wave characteristics and the vertical wall, which is the crest element. In total, four configurations were investigated. The crest element had two different heights (0.05 and 0.08 m), which are included in the crest freeboard R_c as shown in Figure 3.1. A technical drawing of the model set-up is demonstrated in Appendix A. The two crest element heights lead to crest freeboards of 0.35 and 0.38 m, respectively. Additionally, the crest element was located at the water side of the dike crest as well as at the land side. In the latter situation, a combination of a vertical wall with promenade was created with a width of 0.15 m (B in Figure 3.1). As a result of this set-up, it was verified that an extra reduction factor is needed if a promenade in combination with a vertical crest wall is present (Van Doorslaer et al., 2015).

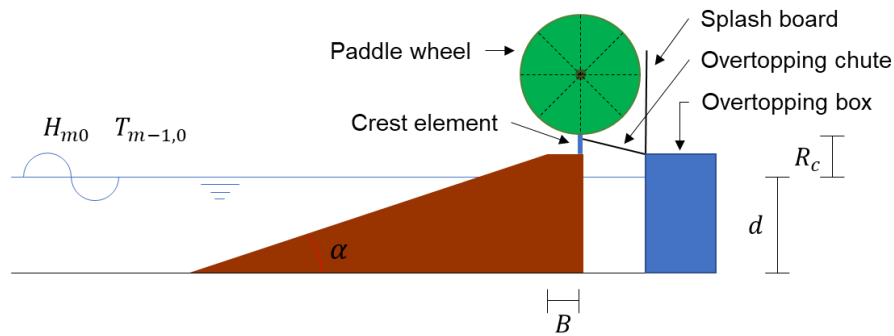


Figure 3.1: Schematic overview of the model set-up with paddle wheel above the seadike with crest wall and promenade.

All tests were performed with and without wind, where wind is schematised using a paddle wheel. This paddle wheel (rotating anti-clockwise in Figure 3.1) mechanically transported all water exceeding the crest level, which could be blown over the dike due to onshore blowing winds, via the chute to the overtopping box. Relating this overtopping discharge to the situation without paddle wheel allowed to determine the maximum wind effect. The splash board was used to make sure all splashing water from the paddle wheel ended up in the overtopping box.

As explained in section 2.4, the maximum wind effect concerns the water volume that would not overtop the dike in case of no wind. This vertical splashing effect against the crest wall is demonstrated in Figure 3.2 for the situation of a dike with a crest wall. A close-up of a splashing event for a crest wall with promenade is included in Figure 3.3. For more figures, the reader is referred to Appendix B.



Figure 3.2: Vertical splashing of water when waves hit the crest wall on the dike with crest wall only.



Figure 3.3: Vertical splashing of water when waves hit the crest wall on the dike with crest wall and promenade.

3.2 Measurement programme

In total, experiments with four different dike configurations were conducted. The vertical wall at the dike crest was located at the water or land side of the crest and it was tested with two different heights as displayed in Figure 3.4. Besides, five different significant wave heights and three wave steepnesses were combined. The overall result was fifteen test series per dike configuration. Furthermore, for each combination of wave characteristics a reference test without crest elements and without wind was carried out. This allowed for a direct comparison with existing guidelines, for example TAW (2002). Several tests with varying water levels were performed as well to investigate the effect of water level variations.

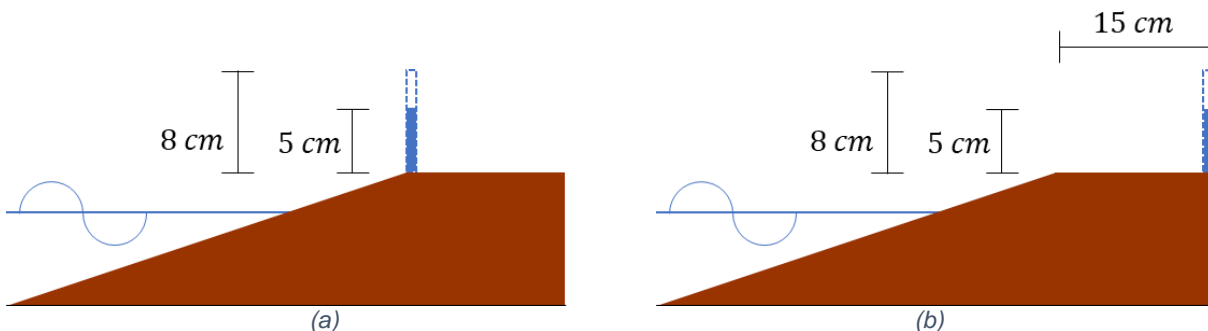


Figure 3.4: Schematic close-up with tested crest wall heights and positions; (a) Crest wall at seaside; (b) Crest wall at land side, thus introducing a promenade.

Each test consisted of approximately 1,000 waves. This series is long enough to schematise a full wave height and period distribution over the frequency domain (Chen et al., 2019). For approximately half of the experiments, the domain for the wave overtopping discharge was within the low overtopping regime, whereas the other tests resulted in higher overtopping discharges. The low overtopping regime means that the dimensionless overtopping discharge as defined in Equation 18 is $2 \cdot 10^{-6} < q^* < 2 \cdot 10^{-4}$. For lower values of q^* , scale effects may dominate the test results, which is why going below the lower limit is not preferable. Higher discharges only require a larger overtopping box or a pumping system within the box. The values for q^* are based on research by Van Doorslaer et al. (2015) and the indicated wave characteristics. An overview of the complete measurement programme is included in Appendix C, but the ranges or values of the most important parameters in the test programme are given in Table 3.1.

Table 3.1: Parameter ranges of the test programme.

Parameter	Symbol	Value/Range
Seaward slope angle [-]	$\tan(\alpha)$	1:3
Relative crest freeboard [-]	R_c/H_{m0}	1.49 – 3.98
Relative promenade width [-]	B/H_{m0}	0 – 1.53
Wave steepness [-]	s_0	0.020 – 0.042
Breaker parameter [-]	ξ_0	1.62 – 3.00
Crest freeboard [m]	R_c	0.2 – 0.48
Crest wall height [m]	h_{wall}	0, 0.05 & 0.08
Incident significant wave height at the toe [m]	H_{m0}	0.098 – 0.202
Promenade width [m]	B	0 & 0.15
Water depth [m]	d	0.6 – 0.85
Mean spectral wave period [s]	$T_{m-1,0}$	1.248 – 2.507

3.3 Froude scaling

Physical modelling comes with scaling of real-life structures to a model scale. Viscosity and surface tension of water are usually not dominant factors when it comes to monophasic physical model tests in hydraulic engineering concerning waves or large gradients in water surface elevation (Schierreck & Verhagen, 2019). Therefore, the Froude scaling law is applied. The main principle in Froude scaling is that the Froude number should be equal for both the model (subscript m) and the prototype (subscript p), defined as

$$\frac{u_m}{\sqrt{g_m L_m}} = \frac{u_p}{\sqrt{g_p L_p}} \quad \text{Equation 19}$$

The variables u , g and L are the velocity, gravitational acceleration and a length, respectively. The scale factor in Froude scaling is defined by parameter n , which characterises the size reduction of the model compared with the prototype.

$$n_L = \frac{L_p}{L_m} \quad \text{Equation 20}$$

When assuming that the gravitational acceleration is not scaled ($g_m = g_p$), and using Equation 19 and Equation 20, the scale for velocities becomes

$$\frac{u_p}{u_m} = \sqrt{n_L} \quad \text{Equation 21}$$

Scales following the Froude scaling rules are used in the set-up of the model, which corresponds to a scale factor of $n_L = 10$ to 20. Based on these equations, the scale factors for time [s] and discharge [m^3/s] are $n_L^{0.5}$ and $n_L^{2.5}$, respectively (Schierreck & Verhagen, 2019).

4

Data analysis

The data analysis of the physical model tests consists of multiple elements and can be roughly divided into two main parts. Part one contains the comparison between the measurements and previous research, qualitatively as well as quantitatively. First, the reference tests are compared with the existing guidelines, such as TAW (2002) and EurOtop (2018) (section 4.1). Second, the relation between the overtopping discharge and the dike configuration and wave characteristics is analysed and verified with expectations based on previous research (section 4.2). After this, the data from the tests with crest elements are compared with TAW (2002) and Van Doorslaer et al. (2015) (section 4.3). When needed, new formulas are proposed, which describe the test results more accurately than the existing ones. Part two focusses on the maximum wind effect (section 4.4). The maximum wind effect and dependencies on wave characteristics and crest elements are researched in this section, which is completed by proposing an influence factor for wind.

During the tests, the overtopping discharge was collected in an overtopping box behind the dike as explained in chapter 3. However, for very large overtopping discharges the box had to be emptied during the test using pumps that were installed in the overtopping box. During this pumping, the overtopping volume was not measured, which means that the average overtopping discharge might have been influenced. Meanwhile, the wave characteristics were continuously measured. As a result, the average wave characteristics during the non-pumping time might differ as well. For one test series ($H_{m0} = 0.2 \text{ m}$; $s_0 = 0.02$), multiple pumping series were needed independent on the dike configuration. Analysing the datapoints with these relatively long and multiple pumping events showed that they systematically lead to deviating discharges. Therefore, these datapoints have not been used in the analysis. Additionally, one test series ($H_{m0} = 0.1 \text{ m}$; $s_0 = 0.04$) resulted in so little overtopping discharge that the measurement might have become inaccurate. This test series was repeated with a higher water level, which led to more overtopping, as expected. This test series is included in the dataset.

4.1 Comparing reference tests with existing guidelines

The physical model reference tests without wind and without crest elements were used to check whether the measurements fit existing overtopping guidelines. In TAW (2002) and EurOtop (2018) the difference was made between breaking and non-breaking waves based on the breaker parameter ξ_0 as defined in Equation 5 (section 2.2). In line with this, the same distinction is made in the analysis here. Figure 4.1 displays the dimensionless overtopping discharge q^* for both breaking and non-breaking waves for the reference tests. The horizontal axis is defined by the relative crest freeboard R_c/H_{m0} . This figure also shows that the wave steepness seems to have significant

impact on the overtopping discharge, although this is not included in Equation 4 for non-breaking waves.

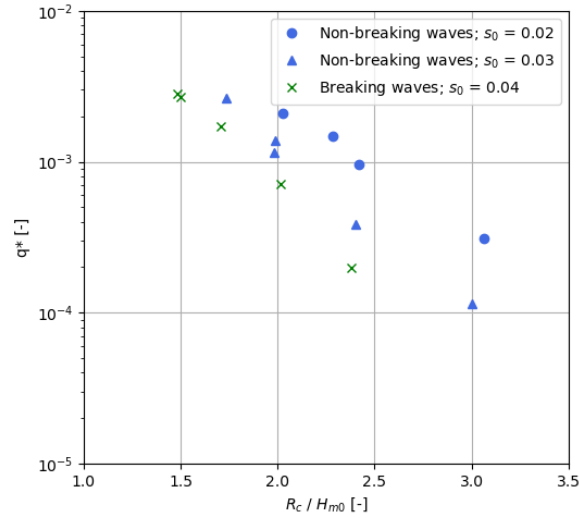


Figure 4.1: Measured overtopping discharges for reference tests, with a distinction between breaking and non-breaking waves, but also between different wave steepnesses.

When analysing breaking and non-breaking waves separately, different findings were made concerning the comparison between the measurements, and the TAW (2002) and EurOtop (2018) equations. From Figure 4.2, it becomes clear that for breaking waves, the deterministic TAW (2002) formula (in red with exponential factor 4.3) is more conservative than EurOtop (2018), where the latter coincides much better with the data. Although the measurements are no more than a factor 3 off, the reason for the conservative TAW (2002) formula for breaking waves was already given by TAW (2002), where it was mentioned that for the deterministic approach, the overtopping formula is on the conservative side. Optimising the exponential factor from 4.3 to 4.7 results in a more suitable fit according to the datapoints for breaking waves (Equation 22). Regarding non-breaking waves, there seems to be some spreading for both guidelines, although this is relatively small compared to the 90 percent confidence intervals for the TAW (2002) formulas.

$$\frac{q}{\sqrt{g H_{m0}^3}} = \frac{0.067}{\sqrt{\tan(\alpha)}} \gamma_b \cdot \xi_0 \cdot \exp\left(-4.7 \frac{R_c}{H_{m0}} \frac{1}{\xi_0 \cdot \gamma_b \cdot \gamma_f \cdot \gamma_\beta \cdot \gamma_v}\right) \quad \text{Equation 22}$$

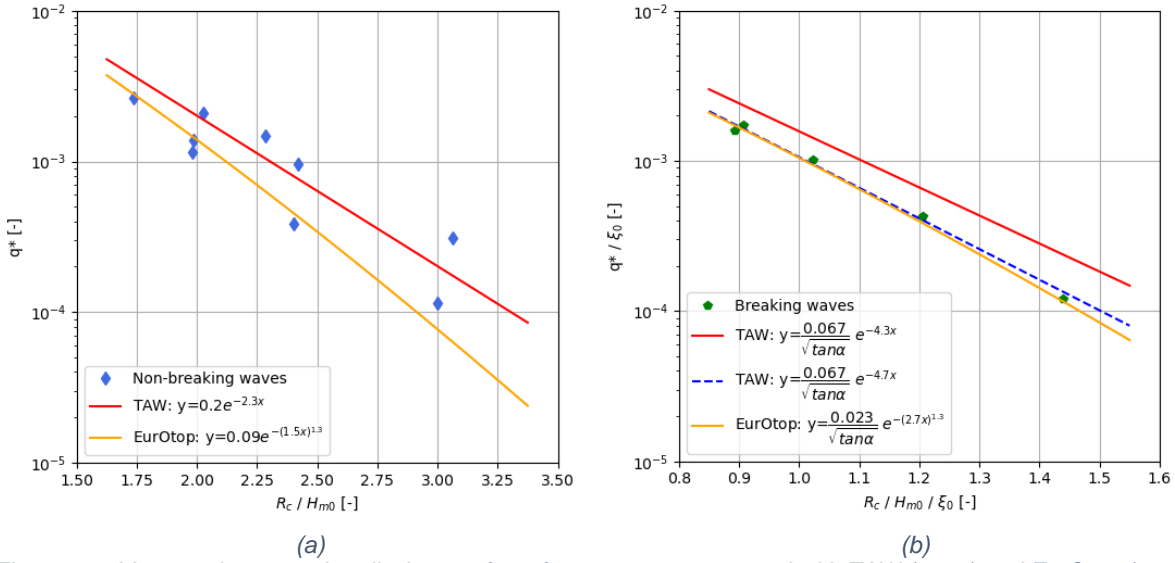


Figure 4.2: Measured overtopping discharges for reference tests compared with TAW (2002) and EurOtop (2018); (a) Non-breaking waves; (b) Breaking waves.

The fact that the wave steepness dependency on the overtopping discharge (Figure 4.1) is not included in guidelines for non-breaking waves was also noticed for breakwaters (Van Gent et al., 2022). Therefore, a new expression (Equation 23) is proposed to account for the wave steepness for non-breaking waves. As Figure 4.3 illustrates, Equation 23 is a better fit than the original TAW (2002) equation in Figure 4.2 (a). It has to be mentioned that it is not investigated in this study if incorporating the breaker parameter would be better than the wave steepness, because the breaker parameter also takes dikes with a different slope angle into account.

$$\frac{q}{\sqrt{g H_{m0}^3}} = 1.1 \cdot 10^{-4} \cdot s_0^{-2} \cdot \exp\left(-2.3 \frac{R_c}{H_{m0}} \frac{1}{\gamma_f \cdot \gamma_\beta}\right) \quad \text{Equation 23}$$

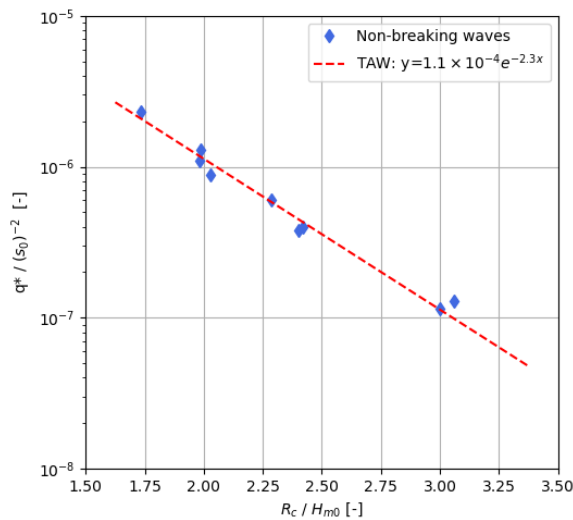


Figure 4.3: Measured overtopping discharges for the reference tests for non-breaking waves compared with the proposed expression in Equation 23.

The root-mean-squared-log error (RMSLE) is used to make quantitative comparisons, and is defined as

$$RMSLE = \sqrt{\frac{\sum_{i=1}^N (\log(q_{measured}^*) - \log(q_{calculated}^*))^2}{N}} \quad \text{Equation 24}$$

where N is the number of tests on which the RMSLE is based (Ma et al., 2022). For datasets spanning a large range, the RMSLE is a better choice than the RMSE (without logarithms) as it presents the relative error. The RMSE presents the absolute error, which is less suitable for datasets spanning a large range as for low values the errors have almost no effect on the RMSE value. Lower RMSLE values imply a better agreement between the measured and calculated overtopping discharges. Optically, Equation 23 is a much better fit than the original TAW (2002) equation for non-breaking waves; the values in Table 4.1 confirm this. The RMSLE values for breaking waves regarding the original and fitted TAW (2002) formula are also included in Table 4.1.

Table 4.1: RMSLE for overtopping discharges of reference tests described by TAW (2002) and the newly proposed Equation 23 (non-breaking waves) or Equation 22 (breaking waves).

	TAW (2002)	Equation 23	Equation 22
Reference tests non-breaking waves	0.2048	0.0604	-
Reference tests breaking waves	0.1975	-	0.0357

4.2 Wave characteristics and dike configuration influencing the overtopping discharge

After analysing the reference tests, the experiments with crest elements are investigated. A few qualitative connections between wave characteristics and dike configurations on the one hand and overtopping discharge on the other hand are inspected. This is to check whether the results are in line with the expectations based on previous research. Both tests with and without wind are taken into consideration since this is important when diving into the maximum wind effect. However, because Figure 4.4 shows an analogy between the tests with and without wind, resulting in a similar analysis for both tests with and without wind, the reader is referred to Appendix D for an elaboration on the tests with wind.

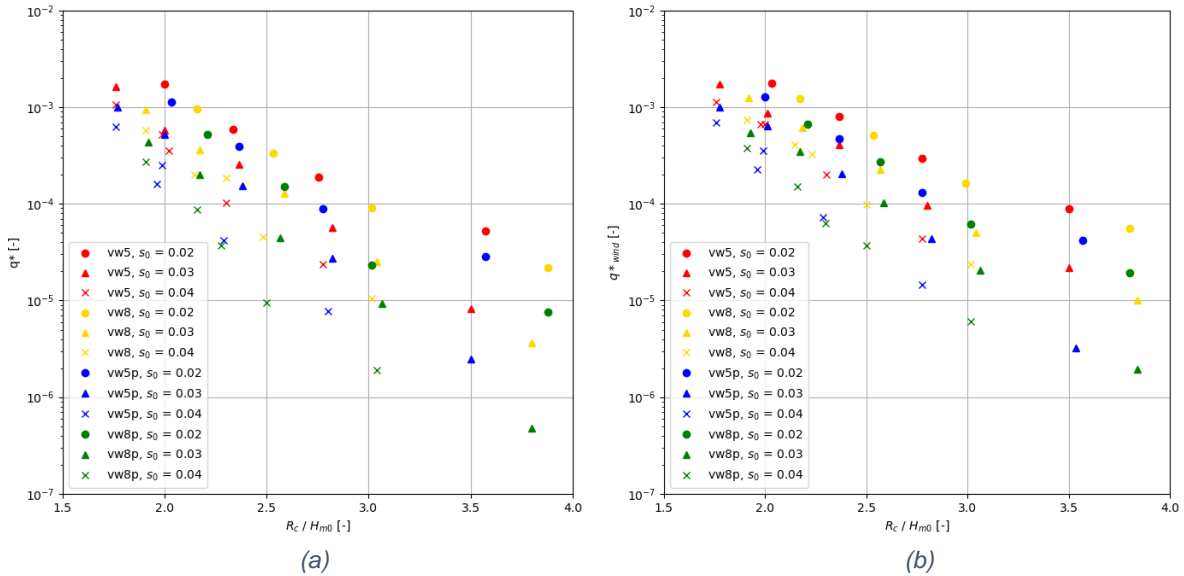


Figure 4.4: Measured overtopping discharges; (a) Measurements in absence of wind; (b) Measurements in presence of wind.

Figure 4.4 contains the total set of measured overtopping discharges for both tests with and without wind. In this figure, the colour of the datapoints indicates the dike configuration, which is a vertical wall of five (vw5) or eight cm (vw8) without promenade or with promenade (vw5p and vw8p). The marker type indicates the wave steepness, increasing from 0.02 towards 0.04.

In order to clarify the dependency of the overtopping discharge on the individual elements, Figure 4.5 and Figure 4.6 display pieces of the total amount of information from Figure 4.4. In general, it can be concluded, from the linear relation on logarithmic scale, that the relation between the relative crest freeboard R_c/H_{m0} is exponential, which is in line with the TAW (2002) and EurOtop (2018) formulas. Next, the effect of introducing a promenade is visible by focussing on the colours in Figure 4.5 where the overtopping discharges are lower in case a promenade is present. Furthermore, there appears to be a negative correlation between the height of the crest wall and the overtopping discharge as well. This is also embedded in the relative crest freeboard. According to Figure 4.6, a lower wave steepness, thus longer waves, creates larger wave overtopping discharges. During the tests, this is observed as well. Longer waves seemed to have more energy, which resulted in higher run-up and run-up velocities thus generating more overtopping discharge. In conclusion, the results are in line with current knowledge. Changes in wave steepness, relative crest freeboard and a promenade in front of the crest wall have significant impact on the overtopping discharge.

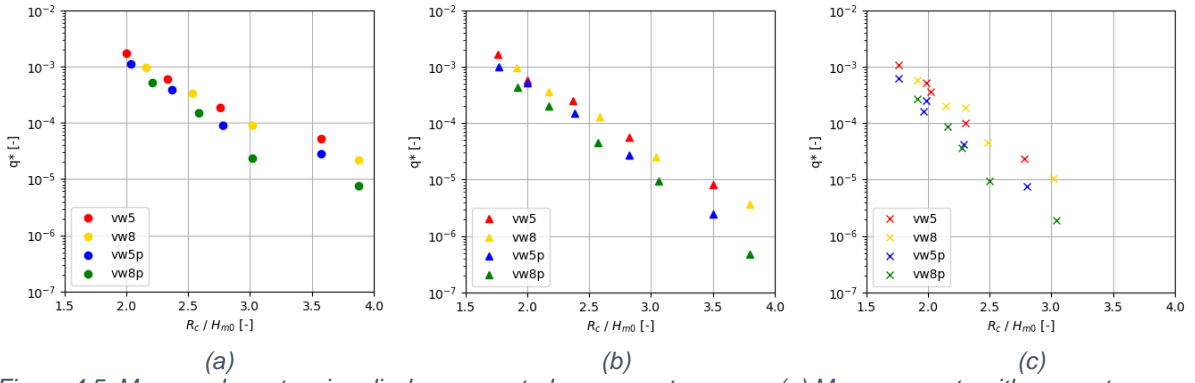


Figure 4.5: Measured overtopping discharges sorted on wave steepness; (a) Measurements with wave steepness of 0.02; (b) Measurements with wave steepness of 0.03; (c) Measurements with wave steepness of 0.04.

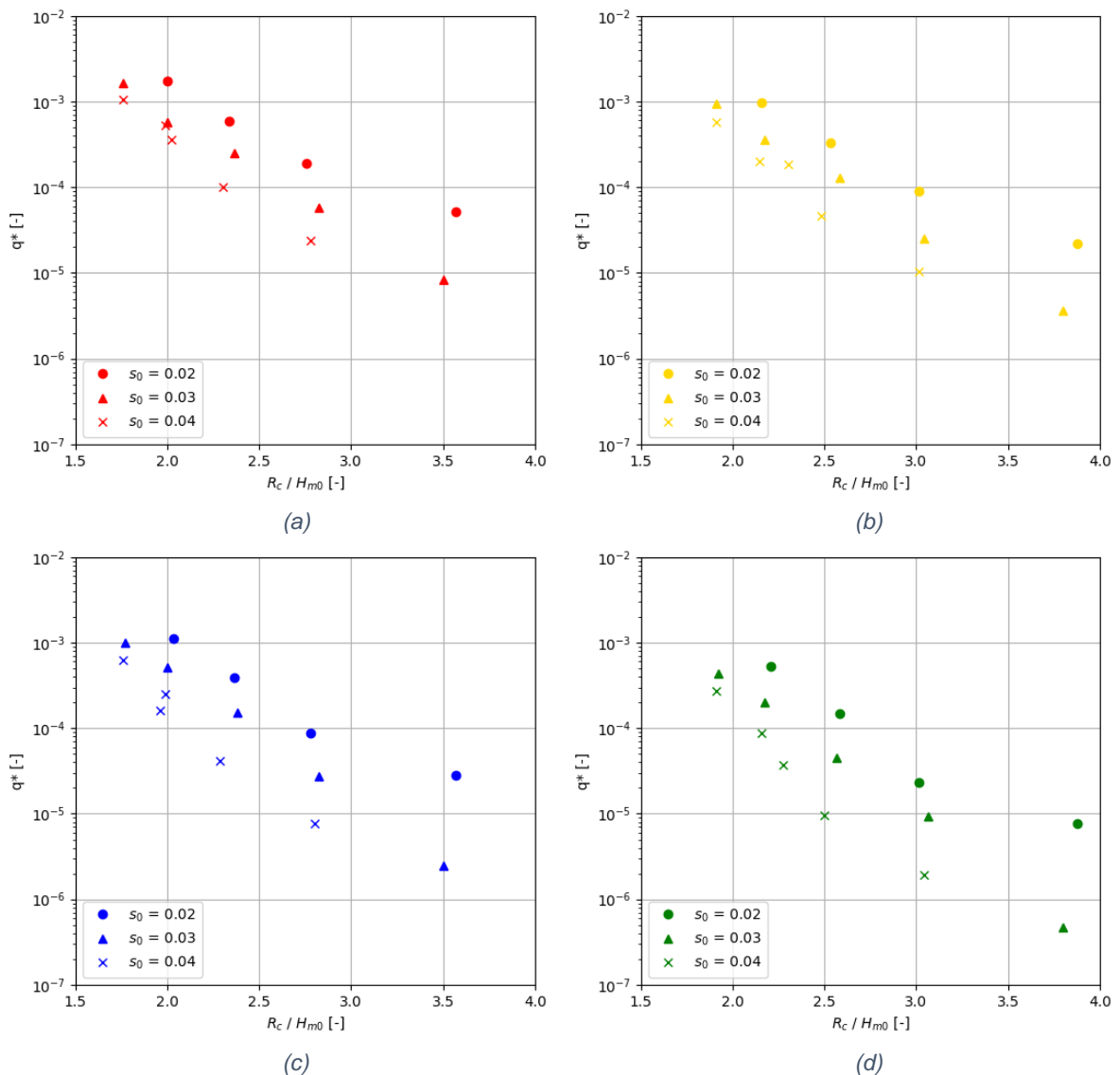


Figure 4.6: Measured overtopping discharges sorted on dike configuration; (a) Measurements with crest wall of 5 cm; (b) Measurements with crest wall of 8 cm; (c) Measurements with crest wall of 5 cm and promenade; (d) Measurements with crest wall of 8 cm and promenade.

In the previous section, it is shown that for tests without crest elements the wave steepness should be included in the TAW (2002) formula to calculate the overtopping discharge for non-breaking waves. Figure 4.7 shows that for tests with crest elements, there is also a wave steepness dependency since the wave steepness is embedded in the breaker parameter ξ_0 . The breaker criterion of ξ_0 is around 1.86, which is the transition from Equation 3 to Equation 4 (TAW, 2002). Even though Figure 4.7 (a) may appear as a point cloud with a large range, there is a positive correlation between the overtopping discharge and the breaker parameter. Not only is this in line with the observation of the wave steepness related to overtopping discharge, but it also coincides with the visual observation made during the tests that plunging breakers cause less overtopping than waves that tend to be more collapsing or surging breakers, which correspond to higher Iribarren parameter values.

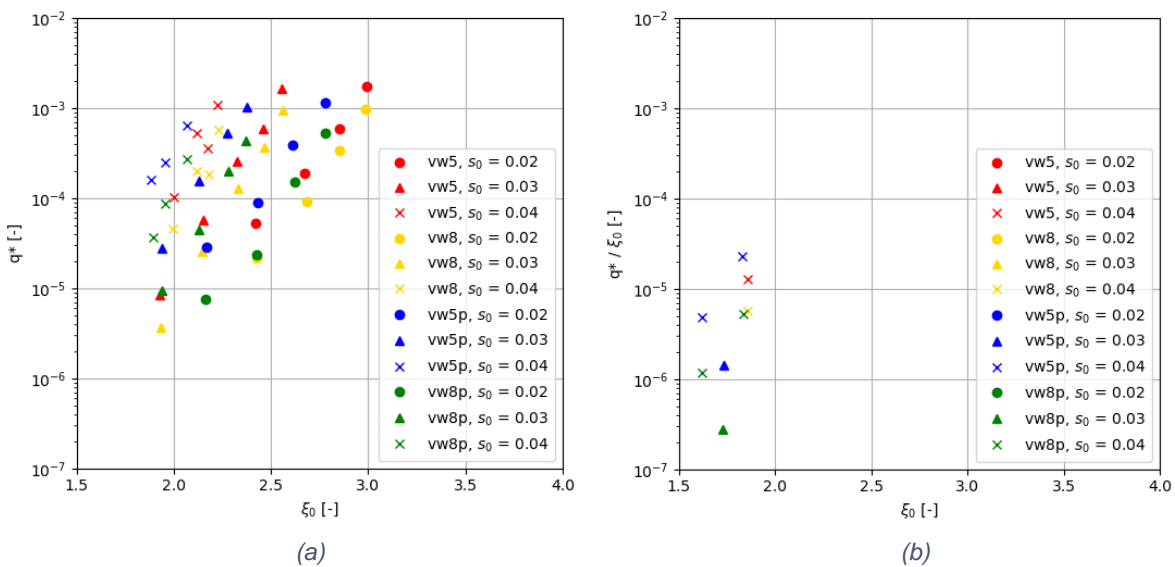


Figure 4.7: Measured overtopping discharge versus breaker parameter; (a) Measurements for non-breaking waves; (b) Measurements for breaking waves.

4.3 Comparing crest element tests with existing guidelines

Van Doorslaer et al. (2015) researched the influence of crest elements on seadikes, such as a vertical wall, promenade, parapet and combinations between those elements. As the present research only includes a vertical wall and a vertical wall in combination with a promenade in the measurement set-up, these are the configurations that are compared with the results from Van Doorslaer et al. (2015).

The previous section shows the relation between wave characteristics and dike configurations on the one hand and overtopping discharge at the other hand. Now, these measurements without wind are compared with existing guidelines. First, the measured dimensionless overtopping discharge is set out against those according to the TAW (2002) formulas in Figure 4.8. The influence factors γ for crest elements for non-breaking waves as shown in subsection 2.3.4 – Equation 14, Equation 15 and Equation 17 – are also taken into consideration (Van Doorslaer et al., 2015). Therefore, the equations used for Figure 4.8 are Equation 3 for breaking waves and Equation 13 for non-breaking waves.

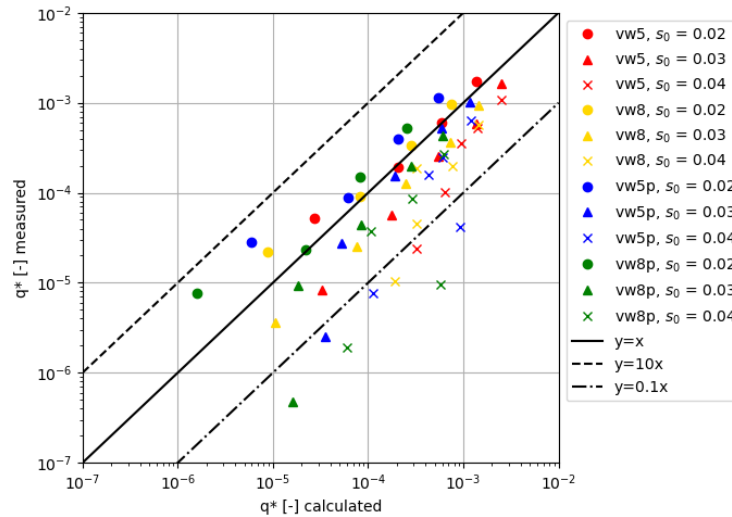


Figure 4.8: Measured overtopping discharges without wind compared with the TAW (2002) and Van Doorslaer et al. (2015) formulas.

Table 4.2: RMSLE for overtopping discharges of crest element tests described by TAW (2002) and Van Doorslaer et al. (2015).

	vw5	vw8	vw5p	vw8p
$s_0 = 0.02$	0.1517	0.2094	0.4039	0.3956
$s_0 = 0.03$	0.4191	0.3630	0.5316	0.7143
$s_0 = 0.04$	0.6987	0.7561	0.8482	1.0975

While most measurements are relatively close to the calculated overtopping discharges using the current guidelines, there are some measurements that differ more than a factor 10 from the calculated overtopping discharges and are overestimated by the guidelines. Most of these measurements are related to a high wave steepness with a large RMSLE. Besides, the promenade tests show an overall increase in the RMSLE, whereas an evident dependency of the crest wall height on how well the measurements fit the guidelines appears to be absent (Table 4.2). Nevertheless, the fact that the influence factors for crest elements proposed by Van Doorslaer et al. (2015) are only embedded in the formula for non-breaking waves (Equation 13) and not in the one for breaking waves (Equation 3) may be the problem. Although an influence factor for crest walls is included in the TAW (2002) formula for breaking waves, its application area is between $1.2 \cdot H_{m0}$ below and above the still water level. As this is not the case for the measurements in this test series, more research needs to be conducted before a conclusion can be drawn.

Crest elements might influence overtopping for breaking waves as well. This hypothesis is fortified by Figure 4.9, where the current guidelines clearly overestimated the measured overtopping discharge for breaking waves. It is therefore reasonable to conclude that crest elements should be considered for breaking waves as well. This is elaborated in subsection 4.3.2, after discussing the influence factor for non-breaking waves.

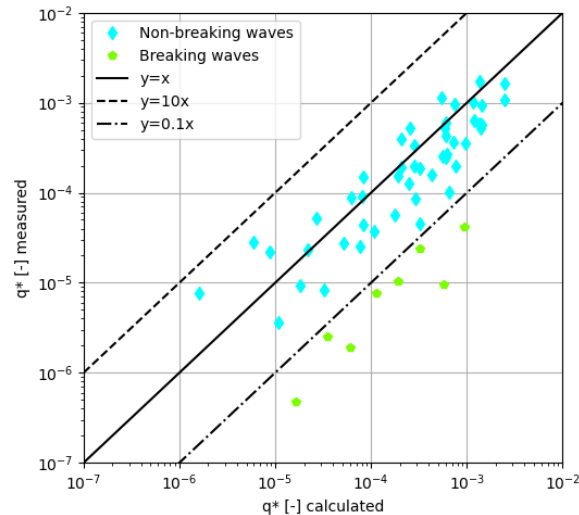


Figure 4.9: Comparison of measured overtopping discharges with calculated overtopping discharges for breaking and non-breaking waves (TAW, 2002); (Van Doorslaer et al., 2015).

4.3.1 Influence factors of crest elements for non-breaking waves

A formulation for the influence factor corresponding to a vertical wall was implemented into Equation 13 (Van Doorslaer et al., 2015). In Figure 4.10, the cyan points depict the hypothetical γ values needed to couple Equation 13 with the measured overtopping discharges. If these values are exactly on the linear function, they are in line with the formulation for the influence factor according to Equation 14. Figure 4.10 shows wide vertical spreading of the results, which might be the reason for the spreading around the line $y=x$ for non-breaking waves in Figure 4.9 as well. It has to be mentioned that the results by Van Doorslaer et al. (2015) themselves also indicated a large spreading of the influence factor.

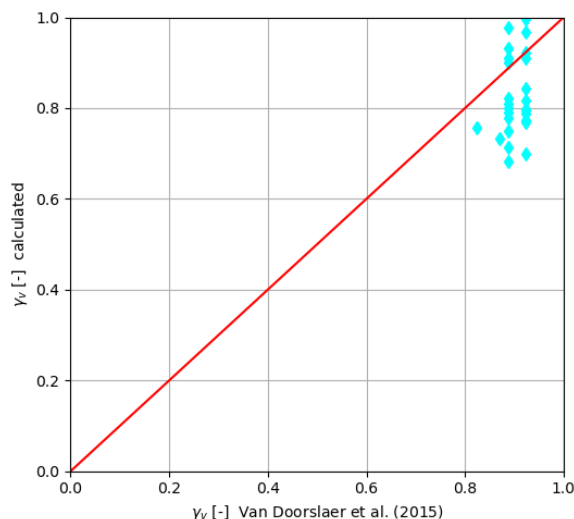


Figure 4.10: Comparison of the hypothetical influence factors for a crest wall, which are needed to connect the measurements with the TAW (2002) formula, with the proposed formula by Van Doorslaer et al. (2015) for non-breaking waves.

Using the formula proposed by Van Doorslaer et al. (2015) (Equation 14), Figure 4.11 displays the effect of adding this influence factor. Despite the spreading illustrated in Figure 4.10, the measured overtopping discharge is in relatively good agreement with previous research when taking the influence factor into account. Moreover, in section 4.2, it is observed that the overtopping discharge for non-breaking waves is dependent on the wave steepness, thus also on the breaker parameter. The influence factor is originally fitted to the original TAW (2002) formula, therefore part of the error margin – due to not taking the breaker parameter into account – is deducted. However, if the newly proposed overtopping formula (Equation 23) is employed, the spreading significantly decreases, which can be seen in Figure 4.12. The power of the wave steepness for the reference tests is optimised to reduce the error margin further, as displayed in Table 4.3. The improvement for this small deviation in power is caused by a better fit for the crest wall tests.

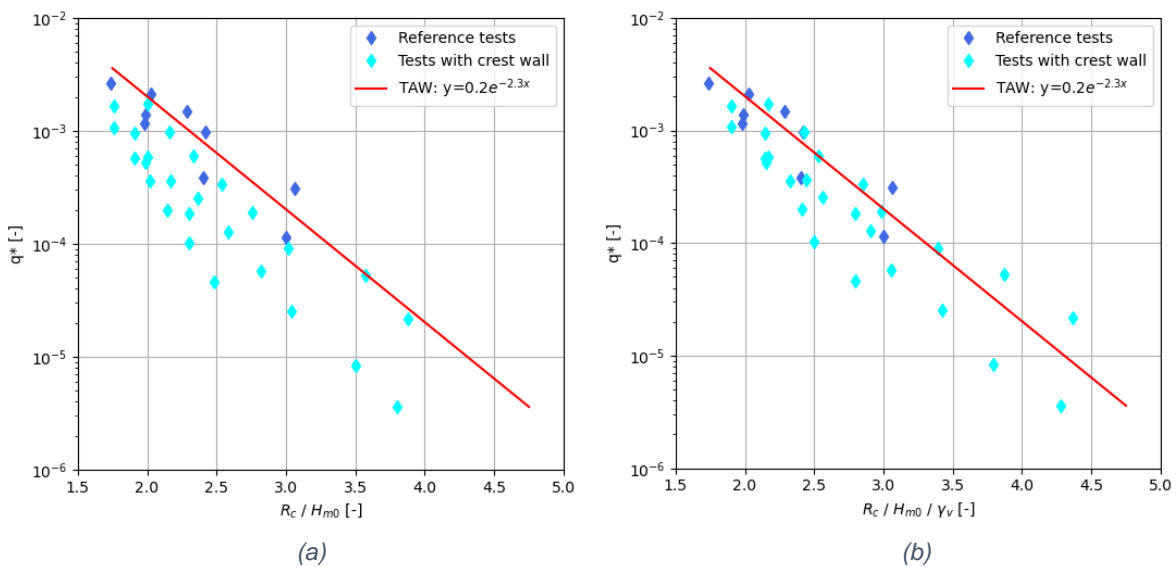


Figure 4.11: Measured overtopping discharges and the effect of adding the influence factor for a crest wall for non-breaking waves; (a) Without taking the reduction factor into account; (b) Taking the reduction factor into account.

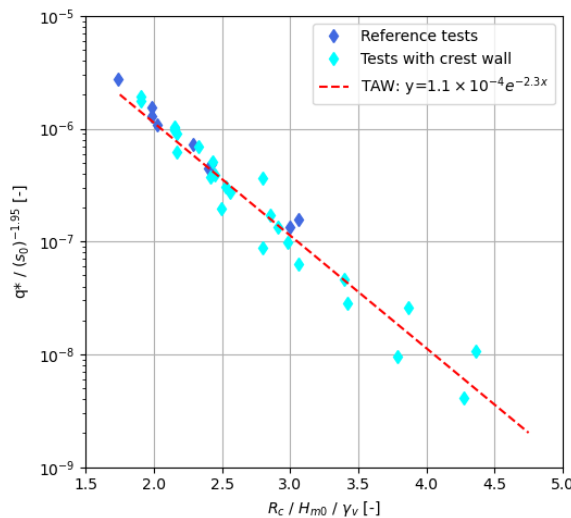


Figure 4.12: Measured overtopping discharges and the effect of adding the influence factor for a crest wall for non-breaking waves compared with the proposed expression in Equation 23, but with $s_0^{-1.95}$ and γ_v .

Table 4.3: RMSLE for overtopping discharges of non-breaking crest wall tests described by TAW (2002) and the newly proposed Equation 23.

	TAW (2002)	Equation 23 with s_0^{-2} and γ	Equation 23 with $s_0^{-1.95}$ and γ
Crest wall tests	0.4035	0.1812	0.1648

When the crest wall is located at the land side of the dike, thus creating a promenade, the results are similar to those demonstrated for a crest wall only. The vertical spread in Figure 4.13 is large, but the influence factor translates the measured overtopping discharge well to the general overtopping formula illustrated in Figure 4.14. Only for the two tests with $H_{m0} = 0.1 \text{ m}$; $s_0 = 0.02$ (horizontal coordinate > 4.5 in Figure 4.14 (b)), the deviations are larger. Possibly, scale effects or measurement errors (see chapter 5) lead to these deviations, but since only two measurements deviate a conclusive statement on the cause of these inconsistencies cannot be made.

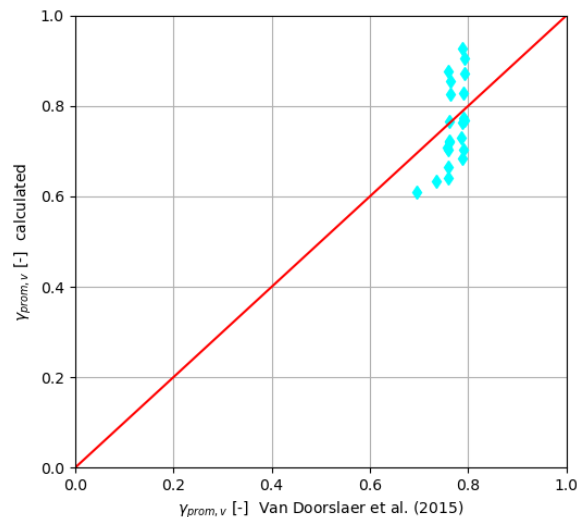


Figure 4.13: Comparison of the influence factors for a crest wall with promenade related to the measurements with the proposed formula by Van Doorslaer et al. (2015) for non-breaking waves.

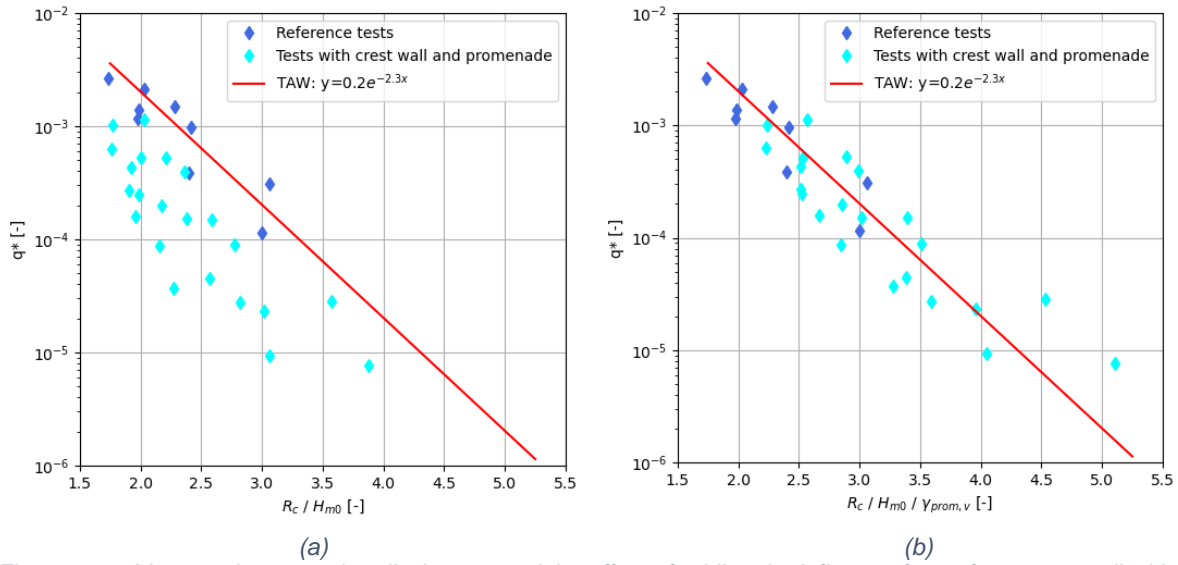


Figure 4.14: Measured overtopping discharges and the effect of adding the influence factor for a crest wall with promenade for non-breaking waves; (a) Without taking the reduction factor into account; (b) Taking the reduction factor into account.

Similar to the tests with a crest wall only, Equation 23 with the wave steepness dependency is compared with the measurements including a crest wall with promenade. Again, the exponent of the wave steepness is optimised to get a better fit (Figure 4.15 and Table 4.4). Because the tests with crest wall and promenade require an exponent which is higher than two and the tests with a crest wall only require an exponent which is smaller than two, overall a value of two seems to be optimal, give only slightly higher RMSLE values than the best fit and fit the reference tests best. This formula is presented in Equation 25.

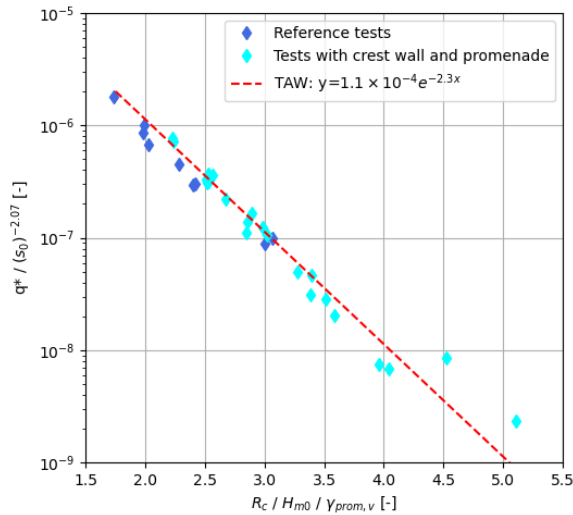


Figure 4.15: Measured overtopping discharges and the effect of adding the influence factor for a crest wall with promenade for non-breaking waves compared with the proposed expression in Equation 23, but with $s_0^{-2.07}$ and γ .

Table 4.4: RMSLE for overtopping discharges of crest wall with promenade tests for non-breaking described by TAW (2002) and the newly proposed Equation 23.

	TAW (2002)	Equation 23 with s_0^{-2} and γ	Equation 23 with $s_0^{-2.07}$ and γ
Crest wall with promenade tests	0.3435	0.1902	0.1567

$$\frac{q}{\sqrt{g} H_{m0}^3} = 1.1 \cdot 10^{-4} \cdot s_0^{-2} \cdot \exp\left(-2.3 \frac{R_c}{H_{m0}} \frac{1}{\gamma_f \cdot \gamma_\beta \cdot \gamma^*}\right) \quad \text{Equation 25}$$

4.3.2 Influence factors of crest elements for breaking waves

The γ factors for crest elements are only prescribed for non-breaking waves by Van Doorslaer et al. (2015). The effect of crest elements on overtopping discharges for breaking waves has not been studied yet, but since the measured values differ significantly from the calculated values in Figure 4.9 it might be interesting to investigate the applicability of the influence factors proposed by Van Doorslaer et al. (2015) for breaking waves as well. Hence, the influence factors for breaking waves applied here are calculated in the same way as for non-breaking waves. Though only two tests with breaking waves and a crest wall were performed, the influence factor needed to fit the guidelines is not in line with the influence factor for non-breaking waves (Figure 4.16). Consequently, this factor does not fit the deterministic TAW (2002) equation nor the optimal coefficient for the reference tests as in Figure 4.17. An exponent of -5.5 would fit the datapoints (Equation 26), but since only two tests are performed, further research is needed to investigate if a different equation is needed to describe the overtopping discharge or if a different influence factor should be constructed.

$$\frac{q}{\sqrt{g} H_{m0}^3} = \frac{0.067}{\sqrt{\tan(\alpha)}} \gamma_b \cdot \xi_0 \cdot \exp\left(-5.5 \frac{R_c}{H_{m0}} \frac{1}{\xi_0 \cdot \gamma_b \cdot \gamma_f \cdot \gamma_\beta \cdot \gamma_v}\right) \quad \text{Equation 26}$$

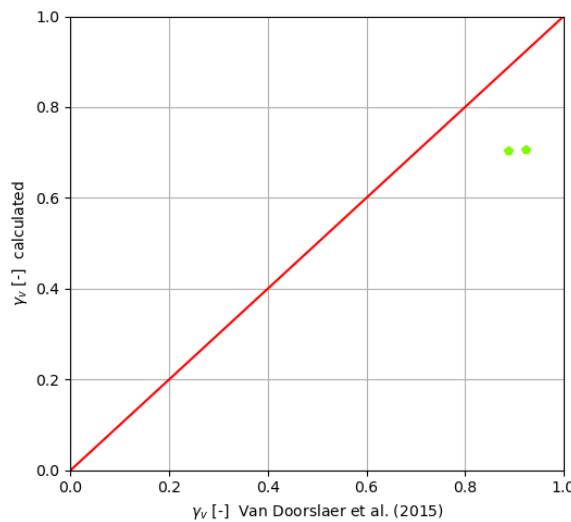


Figure 4.16: Comparison of the influence factor for a crest wall related to the measurements with the proposed formula by Van Doorslaer et al. (2015) for breaking waves.

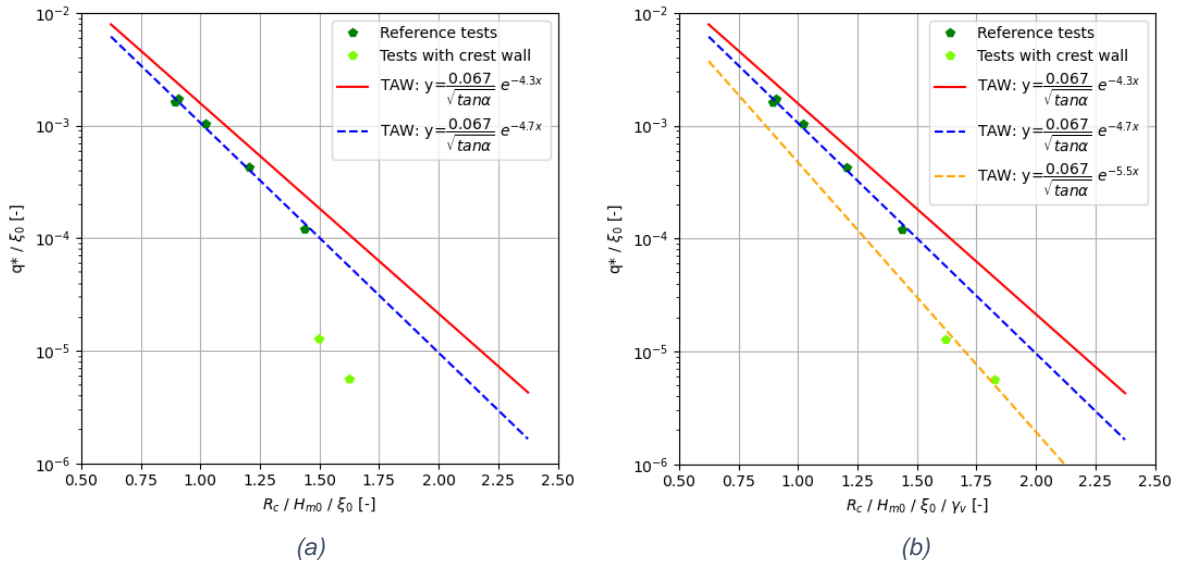


Figure 4.17: Measured overtopping discharges and the effect of adding the influence factor for a crest wall for breaking waves; (a) Without taking the reduction factor into account; (b) Taking the reduction factor into account.

Considering the dike configuration with crest wall and promenade, most datapoints are closer to the Van Doorslaer et al. (2015) factor than for a crest wall only (Figure 4.18). In addition to the deterministic formula used by Van Doorslaer et al. (2015), the less conservative expression (Equation 22) for breaking waves is displayed as well in Figure 4.19. Although most datapoints are not far from the deterministic formula, overall the newly proposed equation is a satisfying compromise. The two datapoints that are overestimated by Equation 22 (the blue line with exponent of -4.7 in Figure 4.19 (b)) are not corresponding to the same test as the two datapoints in Figure 4.17, which are also overestimated. Hence, from these measurements it is reasonable to conclude that the influence factor $\gamma_{prom,v}$ may be used for breaking and non-breaking waves. It is however recommended to employ the new coefficient in the TAW (2002) formula for breaking waves to provide the best estimates for the overtopping discharges.

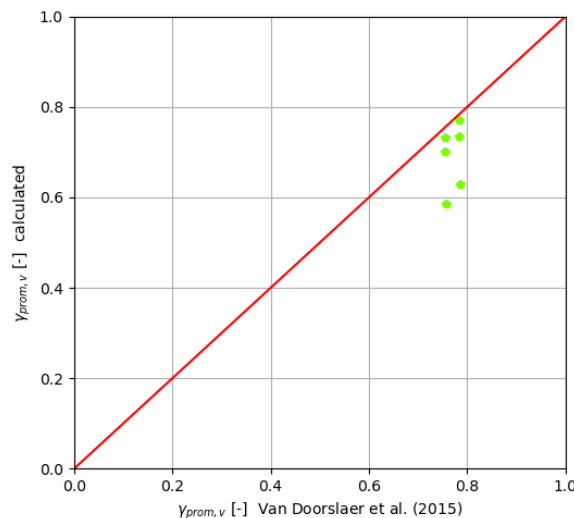


Figure 4.18: Comparison of the influence factor for a crest wall with promenade related to the measurements with the proposed formula by Van Doorslaer et al. (2015) for breaking waves.

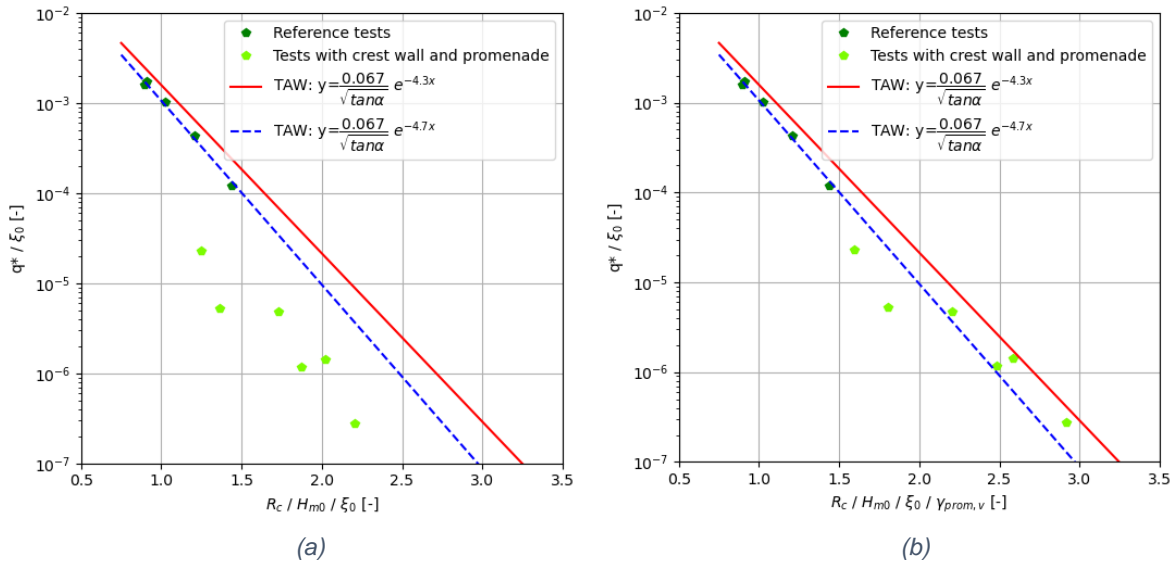


Figure 4.19: Measured overtopping discharges and the effect of adding the influence factor for a crest wall with promenade for breaking waves; (a) Without taking the reduction factor into account; (b) Taking the reduction factor into account.

Table 4.5 quantifies the RMSLE for the crest element tests concerning breaking waves. Employing Equation 22 fits best for the reference tests (see section 4.1) as well as the tests with crest wall and promenade. If there is only a crest wall at the seaside of the dike crest, Equation 26 results in the best fit, although this is not in line with the reference tests. A combination of the tests with a crest wall only and a crest wall with promenade are displayed in Figure 4.20.

Table 4.5: RMSLE for overtopping discharges of crest element tests for breaking waves described by TAW (2002) and the expressions with the fitted exponents (Equation 22 and Equation 26).

	TAW (2002)	Equation 22	Equation 26
Crest wall tests	0.9154	0.6166	0.0698
Crest wall with promenade tests	0.5386	0.3915	-

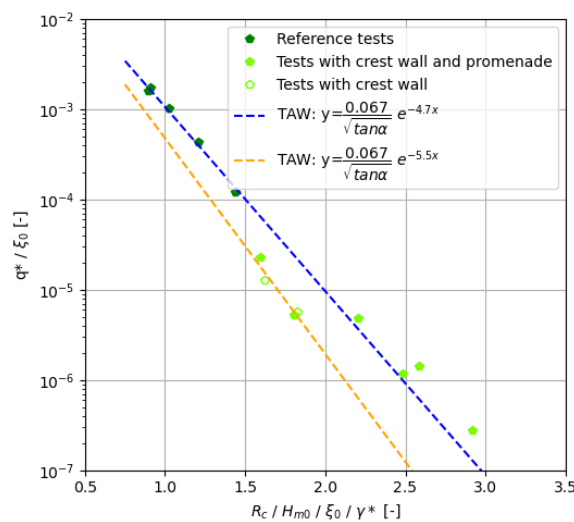


Figure 4.20: Measured overtopping discharges and the effect of adding the influence factor for crest elements for breaking waves compared with the proposed expressions in Equation 22 and Equation 26.

According to the comparison of the data with existing guidelines, several adapted versions of the TAW (2002) formulas are proposed. The basis was provided by the reference tests without crest elements, which led to an optimisation of the coefficients of the overtopping formulas for both breaking and non-breaking waves, in which the wave steepness is included. When focussing on non-breaking waves, only the influence factor for crest elements was added to the expression for the reference tests, which resulted in Equation 25. For breaking waves, the tests with a crest wall only needed a different equation (Equation 26) than the tests with crest wall and promenade. The tests with crest wall and promenade fit to the equation for reference tests (Equation 22), despite some spreading. It has to be mentioned that a relatively small dataset is used to generate the new equations with respect to the TAW dataset.

4.4 Maximum wind effect

The maximum wind effect is defined as the ratio q_{wind}/q , which indicates that this is the overtopping discharge with maximum wind effect due to onshore blowing winds (q_{wind}) over the overtopping discharge without wind effect (q). In section 4.2, several connections are made between the overtopping discharge and parameters that differed during testing, such as significant wave height, wave steepness, the crest wall height and the presence of a promenade. With this information in mind and based on previous research, it is reasonable to suggest that the maximum wind effect differs for various wave characteristics and dike configurations (Wolters & Van Gent, 2007). This section deals with qualitative as well as quantitative results of the maximum wind effect.

4.4.1 The impact of wave characteristics and dike configurations

Before diving into detailed relations for separate segments of the dataset, an overview of the maximum wind effect is given in Figure 4.21. This figure already illustrates the influence of the relative crest freeboard on the maximum wind effect. For decreasing wave heights or increasing crest freeboards, the maximum wind effect enlarges. The maximum wind effect on the vertical axis extends from 1.0 to 4.0 for the conditions tested in this study. If the wind effect is equal to 1.0, it implies that wind doesn't affect the overtopping discharge. Table 4.6 indicates the range for the maximum wind effect for different wave characteristics per dike configuration.

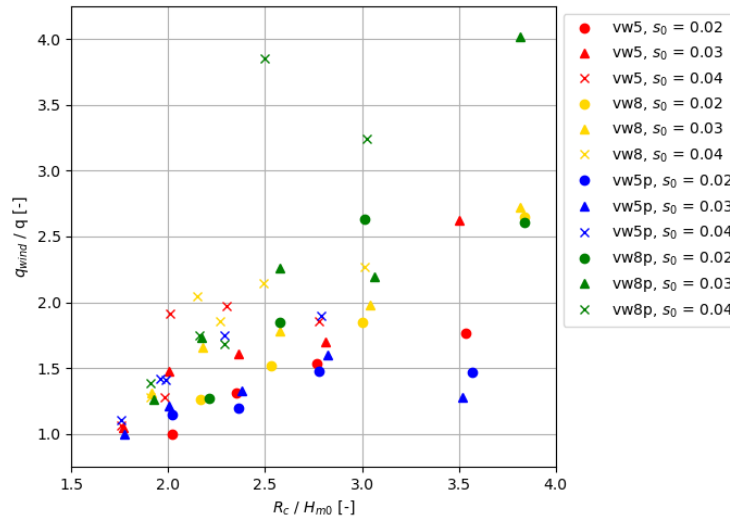


Figure 4.21: The influence of the relative crest freeboard on the maximum wind effect.

Table 4.6: Ranges of the maximum wind effect for different wave characteristics per dike configuration.

Dike configuration	Wave steepness $s_0 [-]$			Significant wave height $H_{m0} [m]$				
	0.02	0.03	0.04	0.1	0.125	0.15	0.175	0.2
vw5	1.0 - 1.8	1.0 - 2.6	1.1 - 2.0	1.8 - 2.6	1.5 - 1.9	1.3 - 2.0	1.0 - 1.5	1.0 - 1.1
vw8	1.3 - 2.7	1.3 - 2.7	1.3 - 2.3	1.9 - 2.7	1.8 - 2.3	1.5 - 2.1	1.3 - 2.0	1.3 - 1.3
vw5p	1.1 - 1.5	1.0 - 1.6	1.1 - 1.9	1.3 - 1.5	1.5 - 1.9	1.2 - 1.7	1.1 - 1.4	1.0 - 1.1
vw8p	1.3 - 2.6	1.3 - 4.0	1.4 - 3.9	1.7 - 4.0	2.2 - 3.2	1.8 - 3.9	1.3 - 1.7	1.3 - 1.4

In Figure 4.22 the data per wave steepness are categorised in order to give a more detailed picture of the different factors influencing the maximum wind effect. This approach allows for a comparison between the dike configurations. On average, two observations were made that remain valid for all three wave steepnesses. First, with a crest wall of eight cm, the promenade has an increasing effect on the wind effect, because the maximum wind effect is larger for the cases with a promenade. The second observation is that this positive correlation between the promenade and wind effect cannot be confirmed for a five cm crest wall. The configuration with a low crest wall and promenade gives a lower wind effect than the configuration with only a crest wall for the same horizontal coordinate in Figure 4.22.

The second observation is of interest as one would expect including a promenade in front of the crest wall would decrease the overtopping discharge, thus enhance the maximum wind effect. The data showed that this is not the case. A possible explanation is that the first part of the wave fills the triangular area above the promenade when a low crest wall is present (Figure 4.23). In this case, the remaining part of the wave would overtop the structure more easily and less water would be forced to move in the vertical direction. Because this could only happen when a promenade is present, the wind effect – which transports vertical spray over the dike – will be less significant for these situations. This situation is less likely to occur with higher crest elements as the triangular volume becomes too large to be filled, resulting in more vertical spray. Accordingly, the effect of a promenade is ambiguous because its impact on the maximum wind effect is dependent on the height of the crest wall.

Another possible situation is that the crest element is too low such that overshooting occurs. This could be achieved if the outer dike slope is extended virtually over the promenade and the crest wall stays below this imaginary line, thus if the ratio of the crest wall height over the promenade width is lower than the outer dike slope. For example, with an outer slope of 1:3 and promenade width of 0.15 m, the crest wall needs to be higher than 0.05 m to prevent overshooting. When overshooting occurs, the water is not forced by the crest wall to move in the vertical direction. The crest wall of five cm would be a borderline case, but there are no visual observations that confirm a lot of overshooting.

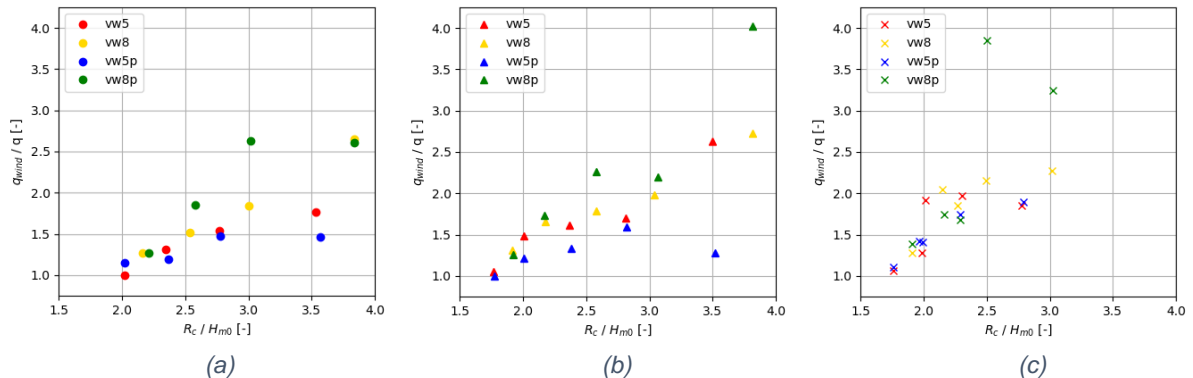


Figure 4.22: Maximum wind effect sorted on wave steepness; (a) Measurements with wave steepness of 0.02; (b) Measurements with wave steepness of 0.03; (c) Measurements with wave steepness of 0.04.

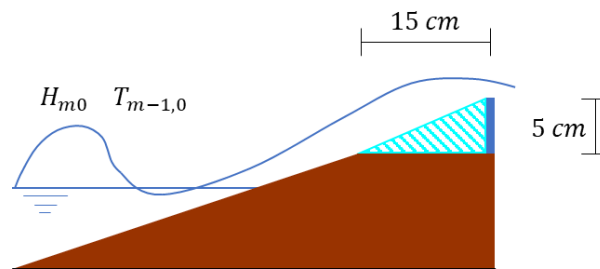


Figure 4.23: Schematic close-up of the dike. When the striped blue triangle above the promenade is filled with water, the wave will overtop the crest element more easily.

Next to the promenade, the crest wall also impacts the maximum wind effect. Figure 4.24 serves to clarify the influence of the height of the crest wall. The set-up of this figure is slightly different since the wave steepness defines the horizontal axis, but the consequence of changing the height of the crest wall becomes more pronounced. Regardless of the presence of a promenade, in general increasing the height of the crest wall results in a larger maximum wind effect. Without a promenade (Figure 4.24 (a)), increasing the crest wall from five to eight cm increases the maximum wind effect utmost with a factor 2.0. For the tests with promenade (Figure 4.24 (b)), this is even a factor 3.1. The impact of introducing a promenade is less spectacular. As explained, for a crest wall of five cm, the maximum wind effect repeatedly decreases, but for a crest wall of eight cm, the maximum wind effect increases with a factor up to 1.8.

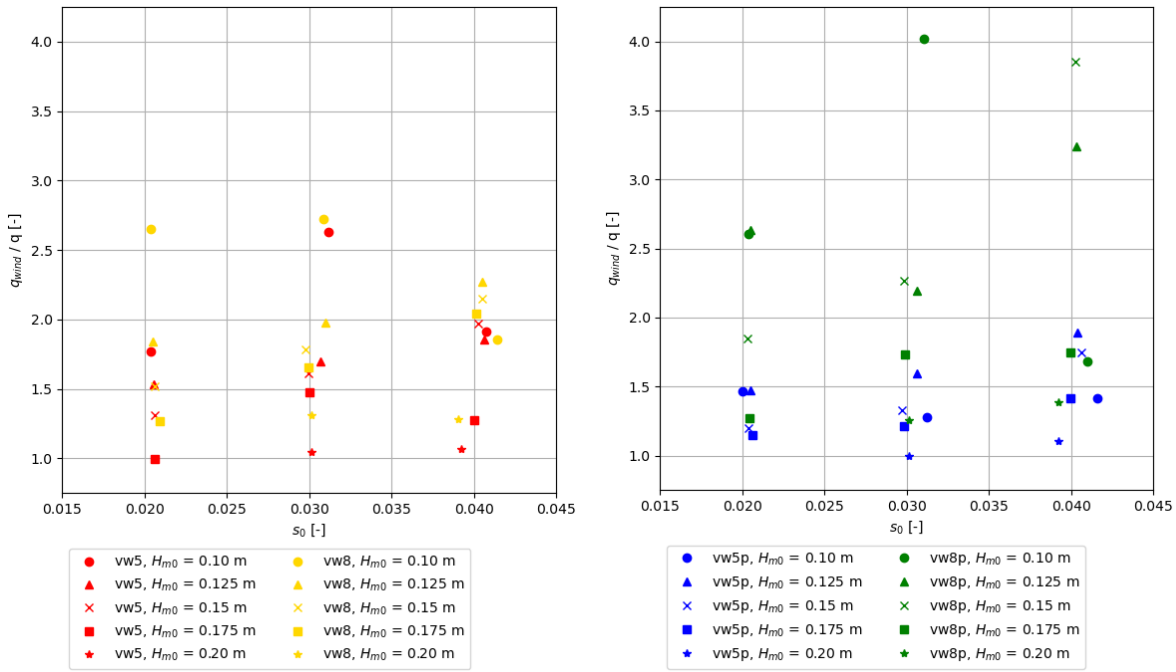


Figure 4.24: The influence of the crest wall height on the maximum wind effect; (a) Measurements with a crest wall only; (b) Measurements with a crest wall and promenade.

The previous findings related to the dike configuration and the maximum wind effect are in line with expectations based on the amount of overtopping discharge. The main idea is that the wind effect is larger for small overtopping discharges. The reasoning behind this arises from the visual observation during the tests that long and high waves overflow the crest element more easily, causing less splash when waves hit the crest element. This vertical splashing of water is the basis for measuring the maximum wind effect, so splashing is less for large overtopping events.

The hypothesis that the wind effect is larger for small overtopping discharges is already illustrated in Figure 4.21, where the relative crest freeboard is plotted on the horizontal axis. This theorem can be derived from Figure 4.21 since there is a positive correlation between the wind effect and relative freeboard. Smaller overtopping discharges arise from smaller waves when the relative crest freeboard is high. The positive correlation between the height of the crest wall and the reasoning behind introducing a promenade is also in line with this concept.

The data can also be sorted based on dike configuration, which can be seen in Figure 4.25. Because a higher wave steepness leads to lower overtopping discharges, it is assumed that the wind effect is larger for higher wave steepnesses. Despite some outliers, Figure 4.25 confirms this expectation. One of the unexpected details in Figure 4.25 (c) is the 0.03 wave steepness datapoint at a relative crest freeboard of 3.5. This point should give a maximum wind effect that is higher than the 0.02 wave steepness datapoint around the same horizontal coordinate. An explanation could be that the overtopping discharge might be inaccurate and affected by scale effects, because it is close to the lower boundary of the low overtopping regime.

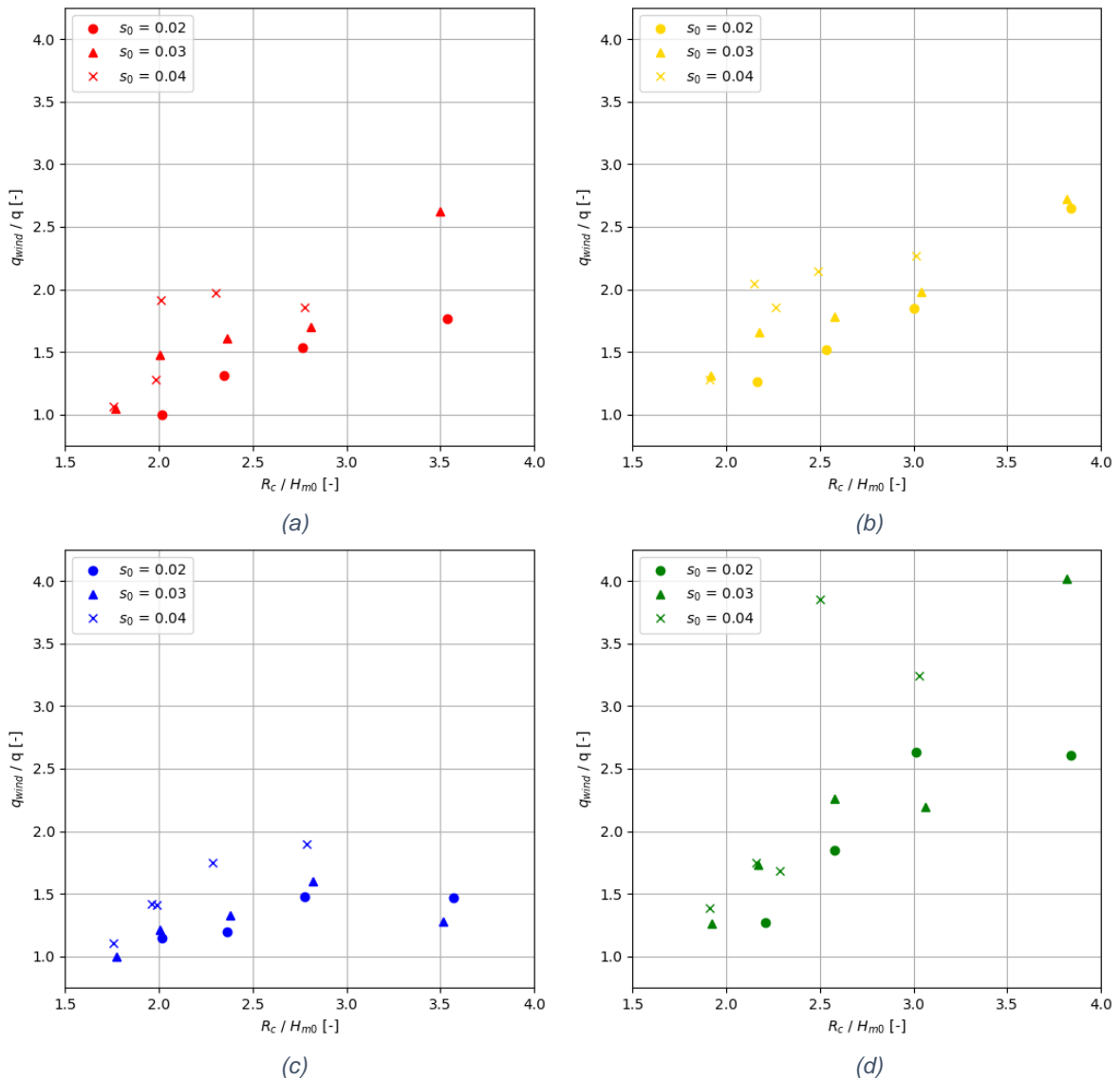


Figure 4.25: Maximum wind effect sorted on dike configuration; (a) Measurements with crest wall of 5 cm; (b) Measurements with crest wall of 8 cm; (c) Measurements with crest wall of 5 cm and promenade; (d) Measurements with crest wall of 8 cm and promenade.

Furthermore, it might not only be interesting to look at dike configurations and wave characteristics such as wave height and steepness, but also to know if the type of wave impacts the wind effect. Therefore, the breaker parameter ξ_0 was investigated. For higher breaker parameter values, the wave steepness needs to be lower, hence the overtopping discharge is larger. Consequently, it is presumed that the maximum wind effect decreases for higher breaker parameter values. Additionally, one could argue this based on the different wave types with respect to the overtopping discharge, but also lose energy while breaking (Wolters & Van Gent, 2007). Overall, plunging waves will most likely result in lower overtopping discharges than collapsing and surging waves, which lose less energy when reaching the dike crest and are related to higher breaker parameter values. From both views, Figure 4.26 is in line with the theory; lower breaker parameters seem to correspond to a higher maximum wind effect.

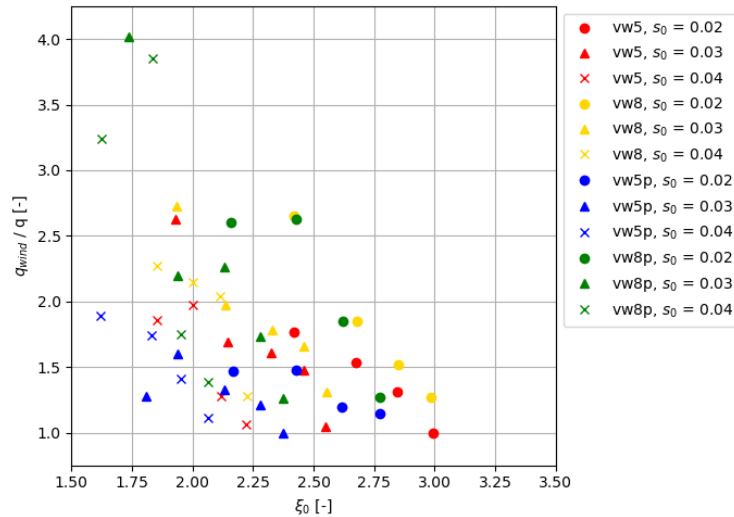


Figure 4.26: The influence of the breaker parameter on the maximum wind effect.

4.4.2 The impact of water level variations

In addition to the regular tests, a couple of test series are performed with varying water levels, which cause variations in the relative crest freeboard for the same wave characteristics and dike configuration. These tests were not analysed previously in this research. The tests were performed with a crest wall of five cm and all contained non-breaking waves. The overtopping discharge itself is in good agreement with the qualitative relation concerning the relative crest freeboard (Figure 4.27). Because the different sets of datapoints seem to be spread, for a qualitative comparison with current guidelines Equation 23 is used for the tests without wind, in which the wave steepness is added to the TAW (2002) formula. Table 4.7 indicates that adding the wave steepness results in a better fit for these measurements as well.

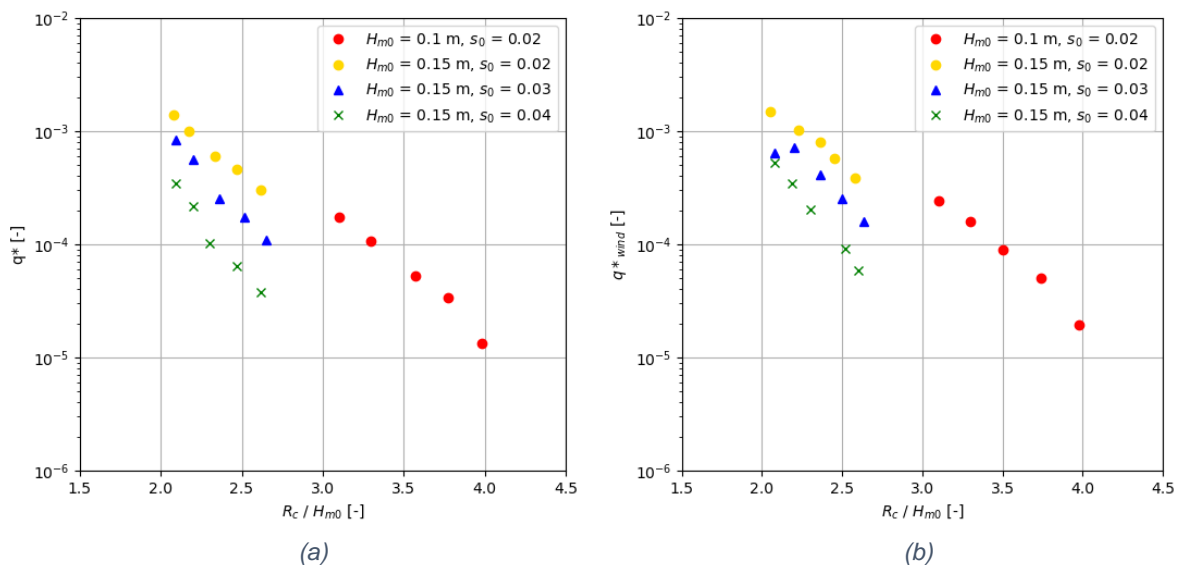


Figure 4.27: Measured overtopping discharges for different tests with variations in water level; (a) Measurements in absence of wind; (b) Measurements in presence of wind.

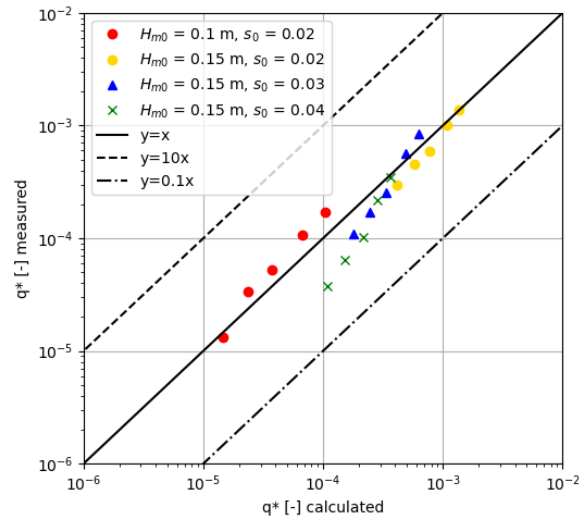


Figure 4.28: Measured overtopping discharges without wind for varied water levels compared with Equation 23.

Table 4.7: RMSLE for overtopping discharges of tests with water level variations described by TAW (2002) and the newly proposed Equation 23 (non-breaking waves).

	TAW (2002)	Equation 23
Tests with water level differences	0.4231	0.1953

Nonetheless, an interesting pattern of the maximum wind effect for these experiments can be observed (Figure 4.29). A similar overview as in Figure 4.21 is expected, but that does not seem to be true. Instead, in general the wind effect seems to have a maximum for a certain water level and decreases for higher relative crest freeboards. Moreover, there is a large variety amongst the test series. This effect is most pronounced for the 0.02 wave steepness datapoints with a significant wave height of 0.1 m. Especially the decreasing trend for decreasing water levels – hence increasing relative crest freeboards – is remarkable. Lower water levels result in low overtopping discharges, but the values in Figure 4.27 are not as low as being possibly inaccurate due to dominating scale effects, which would be the case if the values are below the lower limit of the low overtopping regime. Another observation is that two measurements resulted in a maximum wind effect which is lower than 1.0. Therefore, it is recommended to carry out more research to investigate the effect of water level variations on the maximum wind effect for a wider range of water levels and wave characteristics.

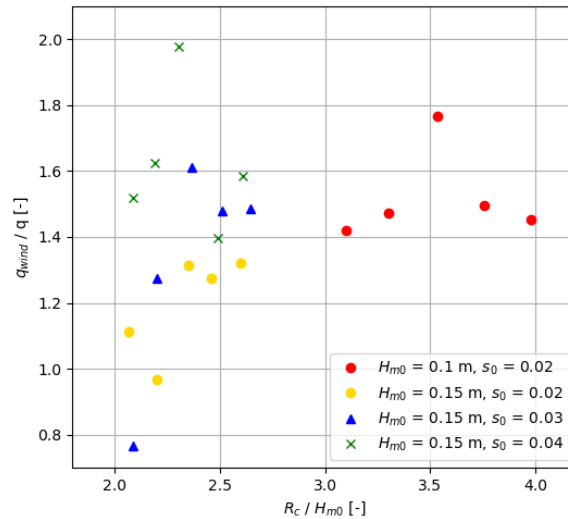


Figure 4.29: Maximum wind effect for different tests with variations in water level.

4.4.3 Creating a wind influence factor

All parameters and influence factors related to the change of the maximum wind effect are embedded in one all-embracing variable: the overtopping discharge itself. The overtopping discharge contains not only wave characteristics such as the breaker parameter, wave steepness and wave height, but also aspects of the dike configuration such as the crest freeboard, crest wall and promenade. Figure 4.30 depicts an overall relation between the overtopping discharge and the maximum wind effect. Low overtopping discharges for the situation without wind result in a large wind effect, which is in line with the theory that for low discharges there is more vertical spray. For each dike configuration, a slightly different formula can be fitted on the data, but the basis is the same (Figure 4.31). Physically, the maximum wind effect should not underrun 1.0 as that would imply a negative wind effect with a lower overtopping discharge for tests with wind. Offshore blowing winds could induce this. A vertical asymptote is defined by the overtopping discharge, which cannot be negative. In theory, one water droplet that overtops the structure due to wind, but not in the case without wind results in an infinitely large maximum wind effect. Hence, mathematically speaking, the equations' range is from 1.0 till infinity and the domain is from zero to infinity, resulting in a hyperbole.

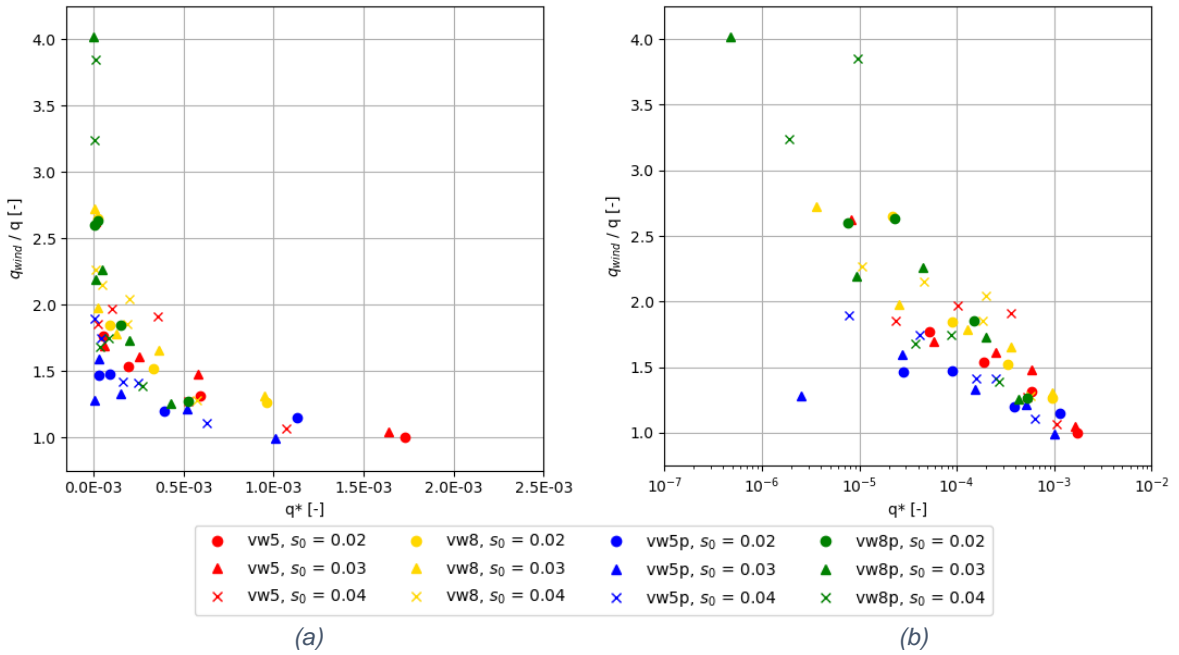


Figure 4.30: The influence of the overtopping discharge on the maximum wind effect; (a) Maximum wind effect on linear scale; (b) Maximum wind effect on logarithmic scale.

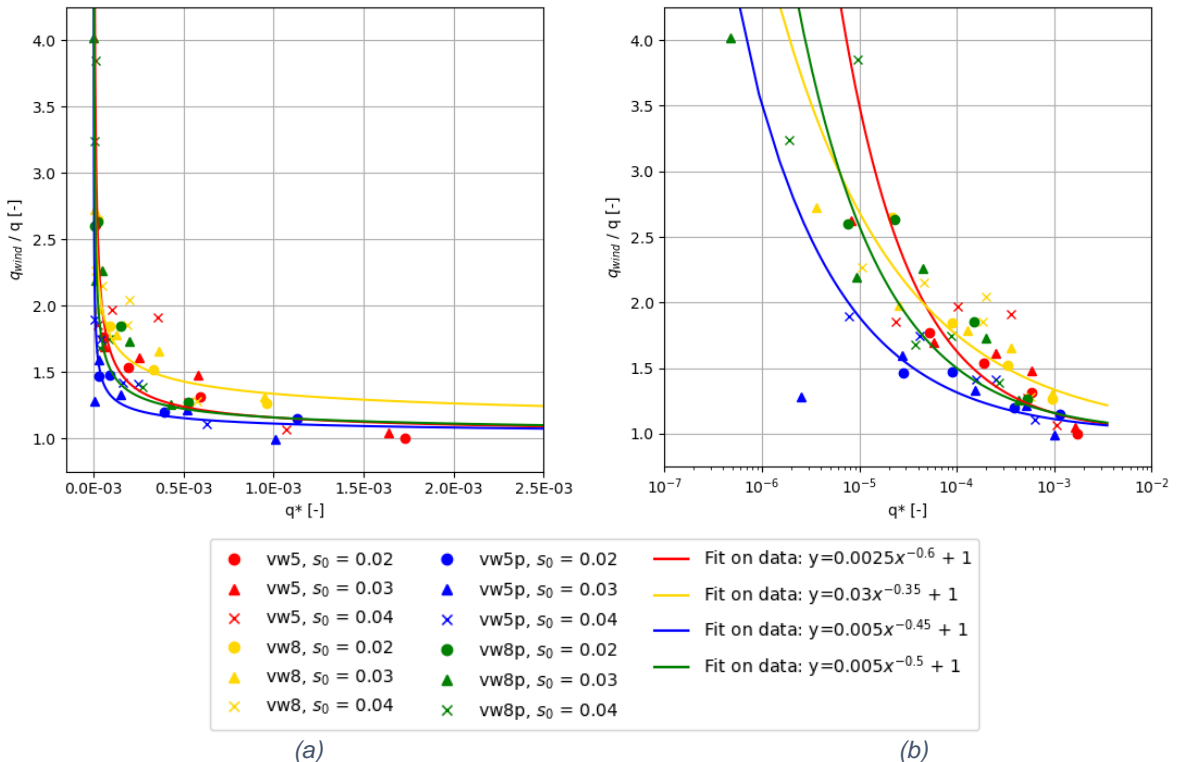


Figure 4.31: The influence of the overtopping discharge on the maximum wind effect and fitted curves (Equation 27); (a) Maximum wind effect on linear scale; (b) Maximum wind effect on logarithmic scale.

The relations shown in Figure 4.31 form the basis for a wind influence factor γ_{wind} , although the definition of this factor differs from other influence factors. Where all other influence factors are equal to or lower than 1.0, γ_{wind} increases the overtopping discharge and is defined to be larger or equal to 1.0, hence may be called an

amplification factor. The factor γ_{wind} , which is illustrated in Figure 4.31, is defined in Equation 27 for the specific dike configurations tested in this research, where $\gamma_{wind} = q_{with\ wind}/q_{without\ wind}$.

$$\gamma_{wind} = \begin{cases} 0.0025 q^{*-0.6} + 1 & \text{for crest wall of 5 cm} \\ 0.03 q^{*-0.35} + 1 & \text{for crest wall of 8 cm} \\ 0.005 q^{*-0.45} + 1 & \text{for crest wall of 5 cm and promenade of 15 cm} \\ 0.005 q^{*-0.5} + 1 & \text{for crest wall of 8 cm and promenade of 15 cm} \end{cases} \quad \text{Equation 27}$$

A more general applicable amplification factor is constructed and defined in Equation 28 and displayed in Figure 4.32, together with the 90 percent confidence interval based on the relative error between the measurements and Equation 28. This equation is based on all four dike configurations and has the advantage that upscaling to uncalibrated structures to predict the maximum wind effect is possible as well. Eventually, γ_{wind} can be employed as amplification factor to the overtopping discharge without wind to estimate the overtopping discharge with the maximum wind effect due to onshore blowing winds.

$$\gamma_{wind} = 0.011 q^{*-0.43} + 1 \quad \text{Equation 28}$$

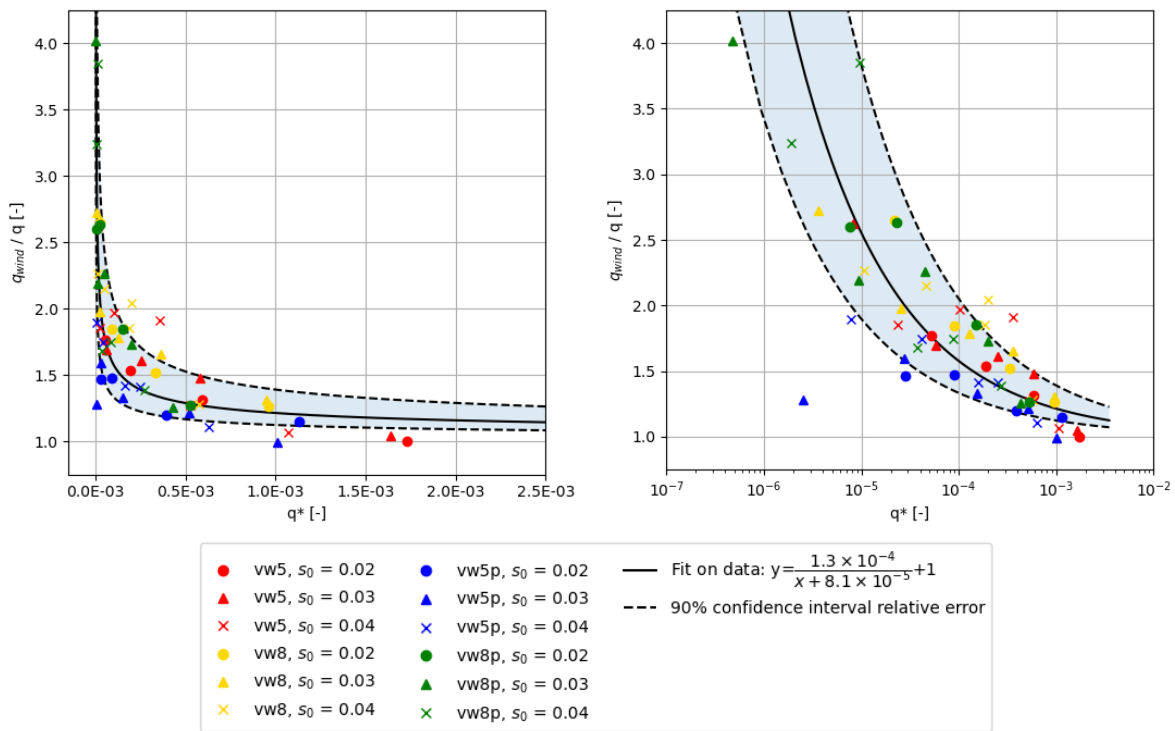


Figure 4.32: The influence of the overtopping discharge on the maximum wind effect and fitted curve (Equation 28) with the 90% confidence interval based on the relative error; (a) Maximum wind effect on linear scale; (b) Maximum wind effect on logarithmic scale.

The root-mean-squared error (RMSE) in Table 4.8 is used to define the spreading around the proposed formulas. The RMSE for the vertical wall of eight cm with promenade is very large due to the 0.03 wave steepness datapoint with overtopping discharge q^* around $4.8E-07$. Without this datapoint, the RMSE would be roughly half

(0.6001 instead of 1.2691). The RMSE for Equation 28 would reduce from 0.6150 to 0.4993 when not considering this datapoint.

Table 4.8: RMSE for the amplification factor γ_{wind} described by the newly proposed Equation 27 and Equation 28.

	Equation 27	Equation 28
All four dike configurations with wind	-	0.6150
vw5 with wind	0.4240	-
vw8 with wind	0.3897	-
vw5p with wind	0.2890	-
vw8p with wind	1.2691	-

To conclude the research, the overtopping discharges of all tests are combined in Figure 4.33 and compared with the proposed equations throughout this chapter. Especially the measurements related to the tests with wind show a good fit with respect to the proposed formula. The RMSLE per category is given in Table 4.9, together with the corresponding equation. Only for the crest element tests for breaking waves, two formulas are applied because the tests with a crest wall and promenade are prescribed by a different formula than the tests with a crest wall only.

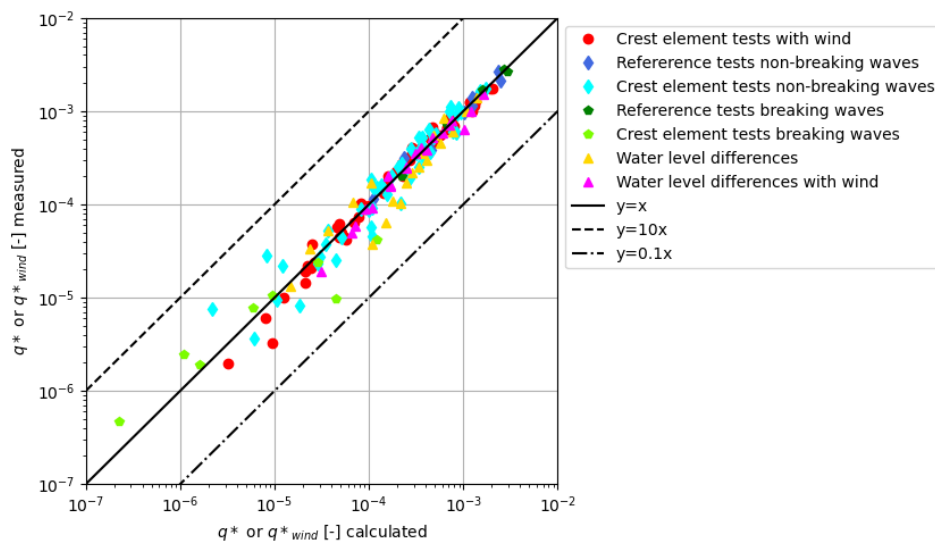
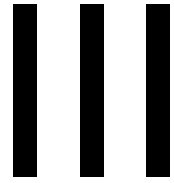


Figure 4.33: Measured overtopping discharges of all tests compared with the proposed equations in Table 4.9.

Table 4.9: RMSLE for overtopping discharges of all tests described by the newly proposed formulas in this thesis.

	Proposed equation	RMSLE value
Crest element tests with wind	Equation 28	0.1002
Reference tests non-breaking waves	Equation 23	0.0604
Crest element tests non-breaking waves	Equation 25	0.1858
Reference tests breaking waves	Equation 22	0.3409
Crest element tests breaking waves	Equation 22 and Equation 26	0.0357
Water level differences	Equation 23	0.1954
Water level differences with wind	Equation 28	0.0853



Wrap-up

5

Discussion

The discussion consists of two sections. The first part is a critical reflection on the physical model tests and the results. This contains possible inaccuracies or how the results might have been affected by certain choices made in the measurement set-up. Second, the limitations of the research are reported.

5.1 Physical model tests

When performing physical model tests, deviations in input parameters are reduced in order to retrieve reliable data. In the present research, one of the sources of uncertainty could be wave gauges, because the wave characteristics as well as the overtopping discharge are measured through these instruments. However, this error is expected to be negligible since the wave gauges measured with millimetre accuracy.

Several inaccuracies in the set-up of the physical model tests could have resulted in differences in the overtopping discharges. A one-metre-wide seadike was tested in the basin. This dike was fixed between two concrete walls that cause some friction on incident waves and a slight reduction of wave energy. To account for wall effects, the overtopping chute width (Figure 3.1) was 0.9 m, but it is unknown how much the side walls affected the overtopping discharge. Regarding the overtopping chute, a smaller chute (width of 0.5 m) was used for the tests with a large overtopping discharge to minimize the number of pumping events. However, visual observations during the tests showed that the wave run-up was not always evenly distributed over the dike width. Therefore, applying a narrow chute may lead to more spreading in the results compared to a wider chute.

Pumping events took place for a few tests. Pumping of the overtopping box negatively impacted the measurements as the pumping time was cut out of the time series and had to be minimised or avoided if possible. The tests with the largest wave height and wave length ($H_{m0} = 0.2 \text{ m}; s_0 = 0.02$) resulted in a large amount of overtopping discharge requiring so intense pumping that the results are considered inaccurate. For the other tests with lower pumped discharges, it did not lead to unexpected outliers. Nevertheless, these overtopping discharges could have been influenced to some extent. The wave characteristics at the toe of the structure were constantly measured throughout the complete test, but when the pumping started this time interval was removed from the overtopping discharge measurement signal. The average overtopping discharge did not take into account waves attacking the dike during pumping, which could either have led to a slight over- or underestimation of the overtopping discharge.

Another point of discussion regarding the set-up of the physical model tests is the paddle wheel used to simulate wind. In theory, every water particle that exceeds the crest wall height during vertical splashing is captured by the paddle wheel and transported to the overtopping box. However, reality differs from this theory on two aspects. First, during the tests, the paddle wheel was placed above the crest wall as close as possible. The closer the paddle wheel is to the crest wall, the more vertical splashing is included in the total overtopping volume, but some space must be left to allow for the wheel to rotate. It is however expected that this effect is negligible, because the space is only a few millimetres. Second, the distance between the blades of the rotating paddle wheel created time for water droplets to land in the basin instead of being transported to the overtopping box via the paddle wheel. Mainly low overtopping discharges, for which scale effects might have been present, were affected as some water droplets that were missed by the paddle wheel had more impact on the total volume than in case of large overtopping discharges. Wolters and Van Gent (2007) determined an optimal rotation speed of that would generate an estimated water transport efficiency of more than 90 percent, which is used in the present research. For lower rotation speeds, the time between the subsequent blades becomes large enough for water droplets to land in the basin in front of the dike instead of being hit by the blades, whereas for higher speeds the wheel would transport the water back to the front into the basin.

Finally, for each test approximately 1,000 waves were generated to schematise a full JONSWAP spectrum. Because each series of 1,000 waves was unique, deviations in overtopping discharges for the same overall wave characteristics could have arisen. One test series using the paddle wheel, but without pumping, was repeated several times to quantify the differences. Table 5.1 displays the outcome and input variables, where deviations were measured in overtopping discharge of almost 10 percent for these tests, even if the input variables were the same (test numbers 2 and 4). On logarithmic scale, however, deviations of 10 percent are relatively small. It has to be mentioned that these tests were performed with an overtopping chute of 0.5 m, which might have caused the deviations as described in this section. Another explanation could be the paddle wheel as described above.

Table 5.1: One test series repeated to measure the deviations in overtopping discharge.

Test number	H_{m0} [m]	$T_{m-1,0}$ [s]	s_0 [-]	q [m ³ /s/m]
1	0.148	1.777	0.03002	1.790E-05
2	0.148	1.782	0.02985	2.090E-05
3	0.148	1.781	0.02988	2.029E-05
4	0.148	1.782	0.02985	1.922E-05

5.2 Applicability and limitations of the research

This research focussed on smooth seadikes with a slope of $\tan(\alpha) = 1:3$. A crest wall, with and without promenade, is tested as a climate adaptation measure and the maximum wind effect is studied for the situation of two crest wall heights and a single value for the promenade. The results show an increase in the maximum wind effect for increasing crest wall heights. Conversely, including a promenade does not lead to an increase in the maximum wind effect for all crest wall heights. For lower crest walls, the space above the promenade could be filled with water leading to less vertical

splash when waves hit the crest wall or overshooting could occur if the ratio of the crest wall height over the promenade width is lower than the outer dike slope. The maximum wind effect is therefore lower than for the situation without promenade. Because this phenomenon is less likely to occur with higher crest walls, it raises the question which crest wall height starts the transition from a decrease to an increase in maximum wind effect when a promenade is added. Moreover, the promenade width itself might also have had influence on this turning point. The presented results and equations for both the maximum wind effect, the reference tests and crest element tests may be accurate outside the range of the test conditions, but the validity is unknown. Based on the present research, the crest wall height for which the maximum wind effect starts to enlarge when adding a promenade cannot be derived. Furthermore, it is advised to validate the proposed equations to a larger database, also because the number of tests with breaking waves was relatively limited.

Next to the dike configurations, the methodology of using a paddle wheel to mechanically simulate wind is limited to the maximum wind effect only, whereas, in reality, wind is highly variable in space, time and strength. Although investigating the maximum wind effect is the governing situation for designing a seadike, wind also influences processes such as the wave characteristics and run-up. The TAW (2002) equations used for determining the maximum wind effect do not account for the wind effect on the wave run-up. Consequently, the quantification of the maximum wind effect might change due to processes that are not covered by the paddle wheel.

The water level is also of importance when the governing situation is concerned. For seadikes, water level variations are relevant due to tides, but also due to storm set-up. The physical model tests performed with varying water levels showed a not-expected pattern, where for increasing relative crest freeboards the maximum wind effect did not increase constantly but seemed to have a limit. An explanation could be that for lower overtopping discharges the paddle wheel missed some water droplets, which did not end up in the overtopping box, and therefore resulted in a lower overtopping discharge. Yet, this would more likely be occasional rather than structural. Hence, the water level differences that are inspected in subsection 4.4.2 should be subjected to further research and reliable conclusions are limited to a water depth of 0.7 m and the tests that have proven to be reliable in chapter 4.

6

Conclusions and recommendations

This chapter presents the conclusions of the research, which answer the research question and sub-questions. The second section covers recommendations for further research.

6.1 Conclusions

As defined in section 1.3, the objective of the research was to investigate the maximum wind effect on wave overtopping at dikes. Furthermore, crest elements may influence wave overtopping and the wind effect. To this end, the following research question was covered in this master thesis. The sub-questions, which together answer the research question, are examined in the following subsections.

What is the maximum wind effect on wave overtopping at dikes with crest elements?

The present study was designed to determine the effect of the wind on the overtopping discharge and the effect of adding crest elements. Physical model tests revealed that the maximum wind effect is distributed between 1.0 and 4.0 for the combination of wave characteristics and dike configurations tested in this research. For lower discharges that are not tested in this study, the maximum wind effect could exceed the value of 4.0. The main answer to the research question is presented as an equation that defines the amplification factor between the overtopping discharge with and without onshore blowing wind. Because this amplification factor γ_{wind} ($= q_{with\ wind}/q_{without\ wind}$) is a function of the overtopping discharge without wind, changes in wave characteristics and dike configuration are included. Nevertheless, for each dike configuration, a more specific formula can be fitted on the data, but the general applicable formula (Equation 28) – thus answer to the research question – is repeated here.

$$\gamma_{wind} = 0.011 q^{*-0.43} + 1 \quad \text{Equation 28}$$

The parameter ranges for which physical model tests were conducted, are displayed in Table 6.1. This includes the wave characteristics, model set-up variables and results such as the overtopping discharge and maximum wind effect.

Table 6.1: Parameter ranges of the test programme used in the analysis and the results.

Parameter	Symbol	Value/Range
Seaward slope angle [-]	$\tan(\alpha)$	1:3
Relative crest freeboard [-]	R_c/H_{m0}	1.49 – 3.98
Relative promenade width [-]	B/H_{m0}	0 – 1.53
Wave steepness [-]	s_0	0.020 – 0.042
Breaker parameter [-]	ξ_0	1.62 – 3.00
Crest freeboard [m]	R_c	0.2 – 0.48
Crest wall height [m]	h_{wall}	0, 0.05 & 0.08
Incident significant wave height at the toe [m]	H_{m0}	0.098 – 0.202
Promenade width [m]	B	0 & 0.15
Water depth [m]	d	0.6 – 0.85
Mean spectral wave period [s]	$T_{m-1,0}$	1.248 – 2.357
Overtopping discharge (without wind) [-]	q^*	4.76E-07 – 1.73E-03
Overtopping discharge (with wind) [-]	q_{wind}^*	1.94E-06 – 1.77E-03
Maximum wind effect [-]	γ_{wind}	1.0 – 4.0

6.1.1 How do wave characteristics, such as the significant wave height and wave steepness, influence wave overtopping at dikes with and without crest elements?

The overtopping discharge is influenced by various wave characteristics. The TAW (2002) formulas quantify the overtopping discharge and distinguish between breaking and non-breaking waves. For both type of waves, the significant wave height H_{m0} plays an important role. Increasing the significant wave height results in an increase in overtopping discharge. The opposite is true for the wave steepness s_0 , where a rise in wave steepness results in less overtopping discharge. This dependency on the wave steepness is seen directly in the data, but also via the breaker parameter ξ_0 . A high wave steepness corresponds to a low breaker parameter. Plunging breakers with a lower breaker parameter lose energy while breaking and result in less overtopping discharge compared to collapsing or surging breakers with higher breaker parameters. Van Gent et al. (2022) also concluded that the wave steepness affects the overtopping discharge for breakwaters, but it is not uniformly included in the TAW (2002) formulas. For breaking waves, the breaker parameter is incorporated. Yet, for non-breaking waves this wave steepness dependency is absent.

The investigation of seadikes with and without crest elements, but without wind, resulted in several formulas, categorised by wave type. The formulas for tests with crest elements are presented in the next subsections, but Equation 22 and Equation 23 are proposed for breaking and non-breaking waves, respectively, that overtop at dikes without crest elements. Therefore, γ_v equals 1.0 in this situation.

$$\frac{q}{\sqrt{g} H_{m0}^3} = \frac{0.067}{\sqrt{\tan(\alpha)}} \gamma_b \cdot \xi_0 \cdot \exp\left(-4.7 \frac{R_c}{H_{m0}} \frac{1}{\xi_0 \cdot \gamma_b \cdot \gamma_f \cdot \gamma_\beta \cdot \gamma_v}\right) \quad \text{Equation 22}$$

$$\frac{q}{\sqrt{g} H_{m0}^3} = 1.1 \cdot 10^{-4} \cdot s_0^{-2} \cdot \exp\left(-2.3 \frac{R_c}{H_{m0}} \frac{1}{\gamma_f \cdot \gamma_\beta}\right) \quad \text{Equation 23}$$

6.1.2 What is the influence of the height of crest elements on the overtopping discharge?

The influence of crest elements, such as a vertical crest wall, promenade, parapet and combinations between those were investigated previously by Van Doorslaer et al. (2015). However, their research focussed on non-breaking waves only. The outcome was a definition of influence factors for crest elements applied on the TAW (2002) equation. The findings of the present research complement those of earlier studies by employing the wave steepness dependency in Equation 25 and do not only incorporate non-breaking waves, but breaking waves as well. The same expression of the influence factor for non-breaking waves is applied here to breaking waves.

Regarding non-breaking waves, the proposed influence factors for both crest wall with promenade and crest wall solely are a good fit and are incorporated as follows:

$$\frac{q}{\sqrt{g} H_{m0}^3} = 1.1 \cdot 10^{-4} \cdot s_0^{-2} \cdot \exp\left(-2.3 \frac{R_c}{H_{m0}} \frac{1}{\gamma_f \cdot \gamma_\beta \cdot \gamma^*}\right) \quad \text{Equation 25}$$

where γ^* is γ_v or $\gamma_{prom,v}$ as defined in subsection 2.3.4.

Regarding the sub-question, a higher crest wall causes less overtopping discharge, which is in line with the theory that the influence factor becomes lower. Hence there is further reduction on the overtopping discharge for higher crest walls. Moreover, the crest wall height is embedded in the crest freeboard R_c as well, leading to the same result. This study demonstrates that this concept is generally applicable for non-breaking as well as for breaking waves. For breaking waves, the exponential coefficient of the TAW (2002) formula is modified, which results in Equation 26 for a crest wall only although this formula is based on very little data.

$$\frac{q}{\sqrt{g} H_{m0}^3} = \frac{0.067}{\sqrt{\tan(\alpha)}} \gamma_b \cdot \xi_0 \cdot \exp\left(-5.5 \frac{R_c}{H_{m0}} \frac{1}{\xi_0 \cdot \gamma_b \cdot \gamma_f \cdot \gamma_\beta \cdot \gamma_v}\right) \quad \text{Equation 26}$$

6.1.3 What is the influence of the position of crest elements on the overtopping discharge?

According to the data analysis, the theory behind adding a promenade in front of the crest wall is in line with previous research. Overall, this study strengthens the idea that the promenade has a reducing effect on the overtopping discharge. For the promenade with a width of 0.15 m tested, the overtopping formula for non-breaking waves is Equation 25 from the previous subsection. Nonetheless, different formulas apply for breaking waves depending on the crest element. For a crest wall with promenade, Equation 22 fits the measurement, where the influence factor $\gamma_{prom,v}$ should be added in the exponent.

6.1.4 How do wave characteristics, such as the significant wave height and wave steepness, influence the maximum wind effect on wave overtopping at dikes with crest elements?

From the overtopping discharge, which is compared with previous research, the focus is shifted towards the maximum wind effect. It is expected for low overtopping discharges to have more vertical splash when waves hit the crest element, hence the maximum wind effect is large. The results from the physical model tests indeed identify this behaviour. Both an increase in significant wave height and decrease in wave steepness are related to a decrease in maximum wind effect due to large overtopping discharges. The type of breaker indicated by the breaker parameter is also in line with this concept and visual observations during the tests match as well. Surging or collapsing waves with a low wave steepness (thus high breaker parameter) seem to overflow the crest element more easily than waves that tend to be more plunging, hence causing significantly less vertical splash.

6.1.5 What is the influence of the height of crest elements on the maximum wind effect on wave overtopping at dikes with crest elements?

Raising the crest wall height alters the maximum wind effect more than adding a promenade. For the dike configuration without a promenade, the maximum wind effect almost doubles when the crest wall height is raised from five to eight cm. In the case that a promenade is present, and the crest wall height is increased, the maximum wind effect could even enhance with a factor 3.1. Therefore, in general a positive correlation exists between raising the crest wall height and the maximum wind effect. This finding is in line with previous research, stating that the maximum wind effect increases for lower overtopping discharges, hence higher crest walls.

6.1.6 What is the influence of the position of crest elements on the maximum wind effect on wave overtopping at dikes with crest elements?

The influence of a promenade on the maximum wind effect showed interesting results. Following the same line of reasoning as for the crest wall height and wave characteristics, it is expected that adding a promenade enhances the maximum wind effect since it reduces the overtopping discharge. The experiments revealed that this is only true for high crest walls, where introducing a promenade extends the maximum wind effect with a factor up to 1.8. Lower crest walls create an area above the promenade from the seaward slope towards the crest element that may be filled with water from the front part of a wave. If this is the case, the remaining part of the wave will more easily overflow the crest element without creating any vertical splash. The maximum wind effect will therefore be lower.

6.2 Recommendations

There are multiple directions for future research. Future research could be conducted to determine the effectiveness of variations of crest element geometries. Van Doorslaer et al. (2015) proposed an influence factor for a parapet as well, which can be combined with a crest wall with promenade. For the situation without wind, these influence factors need further validation on breaking waves, for instance, since they were initially derived for non-breaking waves only and the dataset on breaking waves

was relatively small in this research. Additionally, as shown in this study, adding a promenade to reduce the overtopping discharge does not always result in a higher maximum wind effect. Therefore, it is recommended to examine more variations in crest element geometries focussing on the influence on the maximum wind effect. Also, the proposed equations are valid for the tested conditions, so it is recommended to validate these against a larger dataset.

Furthermore, experiments using a broader range of seaward slope angles could shed more light on the applicability of the influence factor for the maximum wind effect. This research focussed on seadikes with an outer slope angle of $\tan(\alpha) = 1:3$, but for less steep dikes the maximum wind effect might significantly differ. The reason is that, although the slope is included in the TAW (2002) overtopping formulas, the waves break differently on gentler slopes, which affects the overtopping discharge and the vertical splash when waves hit the crest element. Also, the wave steepness is included in the newly proposed equations in this study, but to account for different slope angles, it has to be researched if the breaker parameter would be a better choice. Investigating multiple slope angles widens the applicability of the wind influence factor.

As explained in subsection 4.4.2, water level differences may lead to unexpected changes in the maximum wind effect. This behaviour in itself is already a reason to carry out more research, but from a practical point of view it is also relevant. In reality, the water level at the seaside of the dike is constantly changing. Not only the tide creates water level variations, but storms and wind in general do so as well. In addition to the water level variations, an increasing amount of studies is performed to investigate the effect of different climate adaptation measures and combinations of those. The contribution of these measures to the overtopping discharge influences the maximum wind effect.

The present study focussed on wave overtopping for specific wave conditions at the toe, not on the effect of wind on the wave conditions itself. Moreover, this research only focussed on the maximum wind effect, which is a case valid for very strong onshore winds only. However, wind scaling might be difficult if the maximum wind effect is not researched (De Waal et al., 1996). Therefore, field measurements could be performed to validate the small-scale physical model test results. The advantage of these field measurements is that the variability of wind can be considered. The wind direction and strength are out of the scope for this research, but future studies regarding the role of the variability of wind would be worthwhile.

Throughout the research, the overtopping discharge is used. It describes the average volume of water overtopping a dike during a certain time period. However, in order to determine the strength of the dike, hence the resistance against dike failures, individual overtopping waves are important as well. Individual waves may result in excessively large overtopping volumes exceeding the average discharge. Although for large overtopping discharges this study proves that the maximum wind effect is low, the functionality of different crest elements might need to be further explored.

References

- Bakkenist, S., Van Dam, O., Van der Nat, A., Thijs, F., & De Vries, W. (2012). *Flood defense system inspection manuals*.
- Chen, W., Van Gent, M. R. A., Warmink, J. J., & Hulscher, S. J. M. H. (2019). The influence of a berm and roughness on the wave overtopping at dikes. *Coastal Engineering* 156, <https://doi.org/10.1016/j.coastaleng.2019.103613>.
- Chen, W., Warmink, J. J., Van Gent, M. R. A., & Hulscher, S. J. M. H. (2021). Numerical investigation of the effects of roughness, a berm and oblique waves on wave overtopping processes at dikes. *Applied Ocean Research* 118, <https://doi.org/10.1016/j.apor.2021.102971>.
- Chowdhury, S. D., Zhou, J. G., Qian, L., Causon, D., Mingham, C., Pullen, T., Hu, K., Russell, M., Manson, S., Stewart, D., Wood, M., Winter, H., & Joly, A. (2020). Wind effects on wave overtopping at the vertical sea defence. *Coastal Engineering Proceedings*, (36v), papers.40. <https://doi.org/10.9753/icce.v36v.papers.40>.
- De Lange, P. (2022). *Storm Corrie zorgt enkel op zee voor problemen, op vasteland weinig overlast*. de Volkskrant. <https://www.volkskrant.nl/nieuws-achtergrond/storm-corrie-zorgt-enkel-op-zee-voor-problemen-op-vasteland-weinig-overlast-bb7e6041/>
- De Waal, J. P., Tönjes, P., & Van der Meer, J. W. (1996). Wave Overtopping of Vertical Structures including Wind Effect. *Proceedings of the 25th Int. conf. on Coastal Engineering*, pp. 2216-2229, <https://doi.org/10.9753/icce.v25.%25p>.
- Deltares. (n.d.). *Pacific Basin Deltares*. <https://www.deltares.nl/en/facilities/pacific-basin-2/>
- Den Bieman, J. P., Van Gent, M. R. A., & Van den Boogaard, H. F. P. (2020). Wave overtopping predictions using an advanced machine learning technique. *Coastal Engineering* 166, <https://doi.org/10.1016/j.coastaleng.2020.103830>.
- EurOtop. (2018). Manual on wave overtopping of sea defences and related structures. Van der Meer, J.W., Allsop, N.W.H., Bruce, T., De Rouck, J., Kortenhaus, A., Pullen, T., Schüttrumpf, H., Troch, P., & Zanuttigh, B. www.overtopping-manual.com.
- Holthuijsen, L. H. (2007). *Waves in oceanic and coastal waters*. Cambridge University Press.
- Klaassen, R. (2022). *Teruglezen liveblog: storm Corrie trok over Nederland*. Weerplaza. <https://www.weerplaza.nl/weerinhethetnieuws/live-blog/teruglezen-liveblog-storm-corrie-zorgt-voor-onstuimige-maandagtro/7500/>
- Lorke, S., Bornschein, A., Schüttrumpf, H., & Pohl, R. (2012). *Influence of wind and current on wave run-up and wave overtopping*, <http://resolver.tudelft.nl/uuid:73cb6cbe-8931-4499-b4d6-aa31548f5dda>.
- Ma, C., Zhao, J., Ai, B., Sun, S., & Yang, Z. (2022). Machine Learning Based Long-Term Water Quality in the Turbid Pearl River Estuary, China. *Journal of Geophysical Research: Oceans* 127, <https://doi.org/10.1029/2021JC018017>.
- Marsman, E. R. A., Hoogland, K. J., & Van der Zijpp, N. J. (2007). *Stormverslag Petten 18 januari 2007*.
- Schiereck, G. J., & Verhagen, H. J. (2019). *Introduction to Bed, bank and shore protection*. Delft Academic Press / VSSD.
- TAW. (2002). *Technical report wave run-up and wave overtopping at dikes*.

- Van Doorslaer, K., De Rouck, J., Audenaert, S., & Duquet, V. (2015). Crest modifications to reduce wave overtopping of non-breaking waves over a smooth dike slope. *Coastal Engineering* 101, pp. 69-88, <http://dx.doi.org/10.1016/j.coastaleng.2015.02.004>.
- Van Gent, M. R. A. (2002). Wave overtopping events at dikes. *World Sci. ICCE 2002* 2, <https://doi.org/10.1142/9789812791306>.
- Van Gent, M. R. A. (2019). Climate adaption of coastal structures. *SCARC2019 - International Short Course/Conference on Applied Coastal Research*.
- Van Gent, M. R. A. (2020). Influence of oblique wave attack on wave overtopping at smooth and rough dikes with a berm. *Coastal Engineering* 160, <https://doi.org/10.1016/j.coastaleng.2020.103734>.
- Van Gent, M. R. A., Wolters, G., & Capel, A. (2022). Wave overtopping discharges at rubble mound breakwaters including effects of a crest wall and a berm. *Coastal Engineering* 176, <https://doi.org/10.1016/j.coastaleng.2022.104151>.
- Visser, E. (2022). Storm 'Corrie' trekt maandag over ons land. RTV NOF. <https://www.rtvnof.nl/storm-corrie-trekt-maandag-over-ons-land/554948/>
- Wolters, G., & Van Gent, M. R. A. (2007). Maximum wind effect on wave overtopping of sloped coastal structures with crest elements. *Proceedings of 5th Coastal Structures Conference*, pp. 1263-1274, https://doi.org/10.1142/9789814282024_0111.

IV

Appendices

A

Technical drawing model set-up

The physical model set-up is schematically presented in section 3.1, but a more detailed picture is given in this appendix. A front, side and top view with dimensions (in millimetres) drawn to scale illustrate the structure in Figure A.1, Figure A.2 and Figure A.3, respectively. The colours indicate the different elements, where the paddle wheel is shown in blue, the dike slope and crest elements in green, the overtopping chute in olive-green and the overtopping box in red. Components such as concrete wall on both sides of the dike and the construction for keeping the paddle wheel in place are displayed in black.

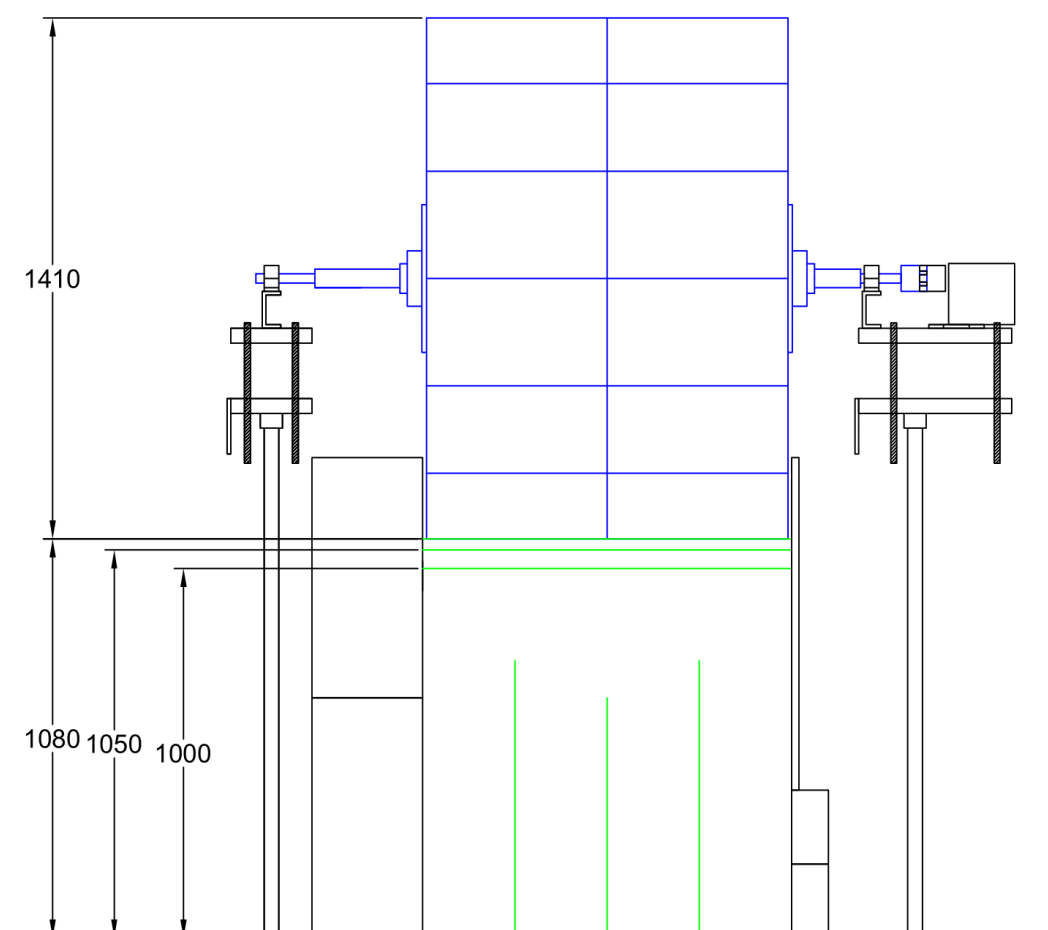


Figure A.1: Front view of the model set-up, which contains the dimensions of the paddle wheel (blue) and the seadike (green) with and without the two crest walls (W. Stet, personal communication, March, 2022).

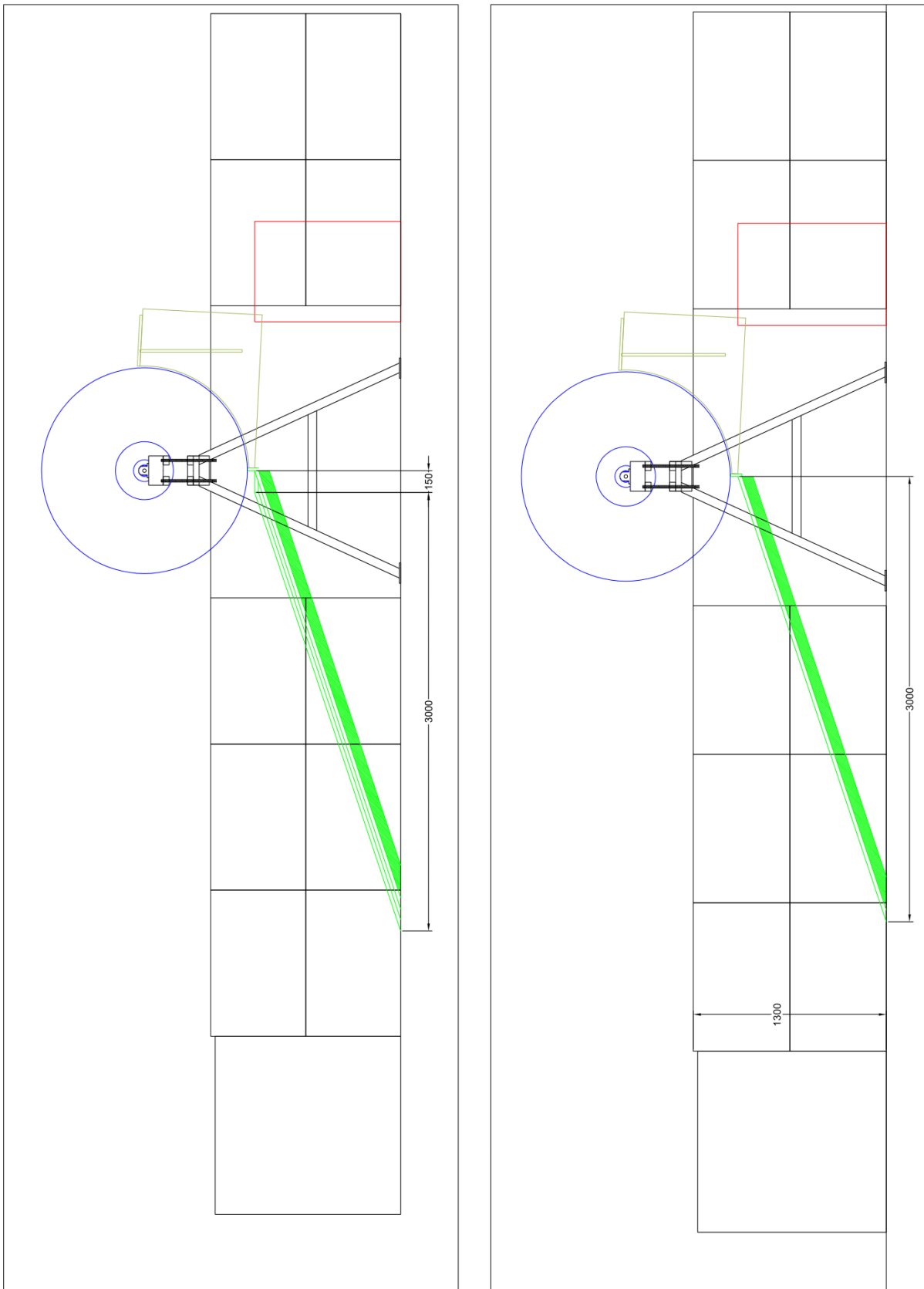


Figure A.2: Side view of the model set-up, which contains dimensions of the promenade, the concrete walls on both sides of the dike and the dike length (W. Stet, personal communication, March, 2022).

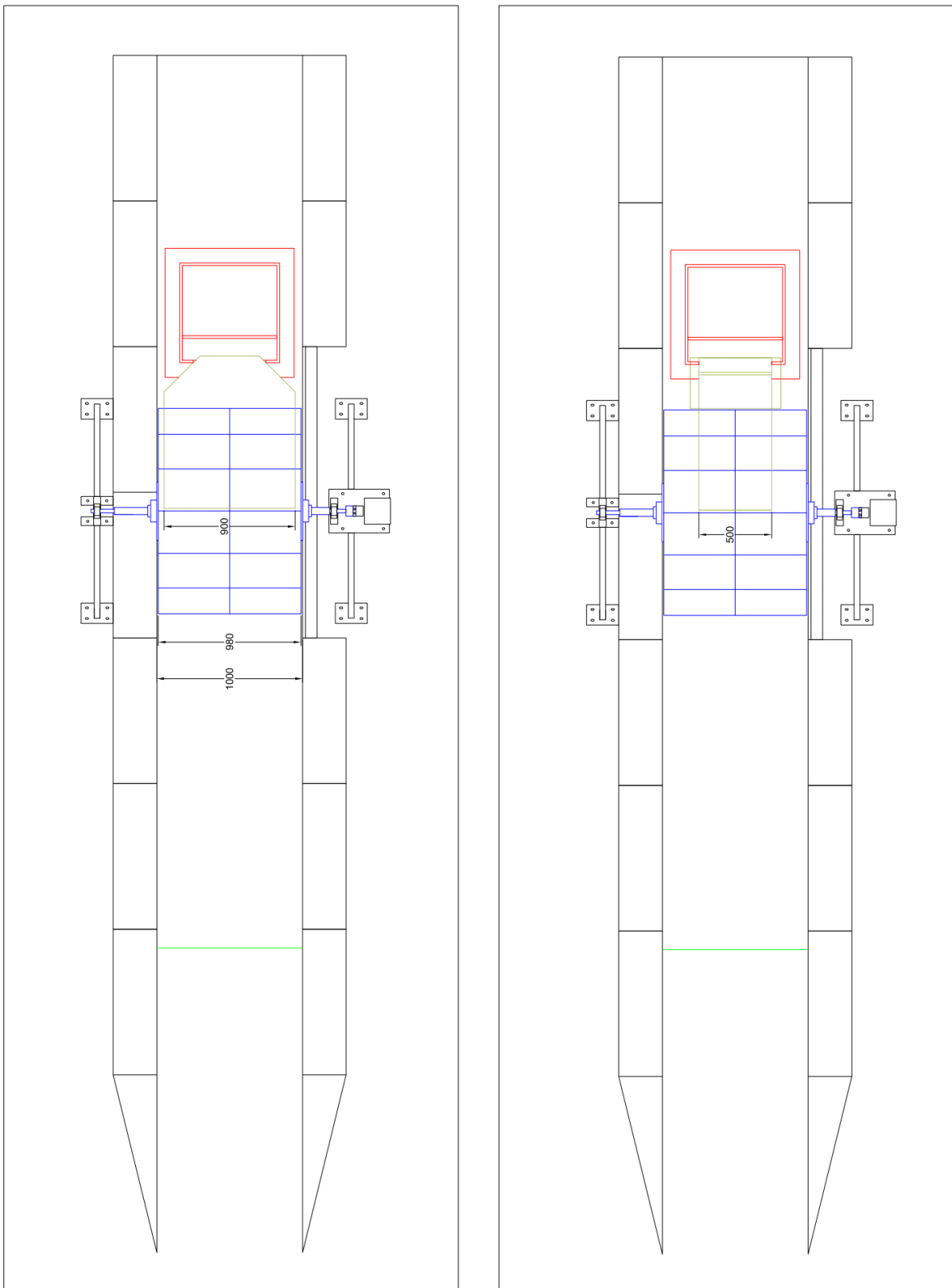


Figure A.3: Top view of the model set-up, which contains the dimensions of the dike width, the width of the paddle wheel and the two different overtopping chutes (W. Stet, personal communication, March, 2022).

B

Pictures from the test facility

To get a more complete overview of the Pacific Basin as a test facility and the model set-up, multiple pictures are added to this appendix.



Figure B.1: Side view; dike configuration with a crest wall and promenade with paddle wheel.



Figure B.2: Front view; dike configuration with a crest wall and promenade with paddle wheel.



Figure B.3: Side view; dike configuration with a crest wall with paddle wheel.

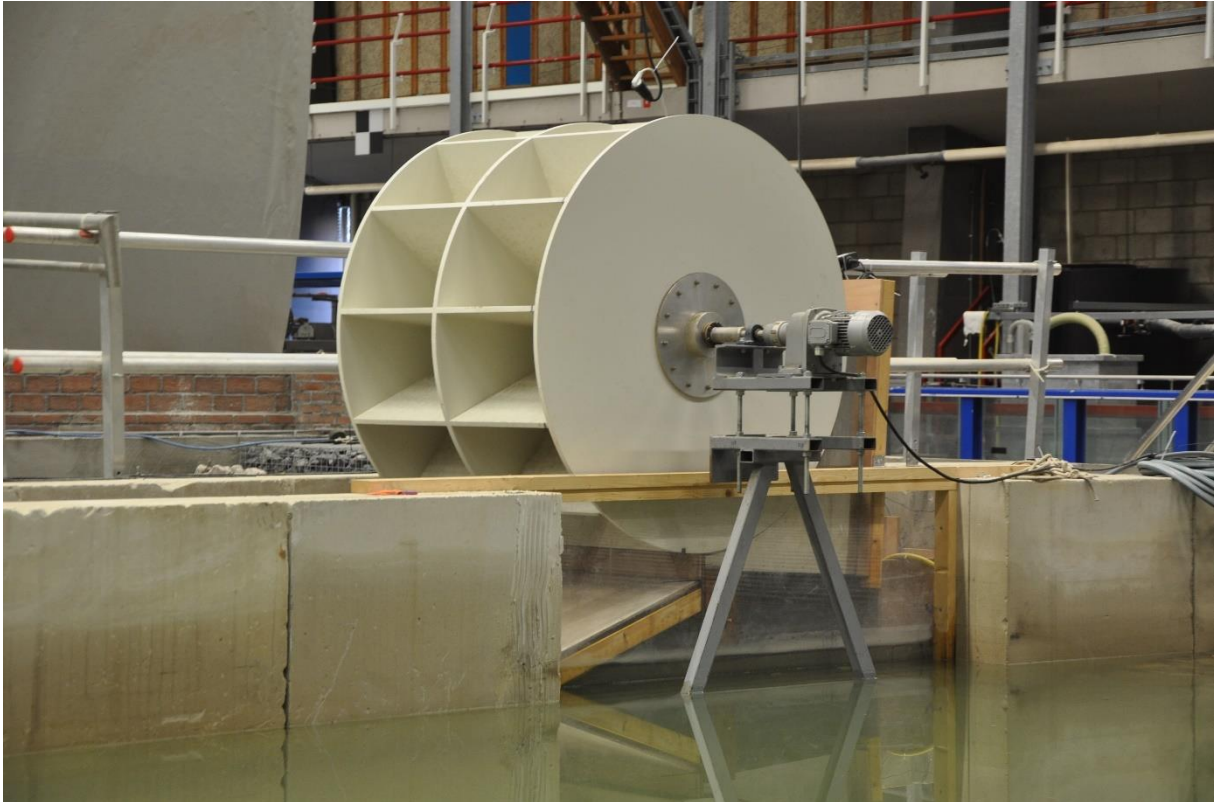


Figure B.4: Side view; dike configuration with a crest wall with paddle wheel.

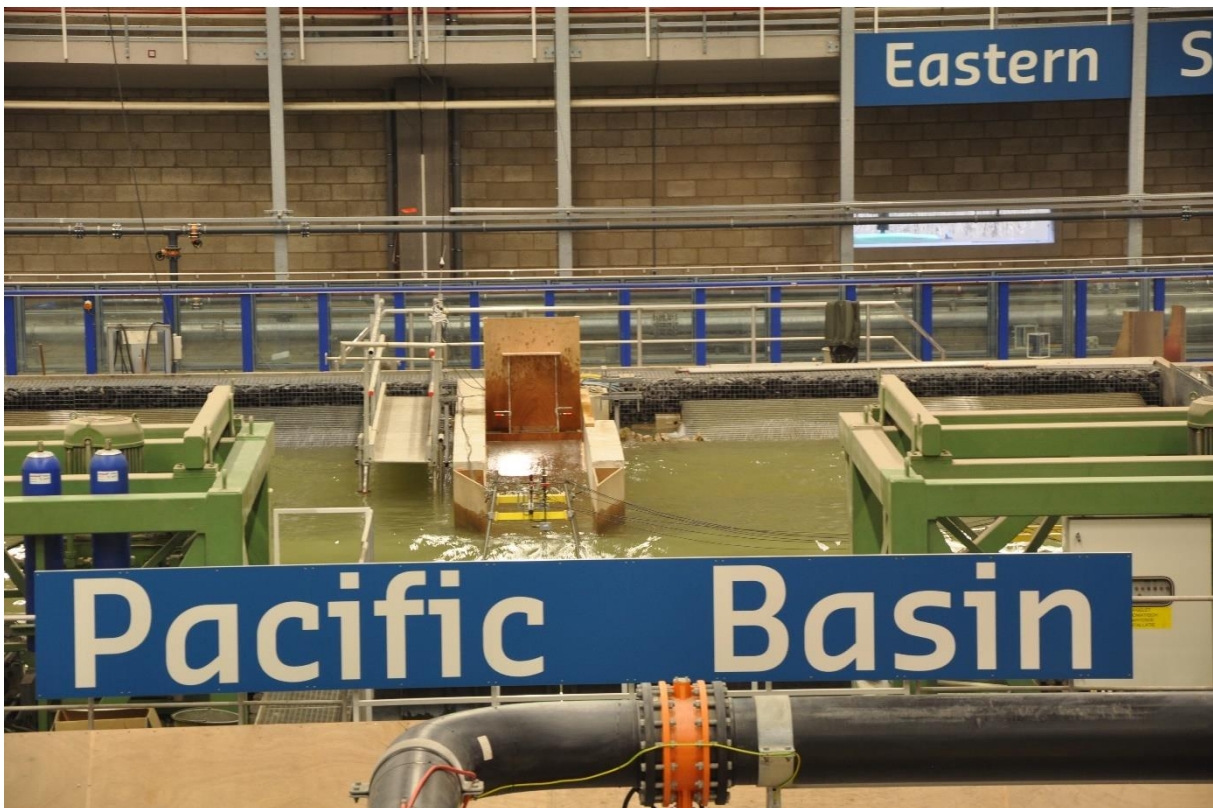


Figure B.5: General overview of the basin with the machines of the wave generator in green; dike configuration with a crest wall.



Figure B.6: Front view with the three wave gauges measuring the wave height and period in front of the dike; dike configuration with a crest wall.

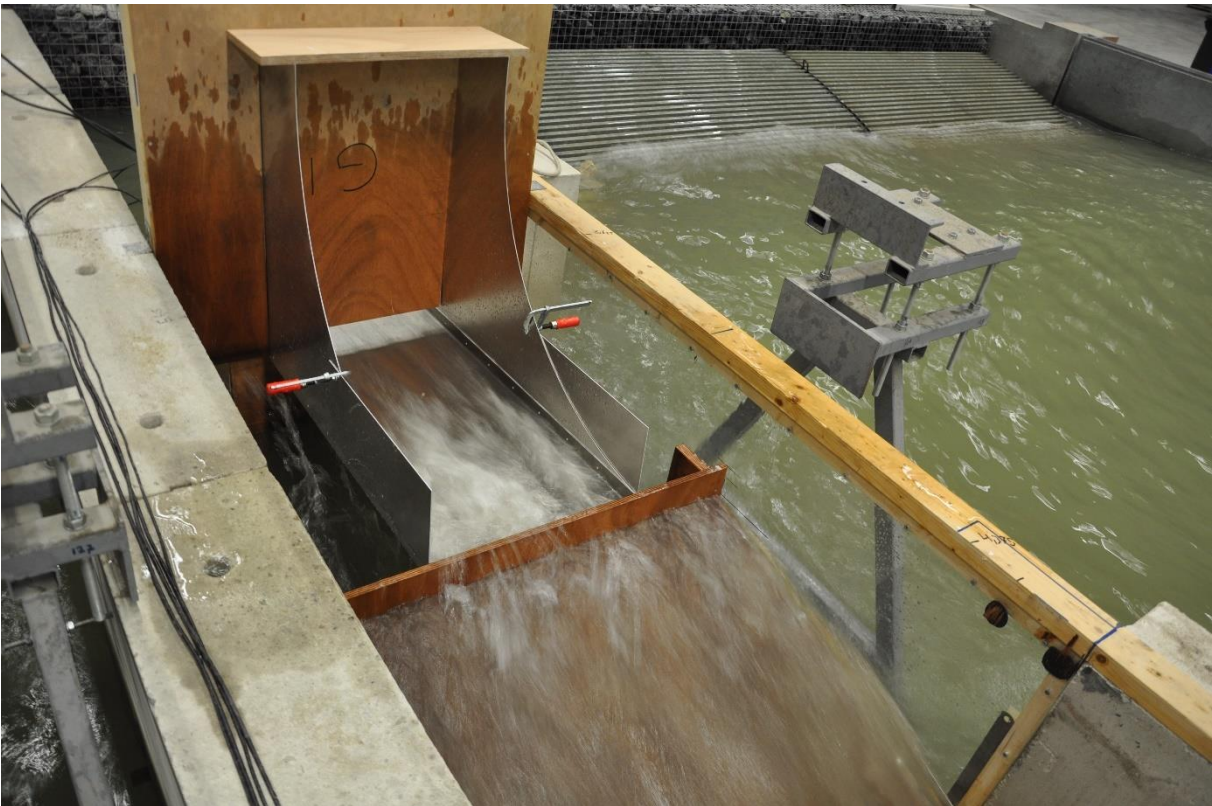


Figure B.7: Side view; dike configuration with a crest wall.

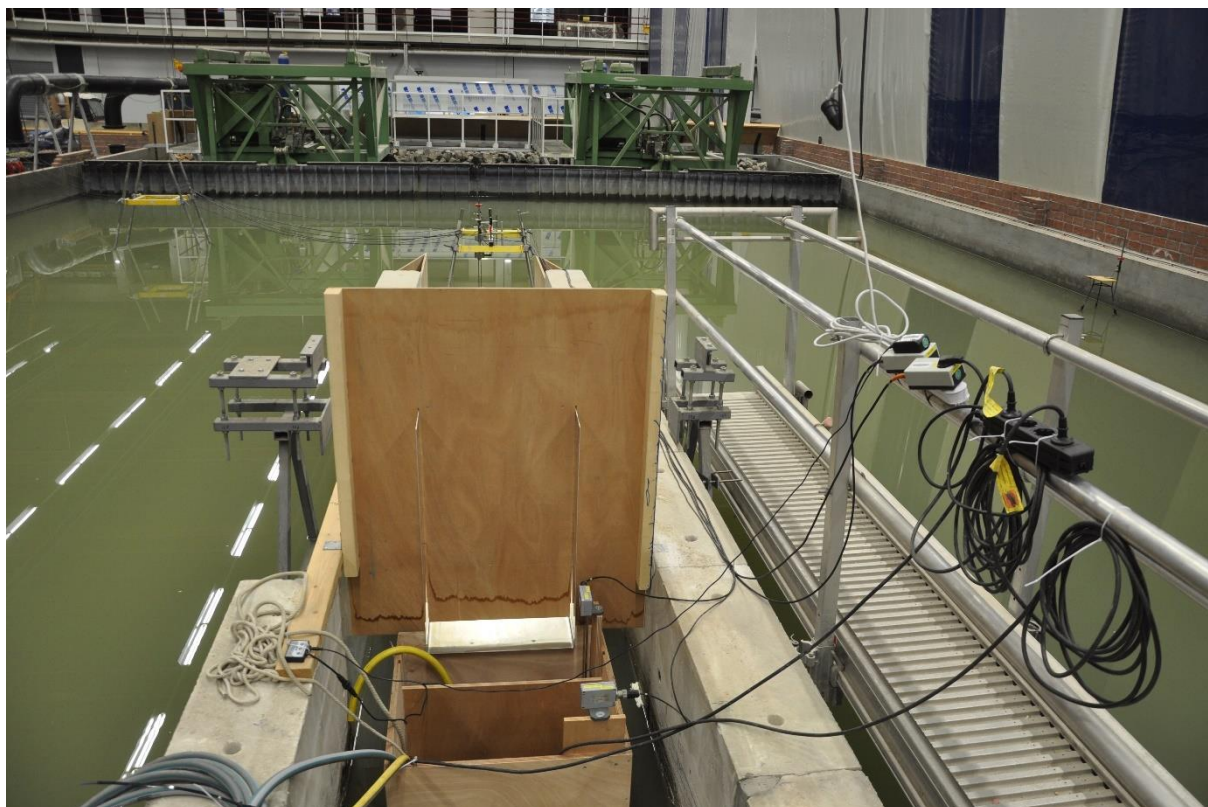


Figure B.8: General overview of the basin from behind the dike; at the top, the wave generator is visible; at the bottom, the overtopping box behind the dike is visible.

C

Measurement programme

Appendix C contains the quantitative details on the measurement programme and defines which wave characteristics were employed for the experiments. Also, the calculated dimensionless overtopping discharges are given for both tests with crest elements and the reference tests.

The different wave characteristics for which the tests were performed are mentioned in Table C.1 and the expected values for the dimensionless overtopping discharge for tests without wind are included in Table C.2. The influence factors in subsection 2.3.4 proposed by Van Doorslaer et al. (2015) for non-breaking waves are used to calculate the overtopping discharges. Besides the tests with crest elements, the reference tests are considered as well.

Table C.1: Wave characteristics for each test series as defined in chapter 2.

Index number	H_{m0} [m]	$T_{m-1,0}$ [s]	T_p [s]	s_0 [-]	Duration of 1,000 waves [min]
1	0.1	1.790	1.968	0.02	33
2	0.125	2.001	2.201	0.02	37
3	0.15	2.192	2.411	0.02	40
4	0.1	1.461	1.607	0.03	27
5	0.125	1.634	1.797	0.03	30
6	0.15	1.790	1.968	0.03	33
7	0.1	1.265	1.392	0.04	23
8	0.125	1.415	1.556	0.04	26
9	0.15	1.550	1.705	0.04	28
10	0.175	2.367	2.604	0.02	44
11	0.2	2.530	2.783	0.02	47
12	0.175	1.932	2.126	0.03	36
13	0.2	2.066	2.273	0.03	38
14	0.175	1.673	1.841	0.04	31
15	0.2	1.789	1.968	0.04	33

Table C.2: Expected dimensionless overtopping discharges for tests without wind based on equations from TAW (2002) and Van Doorslaer et al. (2015).

Index number	q^* [-] reference tests	q^* [-] crest wall 5 cm	q^* [-] crest wall 8 cm	q^* [-] crest wall 5 cm with promenade	q^* [-] crest wall 8 cm with promenade
1	1.75E-04	2.73E-05	8.77E-06	6.00E-06	1.59E-06
2	7.66E-04	2.08E-04	8.16E-05	6.20E-05	2.21E-05
3	1.89E-03	5.97E-04	2.84E-04	2.08E-04	8.22E-05
4	2.02E-04	3.26E-05	1.07E-05	3.50E-05	1.62E-05
5	8.01E-04	1.77E-04	7.66E-05	5.21E-05	1.82E-05
6	2.07E-03	5.52E-04	2.49E-04	1.93E-04	8.40E-05
7	3.82E-03	9.55E-04	3.23E-04	4.29E-04	1.07E-04
8	3.94E-04	3.24E-04	1.89E-04	1.14E-04	6.03E-05
9	1.08E-03	6.45E-04	3.23E-04	9.34E-04	5.76E-04
10	1.04E-03	1.37E-03	7.49E-04	5.47E-04	2.57E-04
11	1.87E-03	7.89E-04	4.67E-04	3.29E-04	1.73E-04
12	3.71E-03	1.37E-03	7.26E-04	5.93E-04	2.82E-04
13	2.10E-03	2.50E-03	1.43E-03	1.17E-03	6.09E-04
14	2.37E-03	1.41E-03	7.73E-04	6.01E-04	2.87E-04
15	4.18E-03	2.50E-03	1.43E-03	1.19E-03	6.17E-04

Information about the tests with water level variations is provided in Table C.3, which includes the corresponding water level, wave characteristics and expected overtopping discharge. These tests were performed only with a crest wall height of five cm.

Table C.3: Wave characteristics and expected dimensionless overtopping discharges for tests with different water levels.

Index number	H_{m0} [m]	$T_{m-1,0}$ [s]	s_0 [-]	d [m]	q^* [-] crest wall 5 cm
1	0.1	1.790	0.02	0.66	1.07E-05
1	0.1	1.790	0.02	0.68	1.71E-05
1	0.1	1.790	0.02	0.70	2.73E-05
1	0.1	1.790	0.02	0.72	5.16E-05
1	0.1	1.790	0.02	0.74	8.16E-05
3	0.15	2.192	0.02	0.66	3.10E-04
3	0.15	2.192	0.02	0.68	4.40E-04
3	0.15	2.192	0.02	0.70	5.97E-04
3	0.15	2.192	0.02	0.72	8.72E-04
3	0.15	2.192	0.02	0.74	1.06E-03
6	0.15	1.790	0.03	0.66	2.84E-04
6	0.15	1.790	0.03	0.68	3.88E-04
6	0.15	1.790	0.03	0.70	5.52E-04
6	0.15	1.790	0.03	0.72	8.11E-04
6	0.15	1.790	0.03	0.74	1.03E-03
9	0.15	1.550	0.04	0.66	3.10E-04
9	0.15	1.550	0.04	0.68	4.40E-04
9	0.15	1.550	0.04	0.70	6.45E-04
9	0.15	1.550	0.04	0.72	8.11E-04
9	0.15	1.550	0.04	0.74	1.03E-03

D

Overtopping discharges with wind

The main parameters determining the overtopping discharge related to this research are analysed in section 4.2. Both tests with and without wind show approximately similar results, hence the results for the tests with wind are situated in this appendix to avoid extensive repetition in the main report. For the complete analysis, the reader is referred to section 4.2, but in short, the figures in this appendix illustrate the following. Increasing the crest wall height or adding a promenade results in lower overtopping discharges (Figure D.1). There is a negative correlation between the wave steepness as well as the relative crest freeboard and overtopping discharge (Figure D.2), whereas the correlation between the overtopping discharge and the breaker parameter is positive (Figure D.3).

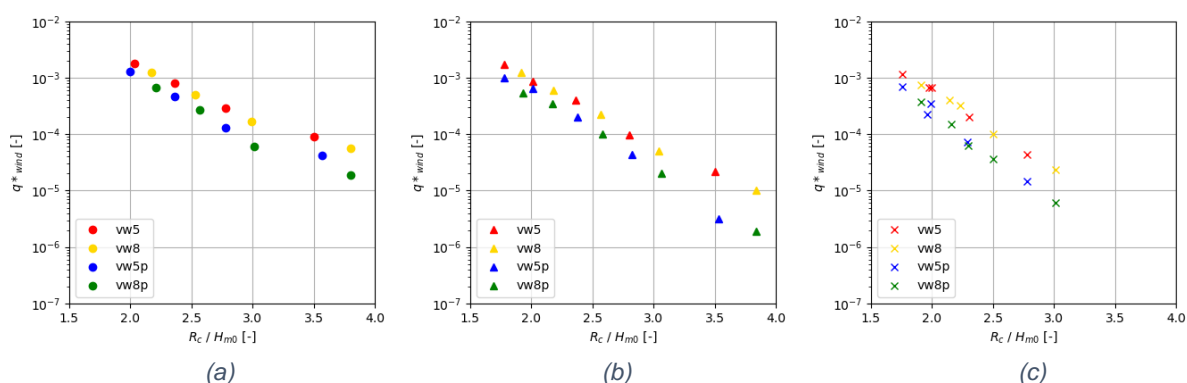
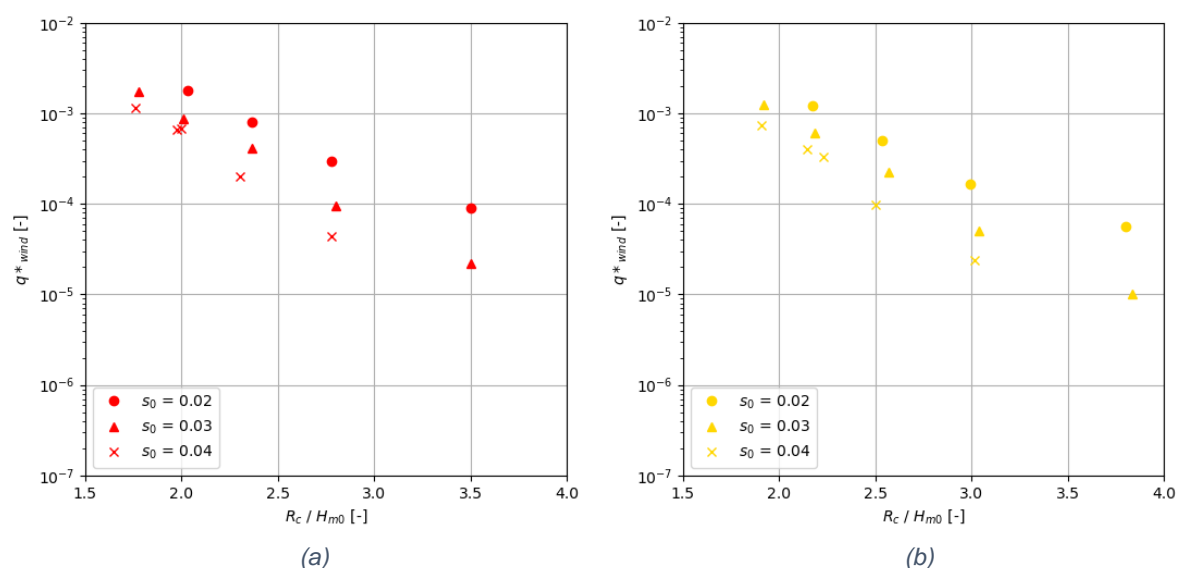


Figure D.1: Measured overtopping discharges with wind sorted on wave steepness; (a) Measurements with wave steepness of 0.02; (b) Measurements with wave steepness of 0.03; (c) Measurements with wave steepness of 0.04.



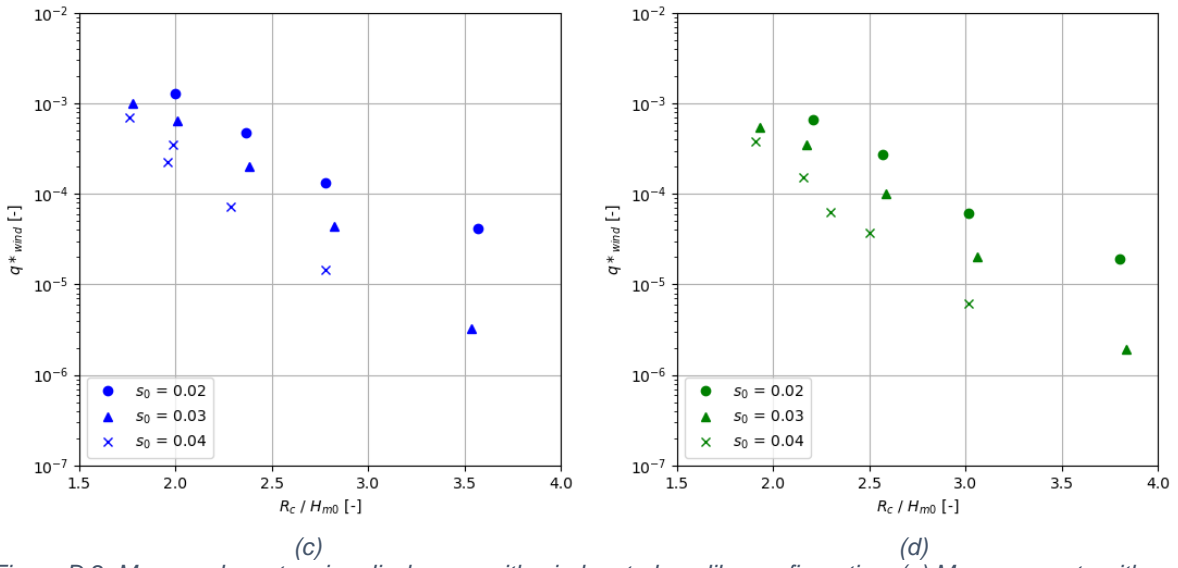


Figure D.2: Measured overtopping discharges with wind sorted on dike configuration; (a) Measurements with crest wall of 5 cm; (b) Measurements with crest wall of 8 cm; (c) Measurements with crest wall of 5 cm and promenade; (d) Measurements with crest wall of 8 cm and promenade.

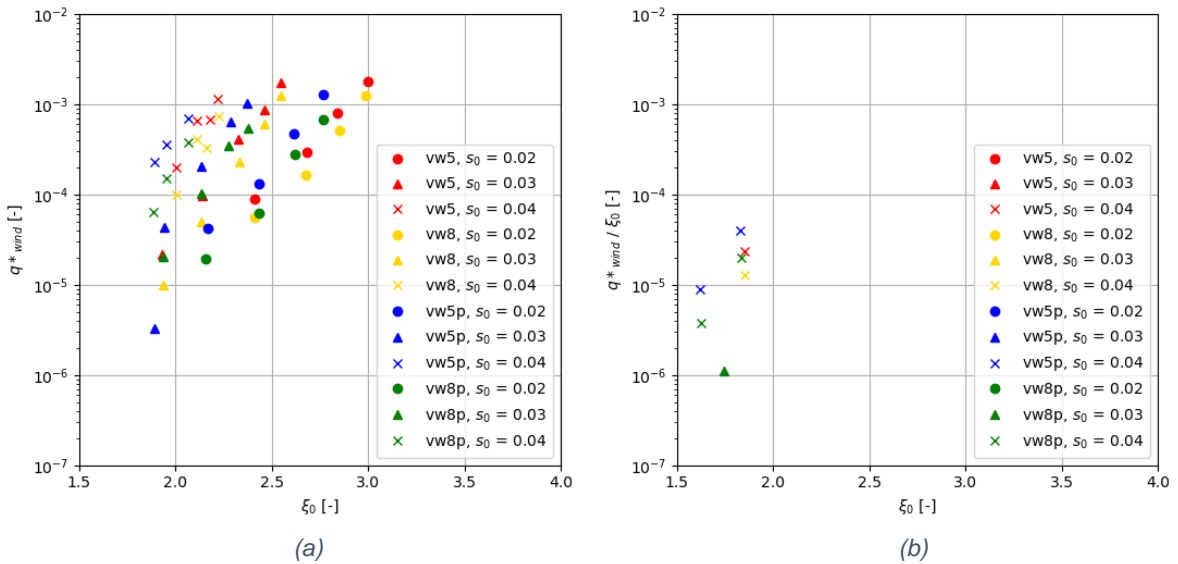


Figure D.3: Measured overtopping discharge with wind versus breaker parameter; (a) Measurements for non-breaking waves; (b) Measurements for breaking waves.